AD_____

Award Number: DAMD17-98-1-8001

TITLE: Role of Nf-kB/Rel in the Etiology of Breast Cancer

PRINCIPAL INVESTIGATOR: Gail E. Sonenshein, Ph.D.

CONTRACTING ORGANIZATION: Boston University Medical Campus
Boston, Massachusetts 02118-2394

REPORT DATE: February 2001

TYPE OF REPORT: Final

PREPARED FOR: U.S. Army Medical Research and Materiel Command
Fort Detrick, Maryland 21702-5012

REPORT DOCUMENTATION PAGE

Form Approved
OMB No. 074-0188

1. AGENCY USE ONLY (Leave blank)	2. REPORT DATE	3. REPORT TYPE AND DATES COVERED
	February 2001	Final (1 Feb 98 - 31 Jan 01)

4. TITLE AND SUBTITLE
Role of Nf-kB/Rel in the Etiology of Breast Cancer

5. FUNDING-NUMBERS
DAMD17-98-1-8001

6. AUTHOR(S)
Gail E. Sonenshein, Ph.D.
.

7. PERFORMING ORGANIZATION NAME(S) AND ADDRESS(ES)
Boston University Medical Campus
Boston, Massachusetts 02118-2394

E-Mail: gsonensh@bu.edu

8. PERFORMING ORGANIZATION REPORT NUMBER

9. SPONSORING / MONITORING AGENCY NAME(S) AND ADDRESS(ES)
U.S. Army Medical Research and Materiel Command
Fort Detrick, Maryland 21702-5012

10. SPONSORING / MONITORING AGENCY REPORT NUMBER

11. SUPPLEMENTARY NOTES

12a. DISTRIBUTION / AVAILABILITY STATEMENT
Approved for Public Release; Distribution Unlimited

12b. DISTRIBUTION CODE

13. ABSTRACT ***(Maximum 200 Words)***

Recent evidence suggests one reason for the rise in breast cancer incidence is increased exposure to and bioaccumulation of environmental pollutants. Work from the PI's laboratory has demonstrated that human breast tumor cell lines and primary breast tumor tissue constitutively express high levels of functional nuclear NF-κB/Rel activity, in contrast to untransformed breast epithelial cells or mammary tissue. Experiments are proposed using cell lines in culture, primary tissue and a transgenic mouse model to test the role of nuclear NF-κB/Rel activity in the etiology of breast cancer. The results of these studies will provide important information on the potential role of NF-κB/Rel factor overexpression in the etiology of breast disease. Rel factors represent an important link between environmental factors and the increased incidence of breast cancer. The different patterns of Rel factor expression in various tumors suggest the possibility that NF-κB/Rel factor represents a new class of potential marker(s) for analysis of progression of breast disease. Importantly, since Rel factor activity is sensitive to treatment with a number of anti-oxidants, demonstration that NF-κB/Rel factors play a role in the etiology of breast cancer would provide a new therapeutic target for the treatment of breast disease.

14. SUBJECT TERMS
Breast cancer, NF-kB, c-myc oncogene, arylhydrocarbon receptor (AhR) antioxidants, green tea, Her-2/neu

15. NUMBER OF PAGES
95

16. PRICE CODE

17. SECURITY CLASSIFICATION OF REPORT	18. SECURITY CLASSIFICATION OF THIS PAGE	19. SECURITY CLASSIFICATION OF ABSTRACT	20. LIMITATION OF ABSTRACT
Unclassified	Unclassified	Unclassified	Unlimited

Table of Contents

INTRODUCTION

The incidence of breast cancer has been steadily increasing over the past 50 years, and is now one of the leading causes of death among American women between the ages of 40-55 (23). In an attempt to find the reasons for this steady increase in incidence, both genetic and environmental factors are being studied. Attention has recently focused on the mechanism by which increased exposure to and bioaccumulation of these pollutants might have an etiologic role in breast cancer (13,20,37,59). The polycyclic aromatic hydrocarbons (PAHs) such as 7,12-dimethylbenz(*a*)-anthracene (DMBA) are specifically of interest (37). The most proximal event in PAH tumorigenesis is the binding of the chemicals to a cytosolic aromatic hydrocarbon receptor (AhR) (10,18,47). The receptor-ligand complex is translocated to the nucleus where it can bind to and alter the transcriptional level of DNA that has AhR-responsive elements. One battery of enzymes whose transcriptional induction is a hallmark of DMBA and other PAH exposure is the Phase I cytochrome P450 enzymes (9,32,37,39,61). These enzymes aid in the oxidative metabolism of both endogenous substances such as steroids, as well as in the breakdown of exogenous substances such as drugs, chemical carcinogens, and environmental pollutants. The products formed by this oxidative metabolism are often reactive oxygen intermediates (61). The potential for increased levels of oxidative stress within the cell resultant from exposure to environmental carcinogens leads us to hypothesize that this might activate expression of the NF-κB/Rel family of transcription factors. This family of factors, which regulates transcription of multiple genes including those involved in the regulation of cell proliferation, such as the c-*myc* oncogene implicated in neoplastic transformation (17,27,31), has been found to be sensitive to the cellular redox state (rev. in 1). In agreement with this model, we have found that malignant breast cancer cell lines and primary breast cancer tissue express significant levels of constitutive nuclear NF-κB/Rel activity (53). The constitutive expression of this factor suggests that NF-κB/Rel may promote aberrant proliferation and thus play an early role in the etiology of breast cancer. A brief introduction to NF-κB/Rel, in particular as it relates to this proposal follows.

NF-κB/Rel Family of Transcription Factors

The transcription factor NF-κB was first identified as a protein specific to mature B lymphocytes that interacted with the B site of the kappa light (L) chain gene enhancer (52). Constitutive nuclear NF-κB activity appeared to occur only in mature B lymphocytes. In most non-B cells, inactive NF-κB protein is present sequestered in the cytoplasm with inhibitor proteins termed IκBs (2). Activation of the NF-κB/IκB complex involves phosphorylation and degradation of IκB (8,24), allowing for translocation of active NF-κB complex into the nucleus where it can bind to κB responsive elements. Activation and nuclear localization can be induced by several agents, including oxidative stress (reviewed in references 1,5,22). NF-κB has been implicated in transcriptional regulation of a number of cellular genes involved in control of cell proliferation, adhesion, and in immune and inflammatory responses (1,5,22). These include the oncogene c-*myc*, several genes encoding growth or chemotactic factors, interleukins or their receptors, and metalloproteases and adhesion molecules such as E-selectin, ICAM-I, and VCAM-I. We demonstrated that the murine c-*myc* oncogene contains two functional κB sites (16,28). The human c-*myc* gene was found to contain similar κB elements (25).

The biochemical characterization of classical NF-κB determined that it is a heterodimer composed of a 50 kDa (p50) and a 65 kDa (p65) subunit. Cloning and sequencing of p50 and p65 led to the discovery that the binding domains of these factors have homology with an approximate 300 amino acid domain of the v-Rel oncoprotein and was thus termed the Rel homology domain (RHD), hence this family is termed the Rel or NF-κB/Rel family (21,29,45). In addition to c-Rel,

other members of the mammalian Rel family include p52 (also called lyt10) (6,41) and RelB (46). Rel-related factors bind as hetero- or homodimers that have different activities depending on subunit composition (58). For example, the p65 subunit is able to potently transactivate promoters driven by κB elements (31,48). The c-Rel protein, which appears to function in an element specific fashion, transactivates more moderately (31, 33,35,56). RelB is also a potent transactivator but only functions as a heterodimer (15,46). The overall effect within a cell is determined by the balance of dimers expressed, and is specific to the gene of interest.

Activation of NF-κB involves release from an IκB molecule and transit to the nucleus. Most studies have focused on the predominant IκB species, IκB-α (43). Several groups have demonstrated a role for CK2 in basal phosphorylation of IκB-α (3,34); these findings implicate CK2 in constitutive activation of NF-κB levels. For induction, phosphorylation, ubiquitination and degradation of IκB-α in the cytoplasm leads to release and subsequent nuclear translocation of NF-κB. The rapid phosphorylation of IκB-α on serine residues 32 and 36 has been shown to correlate with NF-κB induction in a number of cells, e.g., if either of these serine residues are mutated, induction of NF-κB activity is ablated (7). A large, multi-subunit kinase, containing IκB kinase α and β (termed IKKα and IKKβ, respectively), has been implicated in the phosphorylation of these serine residues on IκB-α protein (36,64). Intracellularly, the phosphorylation of these serine residues targets the IκB-α protein for ubiquitination on lysine residues 21 and 22, which marks it for degradation by the proteosome pathway. Several kinases have been implicated in activation of the IKK kinase activities via phosphorylation, and thereby to induction of NF-κB. One of these is the serine/threonine kinase Akt (42); although, there has been some controversy about whether the effects of Akt are mediated via direct phosphorylation of IKK. Overall, our results indicate malignant breast cell lines and primary tissue express active Rel factors, including c-Rel, p50 and p65. Given the potential important role NF-κB/Rel may play in the control of cell proliferation and survival, we proposed further studies of these factors in breast cancer in this application.

BODY AND CONCLUSIONS

Specific Aim 1: Quantitate and compare the levels of the individual subunits of NF-κB/Rel in nuclei of normal and transformed breast cell lines and primary human breast cancer tissue.

a) Work from our laboratory on the analysis of NF-κB expression in breast cancer cell lines was completed during the previous year. Our findings, essentially outlined in the 1ST year Progress Report, have now been published in Carcinogenesis (Kim et al., ref. 65).

b) As discussed above, work from many laboratories has implicated the IKKα and IKKβ of the IKK signalsome and CK2 kinases in activation of NF-κB. Thus, in our recent work we have extended our studies to the analysis of these kinases.

IKK complex kinases are constitutively active in human breast cancer cell lines. To determine whether breast cancer cells are characterized by an increase of activity of kinase components of the IKK complex, we first monitored the level of IKKβ activation. Kinase activity levels in untransformed MCF-10F human mammary epithelial cells (HMECs), and breast cancer cell lines Hs578T and carcinogen-transformed D3-1 and BP-1 cells were compared. D3-1 and BP-1 cell lines were derived from the non-tumorigenic MCF-10F cell by treatment with either the carcinogen DMBA or BaP, respectively (63). As controls for the kinase assay, Hs578T cells were treated with

TNF-α or transfected with plasmids encoding Flag-tagged dominant negative mutated IKKβSS/AA or constitutively active mutant IKKβSS/EE. Whole cells extracts were prepared from cultures of the four cell lines at 70% confluence, and samples containing equal amounts of proteins were immunoprecipitated with an IKKβ kinase specific antibody. Alternatively, a Flag antibody was used with the transfected cell extracts. One third of the immunoprecipitated material was used in *in vitro* phosphorylation assays with full length wild type IκB-α fusion protein (GST-wtIκB-α) as substrate, and protein was labeled with [γ-^{32}P] ATP (Fig. 1A, upper panel). The remainder was subjected to immunoblotting for IKKβ protein or Flag epitope, as indicated (Fig. 1A, bottom panel). Ectopic expression of the dominant negative IKKβ SS/AA resulted in reduced IKKβ kinase activity as judged by decreased IκB-α phosphorylation when compared to expression of IKKβSS/EE (Fig. 1A). This decrease occurred despite the higher total levels of IKKβ protein (Fig. 1A, bottom panel), consistent with a dominant negative effect. The IKKβ kinase activity in Hs578T was modestly stimulated by treatment with TNF-α for 10 min (Fig. 1A). IKK activity was specific for Ser-32 and Ser-36 of IκB-α because replacement with alanine at both sites in the GST-IκB-α substrate eliminated phosphorylation (data not shown).

Comparison of the WCEs from the four cell lines indicated IκB-α kinase activity directed by IKKβ was increased in the tumor cell lines compared to MCF-10F (Fig. 1A). When normalized for level of expression of IKKβ protein detected in the immunoblot (Fig. 1A, bottom panel), values obtained in this and a duplicate experiment for the Hs578T, D3-1 and BP-1 tumor cells were 1.6 and 1.4-, 2.6 and 2.0-, and 1.4 and 1.4-fold, respectively relative to MCF-10F cells. The increases in all of the cells were statistically significant ($p<0.05$). A similar analysis was next performed for IKKα. IKKα kinase activity was significantly lower in the untransformed MCF-10F cells compared

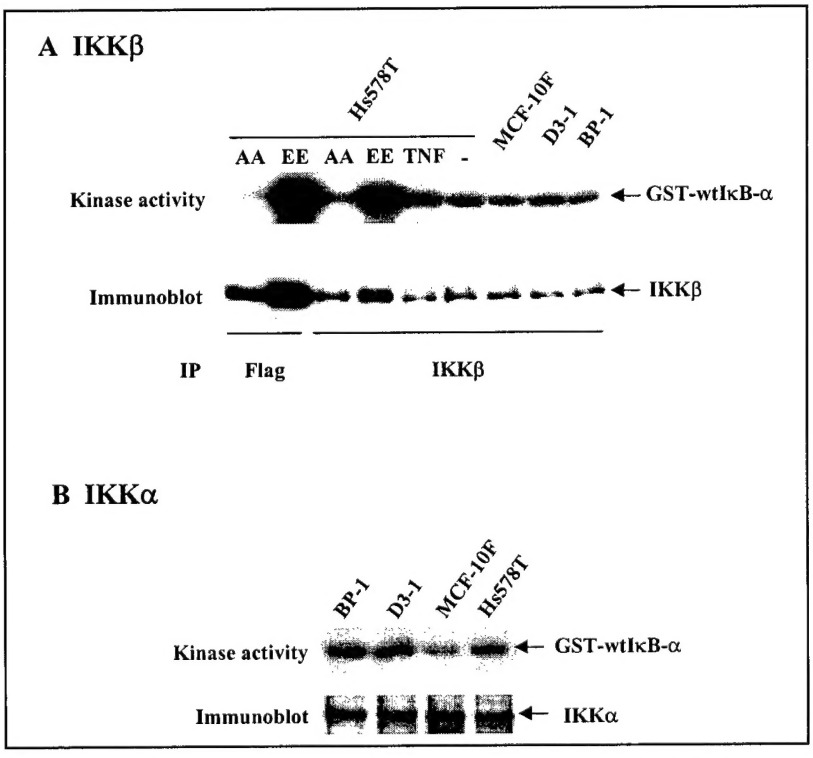

Fig. 1

to all three breast cancer cell lines (Fig. 1B). Immunoprecipitation of IKKα brought down approximately equivalent amounts of endogenous protein from the four lines (Fig. 1B). Compared to the MCF-10F cells, Hs578T, D3-1 and BP-1 tumor cells displayed higher IKKα activities in this and a duplicate experiment of 1.7 and 1.6-fold, 2.0 and 4.2-fold, and 1.9 and 5.0-fold, respectively. Thus, breast tumor cell lines displayed increased IKKα and IKKβ kinase activity compared to untransformed HMECs.

Kinase inactive IKKα or IKKβ inhibits NF-κB activity in Hs578T human breast cancer cells. To assess the role of active IKK kinases in the induction of NF-κB seen in the breast tumor cells, the effects of inhibition of IKKs on NF-κB activity and binding were evaluated. IKK activity was modulated by transfection with plasmids encoding kinase-inactive mutants IKKαSS/AA and IKKβSS/AA. The transcriptional activity of NF-κB was evaluated by co-transfection with a reporter plasmid driven by wild-type (E8-CAT) or mutated (negative control, dmE8-CAT) NF-κB binding elements. In Hs578T cells, functional activation of NF-κB was reduced 1.9-fold ($p<0.05$) upon transfection with IKKαSS/AA and 2.2-fold ($p<0.05$) by IKKβSS/AA compared to the cognate parental vectors (pcDNA3 and pCMV-Neo, respectively). This observation is consistent with the reduction of IKKs kinase activity in transfected cells seen above (Fig. 1A). Thus, these findings suggest that IκB-α turnover is mediated both by active IKKα and IKKβ.

Kinase inactive IKKβ inhibits NF-κB activity in D3-1 and BP-1 human breast cancer cells. We next sought to determine whether inhibition of the IKK complex in the D3-1 and BP-1 cells could similarly reduce NF-κB transcriptional activity and selected the dominant negative IKKβ. D3-1, BP-1 and parental MCF-10F cells were co-transfected with the kinase inactive IKKβSS/AA or parental pCMV-Neo vectors, and the wt and dm E8-CAT reporter constructs, as above. In the presence of the parental pCMV-Neo vector, the two transformed lines displayed higher levels of NF-κB activity compared to the MCF-10F cells, as expected (Fig. 2). The increase in activity was greater with the D3-1 than the BP-1 line. NF-κB activity was greatly reduced in D3-1 and BP-1 cells upon transfection with IKKβSS/AA, while no significant change was observed in the MCF-10F cells (Fig. 2). Thus, inhibition of IKKβ activity reduces NF-κB activity in both the D3-1 and BP-1 transformed breast cancer cell lines.

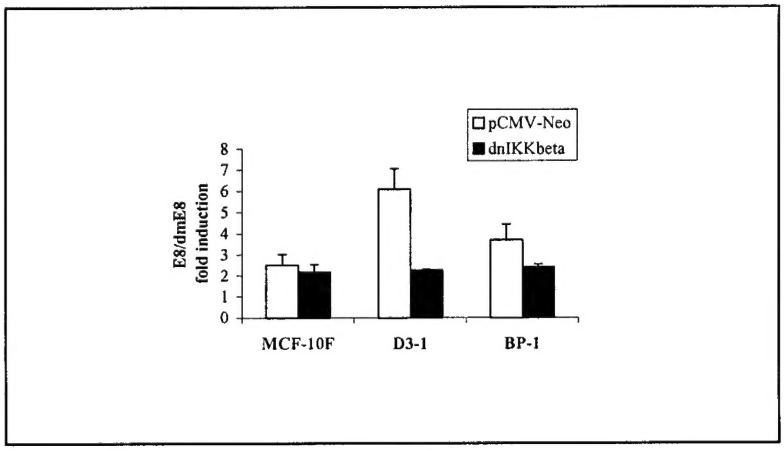

Fig. 2

CK2 kinase activity is increased in human breast cancer cell lines. CK2-mediated phosphorylation of IκB-α in the PEST domain has been implicated in the basal turnover of IκB-α. Thus, to explore the potential role of CK2 on NF-κB levels in breast cancer, a CK2 kinase assay

was developed using IκB-α as a specific substrate. GST fusion proteins of either wild type IκB-α (GST-wtIκB-α), or mutant Δ269-317 IκB-α (GST-Δ2IκB-α), which has a deletion of amino acids 269-317 in the C-terminal PEST domain, were used as positive and negative controls, respectively. Recombinant CK2 enzyme was assayed in the presence of [γ-^{32}P] GTP instead of [γ-^{32}P] ATP, since both ATP and GTP can be used as phosphate donors by CK2 while the IKKs can only use ATP. Recombinant CK2 phosphorylated GST-wtIκB-α to a much greater extent than GST-Δ2IκB-α (Fig. 3A). Similar results were obtained with an IκB-α mutant with three point mutations (S283A, T291A and T299A, GST-3CIκB-α), that had been previously shown to reduce phosphoryl group transfer by CK2 *in vitro* (data not shown).

WCEs were next prepared from Hs578T cells and used directly with GST-IκB-α fusion proteins as substrates in *in vitro* CK2 phosphorylation assays. Kinase assays demonstrated strong preferential phosphorylation of GST-wtIκB-α compared to GST-Δ2IκB-α or GST-3CIκB-α (Fig 3B). To verify the involvement of CK2, two selective pharmacologic inhibitors of CK2 apigenin or emodin were used either with cells in culture or cell extracts. Apigenin is a plant flavonoid that has been shown to be more effective *in vitro*, although, it can also inhibit intracellular CK2 activity (69). Hs578T cells were incubated for 2 h in the presence of 20, 40 or 80 μM apigenin or volume of carrier DMSO equivalent to 80 μM (Fig. 3C, left panel). A decrease of 1.5- to 2-fold in phosphorylation of GST-wtIκB-α was observed with the extracts. Alternatively, WCEs were treated with similar concentrations of apigenin (Fig. 3C, right panel). A dose-dependent inhibition was noted that was more potent than in cells, as seen previously. The natural plant anthraquinone derivative emodin, has been shown to inhibit CK2 activity by competitively binding to its ATP binding site (70). Addition of emodin similarly caused a dose-dependent decrease in CK2 activity both in Hs578T cells or extracts with almost complete inhibition at 25 μg/ml (Fig. 3C). Thus, apigenin and emodin reduced GST-wtIκB-α kinase activity when added to extracts or to cells in culture. Furthermore, addition of the CK2 peptide substrate RRREEETEEE effectively reduced phosphorylation of the GST-wtIκB-α substrate (data not shown). Thus, the assay for CK2 activity using GST-IκB-α as a substrate appears to be specific. Furthermore, the results indicate that Hs578T cells display CK2 IκB-α kinase activity.

We next compared the relative CK2 activity in the untransformed MCF-10F cells with levels in the BP-1, D3-1, and Hs578T breast cancer cells. The CK2 kinase activity was clearly higher in all of the tumor cells compared to the MCF-10F line (Fig. 4A). Compared to MCF-10F cells, the relative increase in CK2 kinase activity was 2.2-, 2.5- and 2.2-fold in Hs578T, BP-1 and D3-1 cells, respectively. Increased CK2 activity is most often due to increased levels of CK2 protein expression. To assess the relative levels of CK2 protein in the cell lines, immunoblot analysis was performed for the CK2α subunit of CK2 using the WCEs (Fig. 4B). The Hs578T, D3-1 and BP-1 cells expressed higher levels of CK2α than MCF-10F cells. Equal loading was confirmed by analysis for β-actin expression. (A slightly lower β-actin level was routinely detected in the Hs578T cells, data not shown.) The results from this and a duplicate experiment were quantified. Compared with the MCF-10F cells, an approximate 2.2+/-0.3-, 1.6+/-0.1- and 1.6+/-0.3-fold increase in the level of CK2α protein was found in the Hs578T, BP-1 and D3-1 transformed lines, respectively. Thus IκB-α kinase activity directed by CK2 is increased in these breast tumor cell lines and this increase can be explained by an increase in levels of CK2α protein.

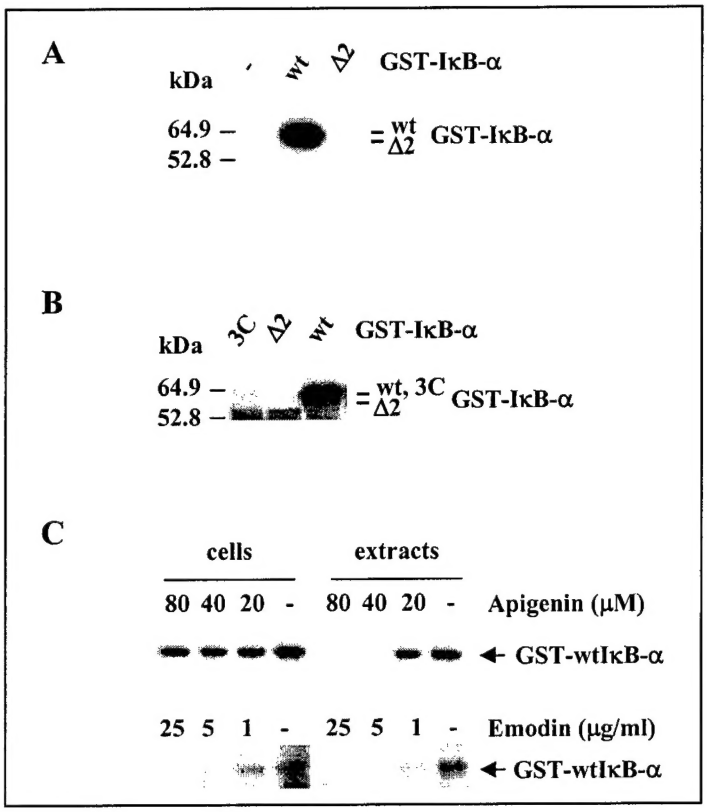

Fig. 3

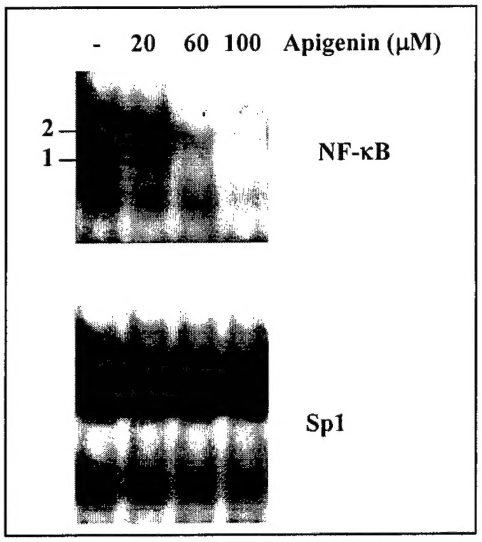

Fig. 5

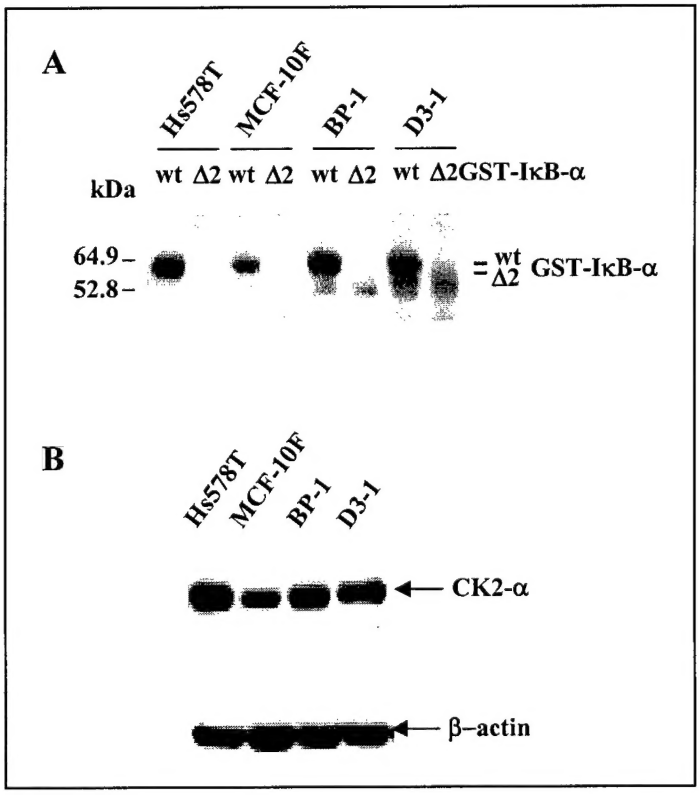

Fig. 4

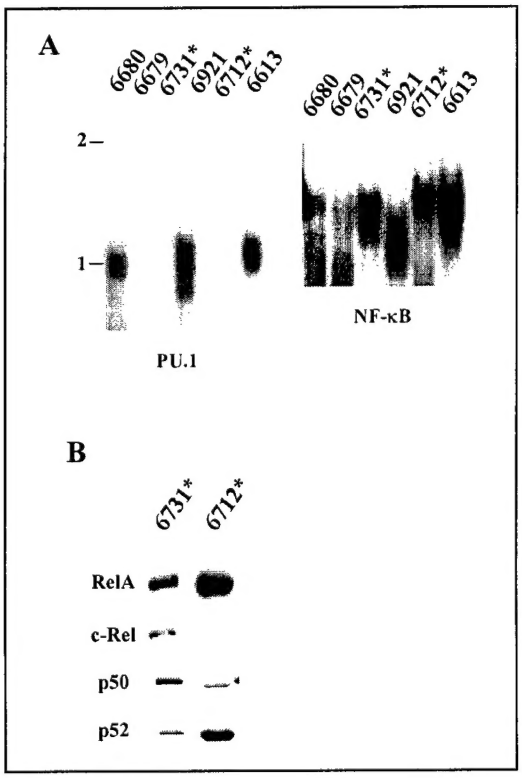

Fig. 6

Inhibition of CK2 reduces NF-κB activity in Hs578T cells. To evaluate the role of CK2 in the constitutive levels of NF-κB in breast cancer cell lines, we chose the CK2-selective inhibitor apigenin. Hs578T cells were incubated for 2.5 h in the presence of 20, 60 or 100 μM apigenin or with the concentration of carrier DMSO equivalent to 100 μM (- apigenin). Nuclear extracts were prepared and analyzed for NF-κB binding activity by EMSA (Fig. 5). Two major complexes were seen in the untreated Hs578T cells. Antibody supershift analysis indicated that complex 2 represents p50/RelA and complex 1 is a homodimer of p50 (data not shown), consistent with our previous observations with this line (65). Apigenin reduced formation of both bands 1 and 2 in a dose-dependent fashion. Little change was noted at 20 μM, while a substantial decline in the upper p50/RelA complex was observed at 60 μM. At a concentration of 100 μM, reduced formation of both complexes was noted. In contrast, little effect was seen on binding of Sp1 (Fig. 5). When these results were scanned and normalized to the Sp1 binding activity, a 70% decrease in classical NF-κB was noted with 60 μM apigenin. At 100 μM apigenin, decreases of 95% and 80% in p50/RelA and p50 homodimers, respectively were observed. We next verified that the NF-κB transcriptional activity is decreased by inhibition of CK2 using either apigenin or emodin. Following transfection with vectors expressing an NF-κB element luciferase reporter plus SV40βgal, for normalization, cells were incubated overnight, and then treated with either 60 μM apigenin or 25 μg/ml emodin. The treatments were performed for 6 h to ensure sufficient time for the transcriptional activity to decline and for decay of the luciferase protein. Apigenin treatment resulted in an approximate 43% decline in NF-κB activity (39.2 +/- 3.8% and 45.6 +/- 6.1% in two separate experiments). Emodin treatment caused an approximate 30% drop in NF-κB activity (35.9 +/- 3.6 and 24.9 +/- 1.8% in two separate experiments). Taken together, these results suggest that inhibition of CK2 leads to a reduction of nuclear NF-κB binding activity in Hs578T breast cancer cells.

c) We then focussed on primary human breast cancer tissue specimens, and similarly expanded our studies to include the IKK and CK2 kinase analyses.

We asked whether these three IκB kinases are activated in primary human breast cancer specimens and whether NF-κB induction correlates with kinase activation. Two sets of human primary breast tumors were studied. The pathological characteristics that were available are shown in Table 1. Nuclear extracts were prepared from frozen breast tumors and used for NF-κB binding by EMSA. Since potential contamination with hematopoietic cells could significantly affect the analysis, our strategy was to also test for such contamination using a binding assay for PU.1 and TCF-1, which are present in B lymphocytes, neutrophils, mast or myeloid cells and T cells. The data obtained from the analysis of the first group of 6 patient samples is shown in Fig. 6 (and Fig. 7 below), and Table 1 presents the findings for every PU.1- and TCF-1-negative sample from the two sets analyzed.

In analysis of the first six specimens, binding of full-length PU.1 protein was detected in sample #6679 (band 2), and a clipped form of PU.1 protein was detected in patients #6680, #6921 and #6613 (Fig. 6A, left panel), and these findings were confirmed using immunoblot analysis (data not shown). Compared to Jurkat T cells, only low and comparable levels of binding to TCF-1 was detected in the tumor extracts (data not shown). Two of the samples (#6731 and #6712) that tested negative for PU.1, were found to express relatively high levels of NF-κB binding (Fig. 6A, right panel). The gels were subjected to densitometry and the results of the analysis of all samples that tested negative for PU.1 and TCF-1 are presented in Table 1.

To identify which NF-κB subunits are present in the nuclear extracts, immunoblot analysis was performed using antibodies specific for RelA (p65), c-Rel, p50, and p52 (Fig. 6B). Both

samples #6712 and #6731 displayed nuclear p65 proteins, as did #6679. When c-Rel was assessed, only #6731 displayed detectable levels of expression. The p50 or p52 subunits were detected in both patient samples. (The p50 in sample #6712 had a slightly faster mobility than p50 in sample #6731.) Sample #6731 displayed somewhat more expression of p50 (band 1) than p52, while sample #6712 expressed more p52 than p50 (Fig. 6B). Thus, sample #6731 contains transactivating subunits RelA and c-Rel while #6712 contains RelA. The data for expression of RelA and c-Rel in the two sets of patient samples are summarized in Table 1. Essentially all of the tumors tested positive for the p50 or p52 subunit (data not shown). Out of the 10 PU.1/TCF-1-negative breast cancer samples characterized, 3 displayed only low levels of NF-κB binding, while 1 had a minimally elevated level and 6 showed substantially elevated levels of NF-κB binding.

Cytoplasmic extracts from tumors of these patients were then tested for CK2 IκB-α kinase activity, using GST-wtIκB-α as substrate (Fig. 7A and data not shown). Two of the six primary tumor samples from the first set of patients showed elevated CK2 IκB-α kinase activity: patients #6731 and #6712 (Fig. 7A). As a negative control for the kinase assay, two samples were tested with GST-Δ2IκB-α as substrate. The extracts failed to phosphorylate this IκB-α protein containing a deletion of the PEST domain sequences. Lastly, to confirm the specificity of the assay for CK2, the selective inhibitor apigenin was added to the reaction with wild type IκB-α as substrate. Apigenin dramatically reduced IκB-α phosphorylation with samples #6680 and #6731, confirming the reactions were mediated by CK2. The results from the two sets of patients were quantified by densitometry; the data for the PU.1/TCF-1-negative samples are presented in Table 1. Three of the specimens displayed low levels of CK2 activity (between 231 and 415 densitometry units), while the remaining specimens had either modestly increased (758 to 1,106 densitometry units) or substantially elevated levels (1,809 to 6,143 densitometry units) (Table 1). The three specimens with low CK2 also displayed low or minimally elevated NF-κB binding. Six samples displayed elevated levels of CK2 and NF-κB binding, while only one specimen (#6885) showed high IκB-α CK2 kinase activity without detectable high NF-κB nuclear activity.

Activities of the IKKα and IKKβ kinases were evaluated following immunoprecipitation with their specific antibodies, and the data presented in Figures 7B and 7C, respectively. The results for PU.1/TCF-1-negative tumors are shown in Table 1. Tumor samples #6731 and #8364 exhibited modestly increased levels of IκB-α kinase activity directed by IKKα, and increased NF-κB binding activity. Consistent with data obtained with tumor cell lines, increased IKKα activity in primary tumors did not seem to be due to increased levels of protein expression (Fig. 7B and data not shown). In the analysis of IKKβ kinase activity most of the samples yielded values between approximately 100 and 300 densitometry units, however, cytosolic extracts from 3 specimens (#8361, #8364, #8385) displayed greatly elevated IKKβ activity (1,164, 1,395 and 980 densitometry units, respectively). These 3 specimens all displayed high NF-κB binding activity. No phosphorylation was detected using a mutant of IκB-α at Ser-32 and Ser-36 as substrate, confirming the specificity of the kinase assay (data not shown).

CONCLUSIONS: Here we show that human breast cancer cell lines and primary human breast tumor specimens display elevated CK2, IKKβ and/or IKKα IκB kinase activities, which correlate and are therefore likely responsible for the aberrant NF-κB activation in these primary tumors. Inhibition of any of these activities in the breast cancer cell lines resulted in reduced functional NF-κB/Rel. Previously, we demonstrated that primary breast cancer samples from patients are typified by aberrant activation of nuclear NF-κB. In particular, we observed the presence of nuclear p50, p65 and c-Rel protein in multiple breast cancer specimens. These results were extended to

additional patients here. As described below, we have recently identified a signaling pathway, mediated via Her-2/neu that leads to the activation of NF-κB subunits p50, p65 and p52 in mammary tumor cells. Overall, our work begins to elucidate the molecular mechanisms responsible for activation of the NF-κB in breast cancer patients. A manuscript on this work has been accepted pending revision in Cancer Research: Romieu-Mourez, E. Landesman-Bollag, D.C. Seldin, A.M. Traish, F. Mercurio, and G.E. Sonenshein. Roles of IKK kinases and protein kinase CK2 in activation of NF-κB in breast cancer.

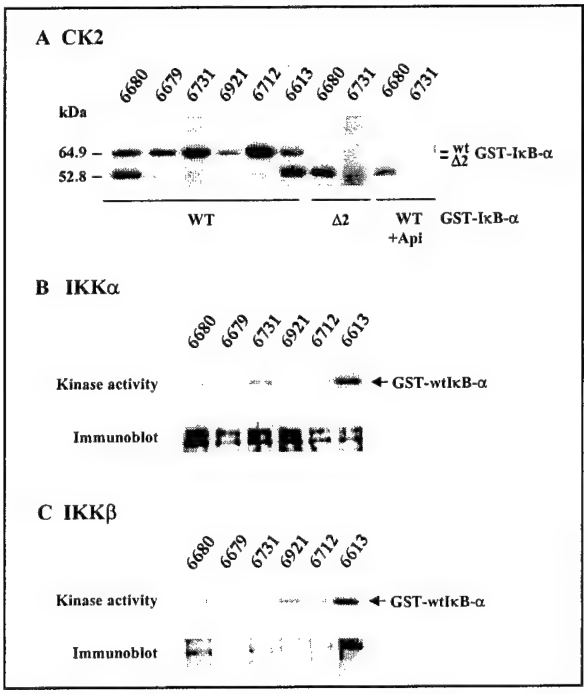

Fig. 7

Table 1. ***IKK and CK2 kinase activity in primary human breast specimens.*** [a]

Patient	Tumor type	NF-κB binding[b]	NF-κB RelA[b]	NF-κB c-Rel[b]	Kinase activity[b] IKKα	Kinase activity[b] IKKβ	Kinase activity[b] CK2
6712	Right Infiltrating Ductal Ca.	3 939	2 578	-	129	178	2 446
6731	Right Breast Mass	4 868	1 137	687	432	114	1 809
6885	Not available	114	-	-	230	316	6 143
8357	Right Invasive Lobular Ca.	970	-	-	-	nd	341
8359	Ductal Ca.	646	-	-	182	276	415
8360	Left Infiltrating Ductal Ca.	344	-	-	-	294	231
8361	Right Breast Mass	6 022	4 764	74	133	1 164	1 106
8364	Not available	1 866	1 713	-	355	1 395	819
8385	Metastatic Ca.	2 840	2 938	652	247	980	758
6698	Left Breast Mass	3 689	-	-	137	243	3 902

[a]Table presents results observed with two groups of 6 and 10 primary human breast specimens.
Data were normalized to a standard WEHI 231 B cell extract

[b]Densitometry, arbitrary units.
"-", no expression/activity detected
nd, not done

c) Determine whether Her-2/neu induces NF-κB.
Overexpression of the epidermal growth factor receptor (EGFR) family member Her-2/neu, seen in approximately 30% of breast cancers, is associated with poor prognosis. Previously, Her-2/neu had been shown to signal via a phosphatidylinositol 3 (PI 3)-kinase to Akt/protein kinase B (PKB) pathway. Since this signaling pathway was recently shown to activate NF-κB, we tested the hypothesis that Her-2/neu can activate NF-κB in breast cancer. Overexpression of Her-2/neu and EGFR-4 in Ba/F3 cells led to constitutive PI 3- and Akt kinase activities, and induction of classical NF-κB (p50/p65) (Fig. 8). Similarly, tumors derived from MMTV-Her-2/neu transgenic mice (Fig. 9) and a tumor cell line isolated from such a tumor (NF639) (Fig. 10 and data not shown) displayed elevated levels of classical NF-κB (p50/p65). Engagement of Her-2/neu receptor downregulated the level of NF-κB (data not shown) (see attached proofs of Pianetti et al., in press; ref 73). NF-κB binding and activity in the cultured cells was reduced upon inhibition of the PI 3- to Akt kinase signaling pathway via ectopic expression of kinase inactive mutants (Fig. 10), incubation with wortmannin (data not shown), or expression of the tumor suppressor phosphatase PTEN (Fig. 11, and see Pianetti et al. in press). Inhibitors of calpain (calpeptin and E64D), but not the proteasome (MG132), blocked IκB-α degradation following inhibition of protein synthesis upon cycloheximide (CHX) addition (Fig. 12). The effectiveness of the MG132 was confirmed in analysis of decay of $p27^{Kip1}$, which occurs via the proteasome (Fig. 12B). Inhibition of Akt did not affect IKK activity (data not shown, see Pianetti et al., in press).

Conclusions: These results indicate that Her-2/neu activates NF-κB via a PI 3- to Akt kinase signaling pathway that can be inhibited via the tumor suppressor PTEN, and is mediated by calpain rather than the IκB kinase complex. A manuscript is in press in Oncogene on this work (Pianetti et al., ref 73).

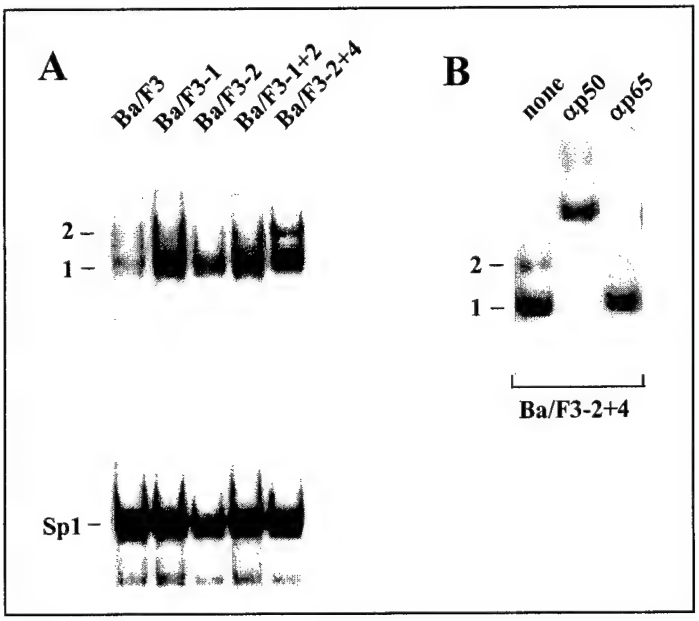

Fig. 8

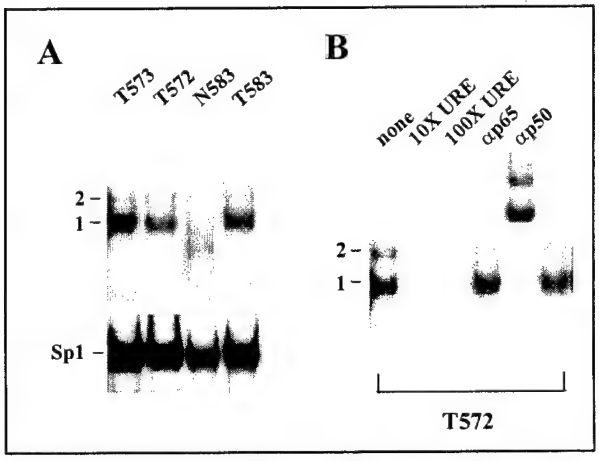

Fig. 9

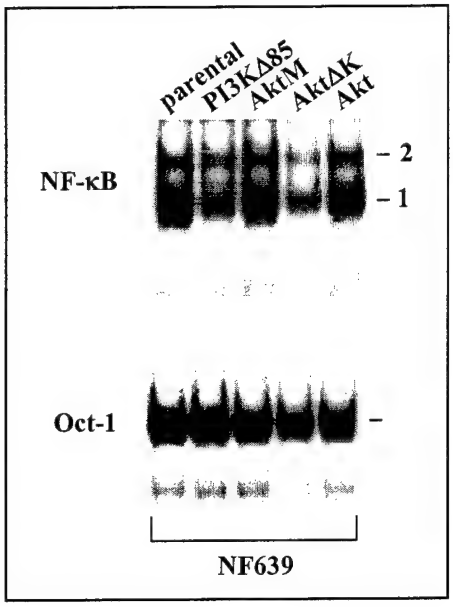

Fig. 10

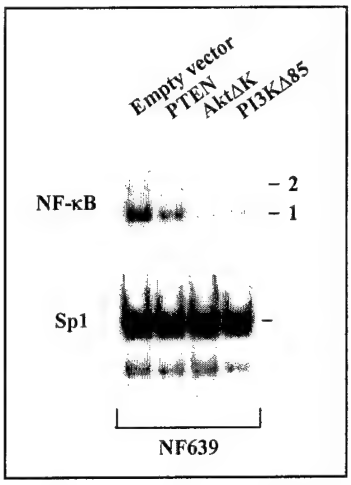

Fig. 11

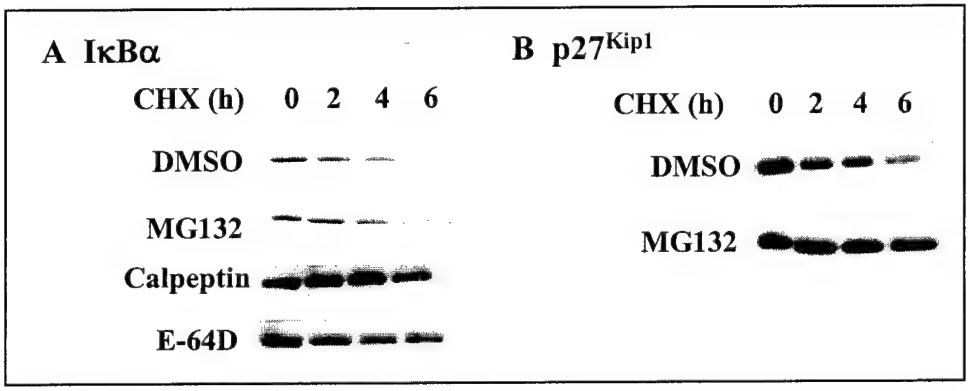

Fig. 12

Specific Aim 2: Test the transactivation activity of Rel specific subunits overexpressed in transformed primary tissue in a breast cell line.

We recently demonstrated that levels of NF-κB and aryl hydrocarbon receptor/transcription factor (AhR), which mediates malignant transformation by environmental carcinogens, are highly elevated and appear constitutively active in breast cancer cells (53, 66). Rel factors have been found to functionally interact with other transcription factors (57). Thus, we tested for the association of AhR with NF-κB subunits. We now demonstrate a physical and functional association between the RelA subunit of NF-κB and AhR resulting in the activation of c-*myc* gene transcription in breast cancer cells. These experiments were described in our 2nd year Progress Report. In brief, we found that

RelA and AhR proteins were co-immunoprecipitated from cytoplasmic and nuclear extracts of non-malignant MCF-10F breast epithelial and malignant Hs578T breast cancer cells. In transient co-transfection, RelA and AhR gene products demonstrated cooperation in transactivation of the c-*myc* promoter, which was dependent on the NF-κB elements, and in induction of endogenous c-Myc protein levels. A novel AhR/RelA-containing NF-κB element binding complex was identified by electrophoretic mobility shift analysis of nuclear extracts from *RelA* and *AhR* co-transfected Hs578T cells. Thus, the RelA and AhR proteins functionally cooperate to bind to NF-κB elements and induce c-*myc* gene expression. These findings suggest a novel signaling mechanism whereby the AhR can stimulate proliferation and tumorigenesis of mammary cells. A paper on this work has now been published in Oncogene (Kim et al., ref. 67). These studies were performed in collaboration with Dr. David Sherr (School of Public Health, Boston University Medical Center), who is a world recognized expert in AhR metabolism and function.

In more recent work we have examined the nature of the sequences mediating AhR/RelA interaction within the NF-κB element. We found that mutation of bases within the core element, which were shown previously to prevent NF-κB binding (68) similarly prevented binding of the AhR/RelA complex. These findings are consistent with the major role of the NF-κB RelA subunit in binding to this site.

CONCLUSIONS: In summary, our results show a physical and functional association of the AhR and the RelA subunit of NF-κB in transactivation of the c-*myc* gene in breast epithelial cells. Specifically, AhR and RelA were physically associated in malignant Hs578T breast cancer and non-malignant MCF-10F HMECs. AhR and RelA induced expression of the endogenous c-*myc* gene in MCF-10F cells. Using transfection analysis, AhR and RelA cooperated to transactivate the c-*myc* promoter in these two lines. As judged by transfection and mobility shift analyses, the RelA and AhR proteins formed a novel complex that binds to the wild type but not mutant NF-κB element of the c-*myc* gene. We postulate it is this complex, binding via the NF-κB element, that transactivates the c-*myc* promoter.

Specific Aim 3: Monitor the effects of antioxidants known to inhibit NF-κB/Rel expression on cellular proliferation of transformed mammary cell lines.
a) Studies demonstrating the inhibitory effects of treatment with the antioxidant pentoxifylline (4) on growth of MCF-7 and 578T cells have been completed, as reported last year.
b) Green tea extracts have been found to be rich in antioxidants. Thus, we have analyzed the effects of two active components of green tea extacts, green tea polyphenols (GTP) and (-)-epigallocatechin-3-gallate (EGCG).

Green Tea Polyphenols Decrease Growth of Hs578T Breast Cancer Cells. In the clinic, ER negative tumors are not responsive to anti-estrogenic treatments such as tamoxifen, and generally indicate a poorer prognosis. Therefore we sought to determine whether treatment with green tea extracts decreases the growth of ER negative breast cancer cells, and first selected the Hs578T cell line. Hs578T cells were treated with concentrations of GTPs ranging from 0-160 μg/ml. Cell growth was assessed every 24 h for a 72 h period by cell numbers using an MTS assay (Fig 13A). Incubation in the presence of 40 μg/ml GTPs had no detectable effect on Hs578T cell growth ($p=0.95$), whereas, 80 μg/ml GTP slowed the growth of these breast cancer cells ($p<0.05$). No growth, i.e., no increase in cell numbers, was seen with a higher dose of 160 μg/ml GTP ($p<0.01$). Similar effects of GTPs were obtained by cell counting using a hemocytometer (data not shown). Thus, treatment with GTPs inhibits growth of Hs578T cells in a dose-dependent fashion.

We next assessed the effects of EGCG, one of the more potent anti-carcinogenic components of GTPs, on growth of Hs578T cells (Fig. 13B). EGCG slowed the growth of the Hs578T cells in a dose-dependent fashion ($p<0.01$ at all doses tested). A slower growth was seen at a EGCG concentration of 40 μg/ml, while no increase in cell numbers was seen at 80 μg/ml EGCG. At 160 μg/ml EGCG, a decline in cell numbers was observed (Fig. 13B). Thus, both GTP and EGCG slow proliferation of Hs578T breast cancer cells. A lower concentration of EGCG (80 μg/ml) than GTP mixture (160 μg/ml) was effective in preventing an increase in cell numbers over time.

The drop in Hs578T cell numbers with the highest dose of EGCG suggested cell death was occurring. To monitor for cell death, trypan blue exclusion analysis was performed (Fig. 14). To ensure that floating, dead cells were not lost during the preparation, cells on the dish and in the media were combined and trypan blue positive and negative cells counted. At 80 μg/ml EGCG, a low percentage of the Hs578T cells stained trypan blue positive at 24 and 48 h (between 7-8%), indicating that the cells were largely viable. A substantial increase in the number of dead cells was seen with 160 μg/ml EGCG (~45% trypan blue positive cells) (Fig. 14). A TUNEL assay indicated apoptosis was occurring at doses of 80 and 160 μg/ml EGCG (data not shown). Taken together, these findings indicate that growth of Hs578T cells begins to slow at 40 μg/ml EGCG, while higher doses of 80-160 μg/ml EGCG inhibit growth and/or cause apoptosis of Hs578T breast cancer cells.

EGCG Slows Growth of Multiple ER Negative Breast Cancer Cell Lines. To determine whether the growth inhibitory effects of EGCG could be extended to other ER negative cells, the MDA-MB-231 and D3-1 breast cancer cell lines were selected. MDA-MB-231 cells displayed an EGCG dose-response curve similar to that of Hs578T cells (Fig. 13C), while the D3-1 cells were somewhat more sensitive (Fig. 13D). The apparent higher sensitivity of the D3-1 line was extended to trypan blue analysis, and a significant level of cell death was detected even at 80 μg/ml, and 90-100% of the cultured cells had died within 48-72 h of incubation in the presence of 160 μg/ml EGCG. Thus, EGCG slows growth and induces death of ER- breast cancer cell lines in a dose-dependent fashion.

$p27^{Kip1}$ Cyclin-Dependent Kinase Inhibitor Expression is Induced by EGCG Treatment. Since the $p27^{Kip1}$ CKI has been implicated in control of cell cycle progression, we measured the effects of EGCG treatment on the levels of $p27^{Kip1}$ CKI protein in Hs578T cells. Cultures of exponentially growing cells were treated for 24 h with 40 or 80 μg/ml EGCG, as appropriate to inhibit cell proliferation. Whole cell extracts were prepared and subjected to immunoblot analysis for $p27^{Kip1}$

protein expression (Fig. 15A). A small increase in the $p27^{Kip1}$ levels was observed in response to treatment with 40 μg/ml EGCG (1.5-fold relative to untreated control cells), which causes a slight decrease in growth. A larger increase in $p27^{Kip1}$ level was noted with 80 μg/ml EGCG (2.8-fold relative to untreated cells). We then assessed the effects of a longer (48 h) period of EGCG treatment (Fig. 15B). Growth for 48 hours alone resulted in an increase in $p27^{Kip1}$ levels, likely due to the increase in cell density (2.8-fold). EGCG treatment clearly elevated the $p27^{Kip1}$ levels even further (5.5-fold). Thus, growth arrest of HS578T cells in response to EGCG treatment is accompanied by an increase in the level of expression of the CKI $p27^{Kip1}$.

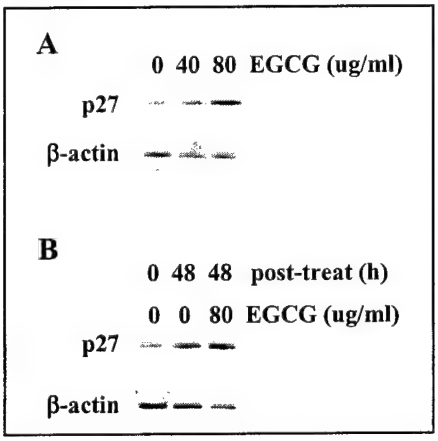

Fig. 15

Ectopic Expression of $p27^{Kip1}$ Arrests Growth of Hs578T Cells. To determine the role of induction of $p27^{Kip1}$ protein in Hs578T breast cancer cell, the LacSwitch inducible expression system was used. Mixed populations of stable Hs578T-*p27S* and Hs578T-*neo* population of cells were isolated. Since we have found that the response of the mixed populations is relatively minimal due to the presence of cells expressing only low levels, three single cell clones of Hs578T- *p27S* cells were isolated by limiting dilution (Hs578T-*p27S* #2, #3, #4). To test for induction of $p27^{Kip1}$ expression, the mixed populations of Hs578T-*p27S* and Hs578T-*neo* cells, and the three Hs578T- *p27S* clones were treated with 0, 10 or 20 mM ITPG, as indicated (Fig. 16A). Total cellular proteins were extracted and samples subjected to immunoblot analysis for $p27^{Kip1}$ expression. A very high level of induction of the $p27^{Kip1}$ protein was detected in the Hs578T-*p27S* cells at both concentrations of IPTG (Fig. 16A, upper panel). In contrast, control Hs578T-*neo* cells showed essentially no induction of the $p27^{Kip1}$ protein. As expected, the Lac I repressor protein was detected at high levels in extracts from both cell populations, confirming equal loading (Fig. 16A, lower panel). One of these clones (Hs578T-*p27S* #3) showed a very high level of $p27^{Kip1}$ induction upon 10 mM IPTG treatment (Fig. 16B, upper panel); whereas, the two other clonal isolates (Hs578T-*p27S* #4, and Hs578T-*p27S*#2) displayed no significant increase in $p27^{Kip1}$ levels (Fig. 16B, lower panel and data not shown). Thus, we selected the Hs578T-*p27S* mixed population and Hs578T-*p27S* #3 for study of the effects of $p27^{Kip1}$ induction on cell cycle, while the Hs578T-*neo* mixed population and Hs578T-*p27S* #4 cells served as negative controls.

The Hs578T-*p27S*, Hs578T-*neo*, Hs578T-*p27S* #3 or Hs578T-*p27S* #4 cells were treated, in triplicate, with IPTG for 24 h and analyzed on a Becton-Dickson FACScan flow cytometer. Approximately, 64.4 +/- 0.4 % of the Hs578T-*p27S* cells treated with IPTG were in the G0/G1 state, compared to 57.2 +/- 1.9 % when untreated. As expected, the Hs578T-*neo* cells had essentially

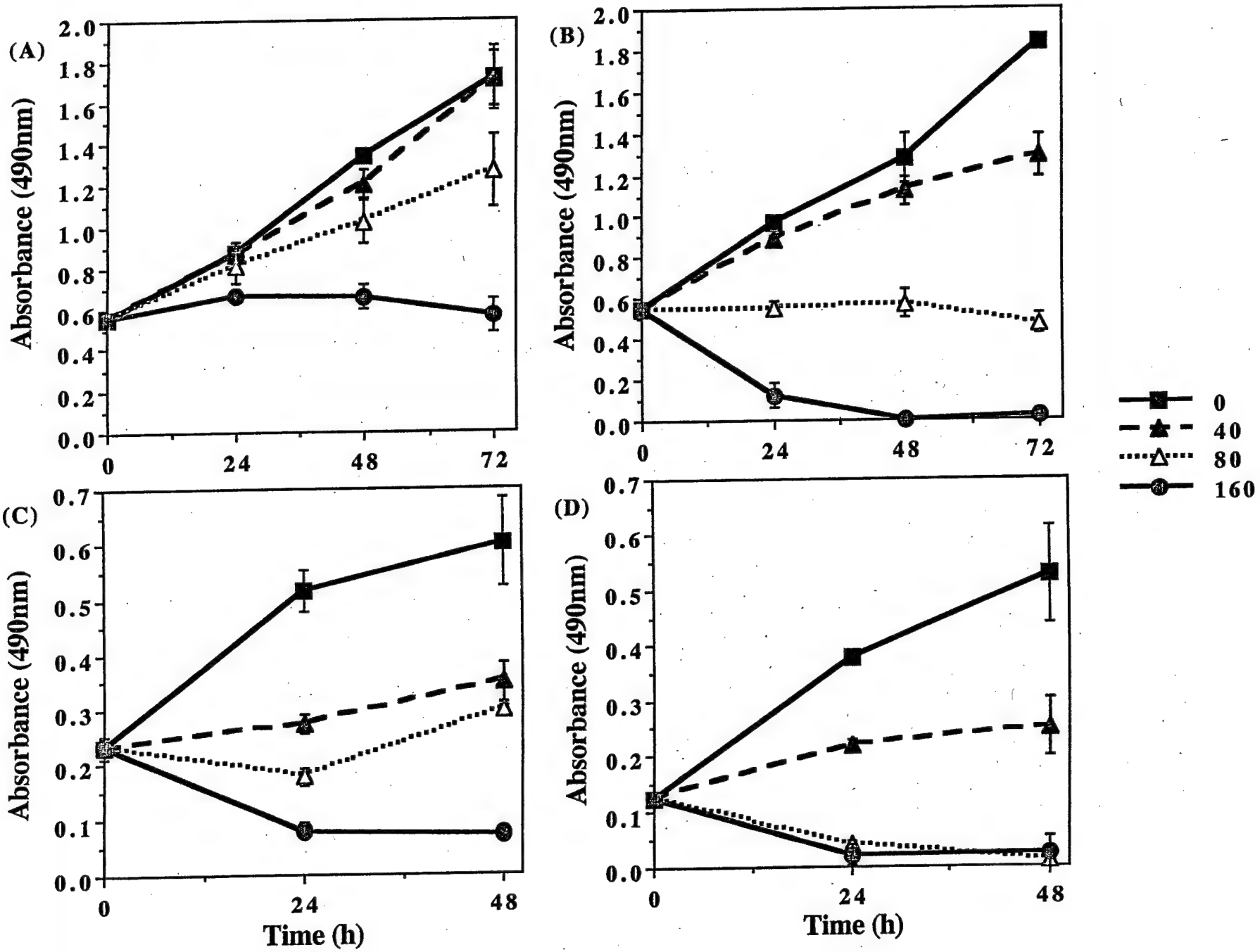
(A)
(B)
(C)
(D)
Absorbance (490nm)
Time (h)
0
24
48
72
0.0
0.2
0.4
0.6
0.8
1.0
1.2
1.4
1.6
1.8
2.0
0.1
0.3
0.5
0.7
0
40
80
160

Fig. 13

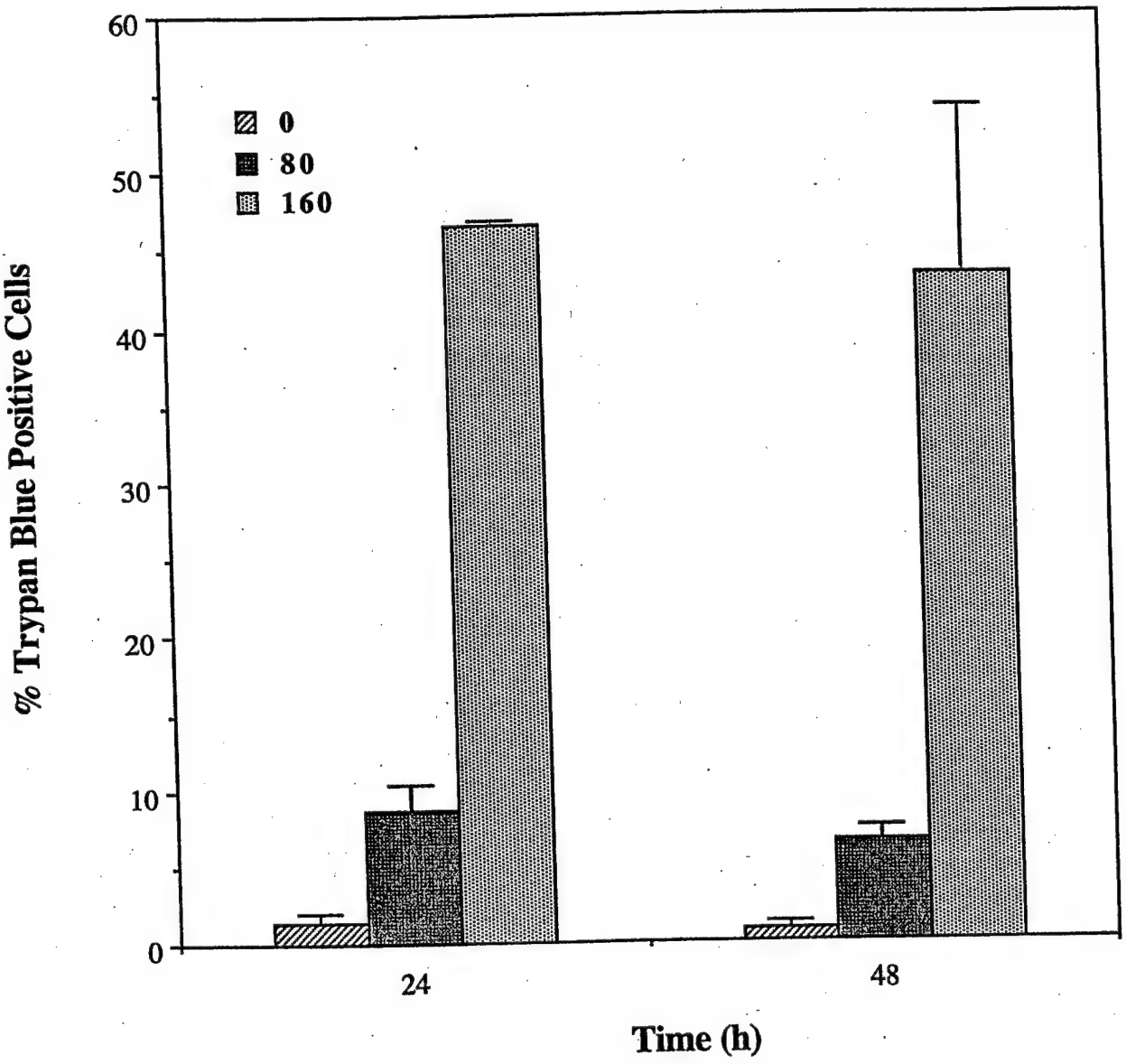
60
50
40
30
20
10
0
0
80
160
% Trypan Blue Positive Cells
24
48
Time (h)

Fig. 14

equivalent cell cycle distribution in the presence or absence of IPTG (56.0 +/- 1.1 vs 58.4 +/- 1.1). IPTG treatment of Hs578T-*p27S* #3 cells resulted in G0/G1 arrest of 82 +/- 0.5 %, compared to 62.5 +/- 1.9 % in untreated cells. Clone Hs578T-*p27S* #4 cells, which showed no induction of $p27^{Kip1}$ levels, displayed no significant difference in the cell cycle distribution with respect to IPTG treatment (60.6 +/- 1.0 vs 60.6 +/- 1.6). Taken together these results indicate the induction of the $p27^{Kip1}$ protein participate in the G0/G1 arrest of Hs578T breast cancer cells.

CONCLUSIONS: In summary, two components of green tea extracts, GTP and EGCG, which have been shown to have antioxidant properties, inhibit growth of multiple ER- breast cancer cell lines. Slower growth could be related in part to induction of $p27^{Kip}$ protein, which causes an arrest of cells at the G1/S phase transition. Furthermore, in work supported by a previous DOD grant (DAMD17-94-J-4468), we showed that green tea extracts given to S-D rats in their drinking fluid significantly decreased carcinogen-induced tumor burden and invasiveness and significantly increased latency to first tumor. These observations provide both *in vivo* and cell culture evidence in support of a role for green tea components in chemoprevention and, possibly, chemotherapy of breast cancer. A manuscript (Kavanagh et al., ref. 72) has been accepted in the Journal of Cellular Biochemistry on this work.

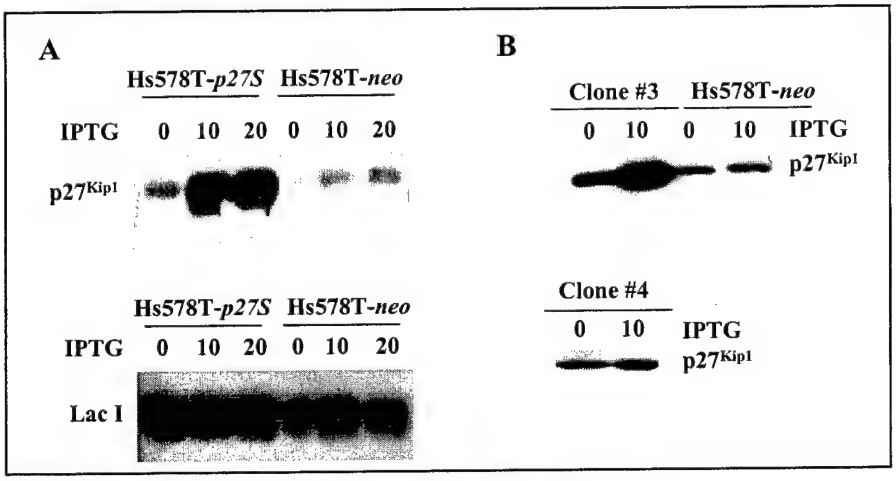

Fig. 16

Specific Aim 4: Use transgenic mice to test the contribution of constitutive NF-κB/Rel subunit expression in the development of breast neoplasias.

a) During the previous period, we completed the generation of the MMTV-c-Rel mouse lines. This includes the previously described preparation of the construct, microinjection of mice, and identification of founders via Southern blotting. The mouse mammary tumor virus long terminal repeat (MMTV-LTR) is a hormonally responsive regulatory element that can direct expression of genes to the mammary epithelium as well as to other epithelial tissues. It is activated by corticosteroids and progestins; thus exogenous genes expressed in transgenic mice using the MMTV-LTR as a promoter are upregulated in females with each cycle of pregnancy. Using timed pregnancies, the overexpression of c-Rel protein in transgenic mice was demonstrated as indicated in the previous report via immunoblotting of nuclear extracts obtained from female mice at 18.5

days of pregnancy. In the course of our analysis of expression, we obtained 8 mammary tumors in four lines of mice at an approximate age of 20.5 months. We are now in the process of breeding two of these lines to obtain 25 female mice to test for percentage of tumor formation. They will be maintained for a 2-year time period. These are being bred with male MMTV-CK2 mice to induce the transgene and to obtain c-Rel/CK2 bitransgenic mice for studies of the effects of overexpression of c-Rel and CK2 on mammary tumor formation. This work will be continued under the aegis of the recently awarded grant: NIH/NCI RO1 CA82742.

KEY RESEARCH ACCOMPLISHMENTS

- Demonstrated elevated basal levels of IKK and CK2 kinase activity in breast cancer cell lines and tumor specimens, and the involvement of these kinases in maintenance of aberrant expression of NF-κB.
- Demonstrated overexpression of Her-2/neu leads to induction of classical NF-κB via a PI3-kinase to Akt signaling pathway that can be inhibited by the tumor suppressor PTEN. This pathway leads to degradation of IκB-α via calpain.
- Showed a physical association of the aromatic hydrocarbon receptor/transcription factor (AhR) and the RelA subunit of NF-κB in breast epithelial cells.
- Demonstrated two components of great tea extracts, GTP and EGCG, inhibit growth of multiple ER negative breast cancer cell lines in culture and reduce carcinogen-induced mammary tumor burden in female Sprague-Dawley rats.
- Prepared and obtained tumors in MMTV-c-Rel transgenic mice. These animals will be used for *in vivo* study of the role of constitutive NF-κB expression in the etiology of breast cancer.

REPORTABLE OUTCOMES

Manuscripts:

1. Sovak, M.A., M. Arsura, G. Zanieski, K.T. Kavanagh, and G.E. Sonenshein, The inhibitory effects of transforming growth factor-β1 on breast cancer cell proliferation are mediated through regulation of aberrant NF-κB/Rel expression. Cell Growth Diff. 10: 537-544 (1999).

2. Kim, D.W., M.A. Sovak, G. Zanieski, G. Nonet, R. Romieu-Mourez, A.W. Lau, L.J. Hafer, P. Yaswen, M. Stampfer, A.E. Rogers, J. Russo, and G.E. Sonenshein. Activation of NF-κB/Rel occurs early during neoplastic transformation of mammary cells. Carcinogenesis 21: 871-879 (2000).

3. Kim, D.W., L. Gazourian, S.A. Quadri, R. Romieu-Mourez, D.H. Sherr, and G.E. Sonenshein. The RelA NF-κB subunit and the Aryl Hydrocarbon Receptor (AhR) cooperate to transactivate the c-*myc* promoter. Oncogene 9: 5498-5506 (2000).

4. Pianetti, S., M. Arsura, R. Romieu-Mourez, R.J. Coffey, and G.E. Sonenshein. Her-2/neu overexpression induces NF-κB via a PI3-kinase/Akt pathway without IKK activation that can be inhibited by the tumor suppressor PTEN. Oncogene (in press).

5. Kavanagh, K.T., L.J. Hafer, D.W. Kim, K.K. Mann, D.H. Sherr, A.E. Rogers, and G.E. Sonenshein. Green tea extracts decrease carcinogen-induced mammary tumor burden in rats and rate of breast cancer cell proliferation in culture. J. Cell Biochem. (manuscript accepted).

6. Romieu-Mourez, R., E. Landesman-Bollag, D.C. Seldin, A.M. Traish, F. Mercurio, and G.E. Sonenshein. Roles of IKK kinases and protein kinase CK2 in activation of NF-κB in breast cancer. Cancer Res. (manuscript accepted pending revision).

Abstracts/Posters:
Quadri SA., Kim DW, Gazourian L, Sonenshein GE and Sherr DH. (2000) The aryl hydrocarbon receptor/transcription factor (AhR) and the Rel A Nuclear Factor-κB subunit cooperate to transactivate the c-myc promoter. Toxicol. Sci, 54, 11.
Quadri, S.A., Trombino, A.F., Matikainen, T, Perez, G.I., Tilly, J.L., Kim, D.W., Sonenshein, G.E., Sherr, D.H. 2001. Cell growth, death, and NF-κB regulation by the aryl hydrocarbon receptor. Toxicol. Sci. In Press.
Romieu-Mourez, R., Kim, D.W., Sovak, M.A., Zanieski, G., Lau, A.W., Hafer, L.J., Rogers, A.E., Landesman-Bollag, E., Seldin, D.C., Russo, J., and Sonenshein, G.E., NF-κB/Rel activation in breast cancer occurs early and is mediated by aberrant kinase activity. Oncogene Meeting, 2000 DOD Breast Cancer meeting, June 8-11, 2000
Landesman-Bollag, E., R. Romieu-Mourez, G.E. Sonenshein, and D.C. Seldin. Protein Kinase CK2 in Mammary Gland Tumorigenesis. Keystone Meeting on Breast Cancer, March 2000
D.W. Kim, M.A. Sovak, G. Zanieski, G. Nonet, R. Romieu-Mourez, A.W. Lau, L. J. Hafer, P. Yaswen, M. Stampfer, A.E. Rogers, J. Russo, and G.E. Sonenshein. Activation of NF-κB/Rel Occurs Early During Neoplastic Transformation of Mammary Cell. Mammary Gland Gordon conference, June 6-11, 1999

Oral Presentations:
4/28/00: The roles of NF-κB in control of cell proliferation, survival and neoplastic transformation. Maine Medical Center Research Institute, South Portland ME.
5/5/00: The roles of NF-κB in control of cell proliferation, survival and neoplastic transformation. Eli Lilly, Indianapolis. IN
9/13/00: The roles of NF-κB in control of cell proliferation, survival and neoplastic transformation. University of Texas Health Science Center at San Antonio, San Antonio TX
10/30/00: The roles of NF-κB in control of cell proliferation, survival and neoplastic transformation. Biology Department, Boston University, Boston MA

Mouse lines:
Prepared MMTV-c-Rel transgenic mice for *in vivo* study of the role of NF-κB in the etiology of breast cancer

Degrees obtained:
Dong W. Kim, Ph.D. degree (returned to medical school to complete MD degree).

Funding received based on work supported by this award:
"Role of NF-κB/Rel in the Pathogenesis of Breast Cancer", G.E. Sonenshein (PI); NIH/NCI; RO1 CA82742, 9/1/99-6/30/04: Specific Aims: 1) Determine the functional role of constitutive NF-κB/Rel activity in breast cancer cells, using transgenic mice expressing a NF-κB subunit and IκB-α; 2) Evaluate the kinase activity in tumor cell lines in culture; 3) Determine the functional role of the c-*myc* oncogene as a target of NF-κB/Rel activation in development of breast neoplasias, including signals mediating growth, apoptosis and neoplastic transformation of cells; 4) Determine whether aberrant activation of NF-κB/Rel occurs prior to neoplastic transformation in human breast disease using immunohistochemistry of primary premalignant atypical hyperplasia.

Funding applied for based on work supported by this award (This grant application received a score of 18% and is likely to be funded.):

"Mechanisms of PAH-induced Mammary Tumorigenesis", David Sherr (PI) NIEHS; RO1 ES10435 Specific Aims: 1) Generate transgenic mice in which high level AhR expression is directed to mammary tissue and use these mice to determine the effects on mammary development and neoplasia; 2) Determine AhR function in transformed human breast cancer cell lines including the effects of AhR and p65 interaction.

Conclusions:

Here we have demonstrated that human breast cancer cell lines and primary human breast tumor specimens display elevated CK2, IKKβ and/or IKKα IκB kinase activities. Inhibition of any of these activities in the breast cancer cell lines resulted in reduced functional NF-κB/Rel. Overall, these activities correlate with, and are therefore likely responsible at least in part for, the aberrant NF-κB activation in human breast cancer. Furthermore, we have shown Her-2/neu that leads to the activation of NF-κB subunits p50, p65 and p52 in mammary tumor cells via a PI3-kinase to Akt signaling pathway. Previously, we demonstrated that primary breast cancer samples from patients are typified by aberrant activation of nuclear NF-κB. In particular, we observed the presence of nuclear p50, p65 and c-Rel protein in multiple breast cancer specimens. These results were extended to additional patients here. Overall, our work begins to elucidate the molecular mechanisms responsible for activation of the NF-κB in breast cancer patients.

Our studies show a physical and functional association of the AhR and the RelA subunit of NF-κB in transactivation of the c-*myc* gene in breast epithelial cells. Specifically, AhR and RelA were physically associated in malignant Hs578T breast cancer and non-malignant MCF-10F HMECs. AhR and RelA induced expression of the endogenous c-*myc* gene in MCF-10F cells. Using transfection analysis, AhR and RelA cooperated to transactivate the c-*myc* promoter in these two lines. As judged by transfection and mobility shift analyses, the RelA and AhR proteins formed a novel complex that binds to the wild type but not mutant NF-κB element of the c-*myc* gene. We postulate it is this complex, binding via the NF-κB element, that transactivates the c-*myc* promoter.

Two components of great tea extracts, GTP and EGCG, which have been shown to have antioxidant properties were shown to inhibit growth of multiple ER- breast cancer cell lines. Slower growth could be related in part to induction of $p27^{Kip}$ protein, which causes an arrest of cells at the G1/S phase transition. Furthermore, in work supported by a previous DOD grant (DAMD17-94-J-4468), we showed that green tea extracts given to S-D rats in their drinking fluid significantly decreased carcinogen-induced tumor burden and invasiveness and significantly increased latency to first tumor. These observations provide both *in vivo* and cell culture evidence in support of a role for green tea components in chemoprevention and, possibly, chemotherapy of breast cancer.

Lastly, we have prepared a mouse model to evaluate the functional role of NF-κB in mammary tumorigenesis. In this model, c-Rel subunit has been put under the control of the MMTV promoter to evaluate the effects of maintenance of expression of NF-κB activity. These mice have begun to bear mammary tumors.

REFERENCES:

1. Baeuerle, P.A. The inducible transcription activator NF-κB: regulation by distinct protein subunits. Biochem. Biophys. Acta 1072:63 (1991).
2. Baeuerle, P.A., and Baltimore, D. IκB: a specific inhibitor of the NF-κB transcription factor. Science 242:540 (1988).
3. Barroga, C.F., Stevenson, J.K., Schwarz, E.M. and Verma, I.M. Constitutive phosphorylation of IκBα by casein kinase II. Proc. Natl. Acad. Sci. USA 92:7637 (1995).
4. Biswas, D. K., Dexube, B. J., Ahlers, C., and Pardee, A. B. Pentoxifylline inhibits HIV-1 LTR-driven gene expression by blocking NF-κB action. J. Acq. Immun. Def. Syn. 6:778 (1993).
5. Blank, V., Kourilsky, P. and Israel, A. NF-κB and related proteins: Rel/dorsal homologies meet ankyrin-like repeats. TIBS 17:135 (1994).
6. Bours, V., Burd, P., Brown, K., Villalobos, J., Park, S., Ryseck, R.-P., Bravo, R., Kelly, K., and Siebenlist, U. A novel mitogen-inducible gene product related to p50/p105 NF-κB participates in transactivation through a κB site. Mol. Cell. Biol. 12:685 (1992).
7. Brown, K., Gerstberger, S., Carlson, L., Franzoso, G. and Siebenlist, U. 1995. Control of IκBα proteolysis by site-specific signal-induced phosphorylation. Science 267:1485.
8. Brown, K., Park, S., Kanno, T., Fransozo, G, and Siebenlist, U. Mutual regulation of the transcriptional activator NF-κB and its inhibitor IκB-α. Proc. Natl. Acad. Sci. U.S.A. 90: 2532 (1993).
9. Buening, M.K., Chang, R.L., Huang, M.-T ., Fortner, J.G., Wood, A.W., Conney, A.H. Activation and inhibition of benzo(a)pyrene and aflatoxin B_1 metabolism in human liver microsomes by naturally occuring flavonoids. Canc. Res. 41:67 (1981).
10. Burbach, K.M., Poland, A., Bradfield, C.A. Cloning of the Ah-receptor cDNA reveals a distinctive ligand-activated transcription factor. Proc. Natl. Acad.Sci. USA 89:8185 (1992).
11. Campisi, J., Gray, H., Pardee, A.B., Dean, M., and Sonenshein, G.E. Cell cycle control of c-*myc* but not c-*ras* expression is lost following chemical transformation. Cell. 36:241 (1984).
12. Cardiff, R. D. The biology of mammary transgenes: five rules. J. Mammary Gland Biology and Neoplasia. 1:61 (1996).
13. DiAugustine, R., and Davis, D.L. A holistic approach to breast cancer. Environ. Health Perspect. 101:116 (1993).
14. Dignam, J., Lebovitz, R., and Roeder, R.G. Accurate transcription initiation by RNA polymerase II in a soluble extract from isolated mammalian nuclei. Nucleic Acids Res. 11:1475 (1983).
15. Dobrzanski, P., Ryseck, R.-P., and Bravo, R. Both N- and C-terminal domains of RelB are required for full transactivation: role of the N-terminal leucine zipper-like motif. Mol. Cell. Biol. 13:1572 (1993).
16. Duyao, M.P., Buckler, A.J., and Sonenshein, G.E. Interaction of an NF-κB-like factor with a site upstream of the c-*myc* promoter. Proc. Natl. Acad. Sci. USA 87:4727 (1990).
17. Duyao, M.P., Kessler, D.J., Spicer, D., Bartholomew, C., Cleveland, J., Siekevitz, M., and Sonenshein, G.E. Transactivation of the c-*myc* promoter by HTLV-1 *tax* is mediated by NFκB. J. Biol. Chem. 267:16288 (1992).
18. Ema, M., Sogawa, K., Watanabe, N., Chujoh, Y., Matsushita, N., Gotoh, O., Funae,Y., and Fujii-Kuriyama,Y. cDNA cloning and structure of mouse putative Ah receptor. Biochem. Biophys. Res. Comm. 184:246 (1992).

19. Escot, C., Theillet, C., Lidereau, R., Spyratos, F., Champeme, M-H., Gest, J., and Callahan, R. Genetic alteration of the c-*myc* protooncogene (*MYC*) in human primary breast carcinomas. Proc. Natl. Acad. Sci. USA 83:4834 (1986).
20. Falk, Jr. F., Ricci, Jr., Wolff, M.S., Godbold, J. and Deckers, P. Pesticides and polychlorinated biphenyl residues in human breast lipids and their relation to breast cancer. Arch. Env. Health 47:143 (1992).
21. Ghosh, S., Gifford, A., Riviere, L., Tempst, P., Nolan, G., and Baltimore, D. Cloning of the p50 DNA binding subunit of NF-κB: homology to *rel* and *dorsal*. Cell 62:1019 (1990).
22. Grilli, M., Chiu, J. and Lenardo, M. NF-κB and Rel: Participants in a multiform transcriptional regulatory system. Int. Rev. of Cytol. 143:1 (1993).
23. Harris, J.R., Lippman, M.E., Veronesi, U., Wellett, W. Breast Cancer. N. Eng. J. Med 327:319 (1992).
24. Henkel, T., Machleidt, T., Alkalay, I., Kronke, M., Ben-Neriah, Y., and Baeuerle, P. Rapid proteolysis of IκB-α is necessary for activation of transcription factor NF-κB. Nature (London) 365:182 (1993).
25. Ji, L., Arcinas, M., and Boxer, L.M. NF-κB sites function as positive regulators of expression of the translocated c-*myc* allele in Burkitt's lymphoma. Mol. Cell. Biol. 14:7967 (1994).
26. Kaltschmidt, C., Kaltschmidt, B., Neumann, H., Wekerle, H., Baeuerle, P. Constitutive NF-κB activity in neurons. Mol. Cell. Bio. 12:3981 (1994).
27. Kessler, D.J., Duyao, M.P., Spicer, D.B., and Sonenshein, G.E. NF-κB-like factors mediate interleukin 1 induction of c-*myc* gene transcription in fibroblasts. J. Exp. Med. 176: 787 (1992).
28. Kessler, D.J., Spicer, D.B., La Rosa, F.A., and Sonenshein, G.E. A novel NF-κB element within exon 1 of the murine c-*myc* gene. Oncogene 7:2447 (1992).
29. Kieran, M., Blank, V., Logeat, F., Vandekerckhove, J., Lottspeich, F., LeBail, O., Urban, M., Kourilsky, P., Baeuerle, P., and Israel, A. The DNA binding subunit of NF-κB is identical to factor KBF-1 and homologous to the *rel* oncogene product. Cell 62:1007 (1990).
30. Kreipe, J., Feist, J., Fischer, L., Felgner, J., Heidorn, K., Mettler, L., and Parwaresch, R. Amplification of c-*myc* but not of c-*erb*B-2 is associated with high proliferative capacity of breast cancer. Cancer Research 53:1956 (1993).
31. La Rosa, F.A., Pierce, J., and Sonenshein, G.E. Differential regulation of the c-*myc* oncogene promoter by the NF-κB Rel family of transcription factors. Mol. Cell. Biol. 14: 1039 (1994).
32. Le Bon, A.M., Siess, M.H., and Suschetet, M. Inhibition of microsome-mediated binding of benzo(a)pyrene to DNA by flavonoids either in vitro or after dietary administration to rats. Chemico-Biol. Interact. 83:65 (1992).
33. Lee, H., Arsura, M., Wu, M., Duyao, M., Buckler, A.J., and Sonenshein, G.E. Role of Rel-related factors in control of c-*myc* gene transciption in receptor-mediated apoptosis of the murine B cell WEHI 231 line. J. Exp. Med. 181:1169 (1995).
34. Lin, R., Beauparlant, P., Makris, C., Meloche, S. and Hiscott, J. Phosphorylation of IκBα in the C-terminal PEST domain by casein kinase II affects intrinsic protein stability. Mol. Cell. Biol. 16:1401 (1996).
35. McDonell, P., Kumar, S., Rabson, A., and Gelinas, C. Transcriptional activity of *rel* family proteins. Oncogene 7:163 (1992).
36. Mercurio, F., H. Zhu, B. W. Murray, A. Shevchenko, B. L. Bennett, J. Li, D. B. Young, M. Barbosa, M. Mann, A. Manning and Rao, A. IKK-1 and IKK-2: Cytokine-Activated IκB Kinases Essential for NF-κB Activation. Science 278:860 (1999).
37. Morris, J.J., and Seifter, E. The role of aromatic hydrocarbons in the genesis of breast cancer. Med. Hypothesis 38:177 (1992).

38. Muller, W. J., Sinn, E., Pattengale, P., Wallace, R., and Leder, P. Single-step induction of mammary adenocarcinoma in transgenic mice bearing the activated c-neu oncogene. Cell. 54:105 (1988).
39. Nebert, D.W. and Gonzalez, F.J. P450 genes: Structure, evolution and regulation. Ann. Rev. Biochem. 56:945 (1987).
40. Nebert, D.W., Patersen, D.D., and Fornace, A.J., Jr. Cellular responses to oxidative stress: The [Ah] gene battery as a paradigm. Env. Health Perspectives 88:13 (1990).
41. Neri, A., Chang, C.-C., Lombardi, L., Salina, M., Corradini, P., Mailo, A., Chaganti, R., and Dalla-Favera, R. B cell lymphoma-associated chromosomal translocation involves candidate oncogene *lyt*-10, homologous to NF-κB p50. Cell 67:1075 (1991).
42. Ozes, O.N., Mayo, L.D., Gustin, J.A., Pfeffer, S.R., Pfeffer, L.M., and Donner, D.B. NF-kappaB activation by tumour necrosis factor requires the Akt serine-threonine kinase. Nature 401:82 (1999).
43. Rice, N., and Ernst, M. In vivo control of NF-κB activation by IκB. EMBO J. 12:4685 (1993).
44. Roux-Dosseto, M., Romain, S., Dussault, N., Desideri, C., Piana, L., Bonnier, P., Tubiana, N., and Martin, P.M. C-*myc* gene amplification in selected node-negative breast cancer patients correlates with high rate of early relapse. Eur. J. Cancer 28A:1600 (1992).
45. Ruben, S., Dillon, P., Schreck, R., Henkel, T., Chen, C.-H., Maher, M., and Rosen, C. Isolation of a *rel*-related human cDNA that potentially encodes the 65 kD subunit of NF-κB. Science 251:490 (1991).
46. Ryseck, R.-P., Bull, P., Takamiya, M., Bours, V., Siebenlist, U., Dobrzanski, P., and Bravo, R. RelB, a new rel family transcription activator that can interact with p50-NF-κB. Mol. Cell. Biol. 12:674 (1992).
47. Safe, S. Polychlorinated biphenyls (PCBs) and polybrominated biphenyls (PBBs): biochemistry, toxicology, and mechansism of action. Crit. Rev. Toxicol. 13:319 (1984).
48. Schmitz, M.L., and Baeuerle, P. The p65 subunit is responsible for the strong transcription activating potential of NF-κB. EMBO J. 10:3805 (1991).
49. Schreck, R., Rieber, P., and Baeuerle, P.A. Reactive oxygen intermediates as apparently widely used messengers in the activation of the NF-κB transcription factor and HIV-1. EMBO J. 10:2247 (1991).
50. Seldin, D.C., and Leder, P. Casein kinase IIα transgene-induced murine lymphoma: relation to theileriosis in cattle. Science 267:894 (1995).
51. Seldin, D.C., Landesman, E., Harrington, A., Cardiff, R.D., and Leder, P. Casein kinase IIa accelerates myc-induced mammary carcinogenesis. Keystone Symposium on Breast and Prostate Cancer, 1996 (abstract).
52. Sen, R., and Baltimore, D. Multiple nuclear factors interact with the immunoglobulin enhancer sequences. Cell 46:705 (1986).
53. Sovak, M.A., Bellas, R.E., Kim, D.W., Zanieski, G.J., Rogers, A.E., Traish, A.M., and Sonenshein, G.E. Aberrant nuclear factor-kappaB/Rel expression and the pathogenesis of breast cancer. J. Clin. Invest. 100:2952 (1997).
54. Sovak MA, Arsura M, Zanieski G, Kavanagh KT, Sonenshein GE. The inhibitory effects of transforming growth factor beta1 on breast cancer cell proliferation are mediated through regulation of aberrant nuclear factor-kappaB/Rel expression. Cell Growth Diff. 10:537 (1999).
55. Steward, R. Dorsal, an embrionic polarity gene in Drosophila is homologous to the vertebrate proto-oncogene c-*rel*. Science. 238:692 (1987).
56. Tan, T.-H., Huang, G., Sica, A., Ghosh, P., Young, H., Longo, D., and Rice, N. κB site-dependent activation of the interleukin-2 receptor-chain gene promoter by human c-Rel. Mol. Cell. Biol. 12:4067 (1992).

57. Tian, Y., Ke, S., Denison, M.S., Rabson, A.B., and Gallo, M.A. Ah receptor and NF-kappaB interactions, a potential mechanism for dioxin toxicity.J. Biol. Chem. 274: 510 (1999).
58. Urban, M.B., Schreck, R., and Baeuerle, P. NF-κB contacts DNA by a heterodimer of the p50 and p65 subunit. EMBO J. 10:1817 (1991).
59. Wolff, M.S., Toniolo, P.G., Lee, E.W., Rivera, M., and Dubin, N. Blood levels of organochlorine residues and risk of breast cancer. J. Natl. Cancer Inst. 85:648 (1993).
60. Wu, M., Lee, H., Bellas, R.E., Schauer, S.L., Arsura, M., Katz, D., FitzGerald, M., Rothstein, T.L., Sherr, D.H., and Sonenshein, G.E. Inhibition of NF-κB/Rel induces apoptosis of murine B cells. EMBO J. 15: (in press).
61. Yao, Y., Hoffer, A., Chang, C.-Y., and Puga, A. Dioxan activates human immunodeficiency virus type 1 gene expression by an oxidative stress pathway that requires a functional cytochrome P450 CYP1A1 gene. The Toxicologist 15:64 (1995).
62. Sinn, E., Muller, W., Pattengale, P., Tepler, I., Wallace, R., and Leder, P. Coexpression of MMTV/v-Ha-ras and MMTV/c-myc genes in transgenic mice: synergistic action of oncogenes in vivo. Cell. 49:465 (1987).
63. Calaf, G. and Russo, J. Transformation of human breast epithelial cells by chemical carcinogens, Carcinogenesis. 14: 483 (1993).
64. Zandi, E., Rothwart, D.M., Delhase, M., Hayakawa, M. and Karin, M. The IκB kinase complex (IKK) contains two kinase subunits, IKKα and IKKβ, necessary for IκB phosphorylation and NF-κB activation. Cell 91:243 (1997).
65. Kim, D.W., M.A. Sovak, G. Zanieski, G. Nonet, R. Romieu-Mourez, A.W. Lau, L.J. Hafer, P. Yaswen, M. Stampfer, A.E. Rogers, J. Russo, and G.E. Sonenshein. Activation of NF-κB/Rel occurs early during neoplastic transformation of mammary cells. Carcinogenesis 21:871 (2000).
66. Trombino, A.F., R.I. Near, R.A. Matulka, S. Yang, L.J. Hafer, P.A. Toselli, D.W. Kim, A.E. Rogers, G.E. Sonenshein, and D. H. Sherr. Expression of the Aryl Hydrocarbon Receptor/Transcription Factor (AhR) and the AhR-regulated *CYP1* gene transcripts in a rat model of mammary tumorigenesis. Breast Cancer Res. and Treatment 63:117 (2000).
67. Kim, D.W., L. Gazourian, S.A. Quadri, R. Romieu-Mourez, D.H. Sherr, and G.E. Sonenshein. The RelA NF-κB subunit and the Aryl Hydrocarbon Receptor (AhR) cooperate to transactivate the c-*myc* promoter. Oncogene 9:5498 (2000).
68. Lawrence, R., L.-J. Chang, U. Siebenlist, P. Bressler and G.E. Sonenshein. Vascular smooth muscle cells express a constitutive NF-κB-like activity. J. Biol. Chem. 269:28913 (1994).
69. Ford, H.L., E. Landesman-Bollag, C.S., Dacwag, P.T. Stukenberg, A.B. Pardee, and D.C. Seldin. Cell cycle-regulated phosphorylation of the human SIX1 homeodomain protein. J. Biol. Chem. 275: 22245 (2000).
70. Battistutta, R., S. Sarno, E. De Molliner, E. Papinutto, G. Zanotti, and L.A. Pinna. The replacement of ATP by the competitive inhibitor emodin induces conformational modifications in the catalytic site of the protein kinase CK2. J. Biol. Chem. 275: 29618 (2000).
71. Cogswell, P., D.C. Guttridge, W.K. Funkhouser, and A.S. Baldwin Jr. Selective activation of NF-κB subunits in human breast cancer. Oncogene 19: 1123 (2000).
72. Kavanagh, K.T., L.J. Hafer, D.W. Kim, K.K. Mann, D.H. Sherr, A.E. Rogers, and G.E. Sonenshein. Green tea extracts decrease carcinogen-induced mammary tumor burden in rats and rate of breast cancer cell proliferation in culture. J. Cell Biochem. (manuscript accepted).
73. Pianetti, S., M. Arsura, R. Romieu-Mourez, R.J. Coffey, and G.E. Sonenshein. Her-2/neu overexpression induces NF-κB via a PI3-kinase/Akt pathway without IKK activation that can be inhibited by the tumor suppressor PTEN. Oncogene (in press).

Carcinogenesis vol.21 no.5 pp.871–879, 2000

Activation of NF-κB/Rel occurs early during neoplastic transformation of mammary cells

Dong W.Kim[1,3], Mika A.Sovak[2,3], Gregory Zanieski[1,3], Genevieve Nonet[4], Raphaëlle Romieu-Mourez[1,3], Alan W.Lau[1,3], Laurie J.Hafer[2,3], Paul Yaswen[4], Martha Stampfer[4], Adrianne E.Rogers[2,3], Jose Russo[5] and Gail E.Sonenshein[1,3,6]

[1]Department of Biochemistry, [2]Department of Pathology and Laboratory Medicine and [3]Program in Research on Women's Health, Boston University Medical School, 715 Albany Street, Boston, MA 02118, [4]Lawrence Berkeley National Laboratory, Berkeley, CA 94720 and [5]Breast Cancer Research Laboratory, Fox Chase Cancer Center, Philadelphia, PA 19111, USA

[6]To whom correspondence should be addressed
Email: gsonensh@bu.edu

NF-κB/Rel is a family of transcription factors which are expressed in all cells; however, in most non-B cells, they are sequestered in the cytoplasm in inactive complexes with specific inhibitory proteins, termed IκBs. We have recently shown that NF-κB/Rel factors are aberrantly activated in human breast cancer and rodent mammary tumors, and function to promote tumor cell survival and proliferation. Here, we have examined the time-course of induction of NF-κB/Rel factors upon carcinogen treatment of female Sprague–Dawley (S–D) rats *in vivo* and in human mammary epithelial cells (HMECs) in culture. We observed that NF-κB/Rel activation is an early event, occurring prior to malignant transformation. In S–D rats, increased NF-κB/Rel binding was detected in nuclear extracts of mammary glands from 40% of animals 3 weeks post-treatment with 15 mg/kg 7,12-dimethylbenz[*a*]anthracene (DMBA); this is prior to formation of tumors which normally begin to be detected after 7–9 weeks. In non-tumorigenic MCF-10F cells, *in vitro* malignant transformation upon treatment with either DMBA or benzo[*a*]pyrene (B[*a*]P) resulted in a 4- to 12-fold increase in activity of classical NF-κB (p65/p50). NF-κB induction was corrrelated with a decrease in the stability of the NF-κB-specific inhibitory protein IκB-α. Ectopic expression of the transactivating p65 subunit of NF-κB in MCF-10F cells induced the c-*myc* oncogene promoter, which is driven by two NF-κB elements, and endogenous c-Myc levels. Furthermore, reduction mammoplasty-derived HMECs, immortalized following B[*a*]P exposure, showed dysregulated induction of classical NF-κB prior to malignant transformation. Together these findings suggest that activation of NF-κB plays an early, critical role in the carcinogen-driven transformation of mammary glands.

Introduction

NF-κB/Rel is a family of dimeric transcription factors distinguished by the presence of a Rel homology domain of about 300 amino acids in length which determines much of its function. Classical NF-κB is a heterodimer composed of p65 and p50 subunits (1). Other members of the mammalian Rel family include c-Rel, p52 (also called lyt10) and RelB. The p65 and RelB, and c-Rel subunits, have either potent or moderate transactivation potential, respectively, whereas the p50 and p52 subunits bind avidly, but have only modest transactivation abilities (1). In most cells, other than B lymphocytes, NF-κB/Rel proteins are sequestered in the cytoplasm, bound to one of the specific inhibitory proteins, termed IκBs, of which IκB-α is the paradigm. A variety of agents can induce NF-κB/Rel (2). Activation of NF-κB involves phosphorylation, followed by ubiquitination and proteosome-mediated degradation of IκB, which allows for translocation of active NF-κB complex into the nucleus where it can bind to κB responsive elements (2).

NF-κB/Rel has now been established as a factor promoting survival from apoptosis (3). An anti-apoptotic function for constitutively expressed NF-κB/Rel factors has been demonstrated in several cell types, including B lymphocytes (4,5) and hepatocytes (6,7). Several groups also found that induction of NF-κB/Rel upon treatment with tumor necrosis factor α (TNF-α), radiation and chemotherapeutic agents can protect cells from apoptosis (8–11). More recently, we showed that aberrant activation of NF-κB/Rel occurs in human breast cancer cells and that specific inhibition of this activity leads to the induction of apoptosis (12). There is also increasing evidence that the NF-κB/Rel family is important in control of cell proliferation and oncogenesis, e.g. correlation of factor activation has been reported in various types of cancer (13).

It has been suggested that some of the rise in breast cancer rates reflects increased exposure to and bioaccumulation of lipophilic environmental pollutants such as polycyclic aromatic hydrocarbons (PAHs), like benzo[*a*]pyrene (B[*a*]P), and related organochlorines (14). This hypothesis has been drawn, in part, from epidemiologic studies associating elevated breast cancer rates with PAH exposure (15–18) and from studies demonstrating increased levels of aromatic hydrocarbons in breast carcinomas (19,20), and in sera from breast cancer patients (18). Furthermore, many studies have shown that PAHs can cause malignant transformation of rodent models *in vivo* (21) and human mammary epithelial cells (HMECs) *in vitro* (22). For example, in Sprague–Dawley (S–D) rats, a single intragastric dose of DMBA induces mammary tumors within 7–20 weeks (21). While much has been learned about the effects of carcinogen treatment on gene activation and DNA adduct formation (23), the exact molecular mechanism(s) by which this transformation occurs has yet to be elucidated. Recently, we observed that NF-κB/Rel factors are aberrantly activated in 86% of the mammary tumors induced by DMBA-treatment of S–D rats compared with the normal mammary glands of the age-matched, vehicle-treated control animals (12). Here, we have examined the time course of carcinogen-mediated induction of NF-κB/Rel using the S–D rat model and the

Abbreviations: B[*a*]P, benzo[*a*]pyrene; CAT, chloramphenicol acetyltransferase; DMBA, 7,12-dimethylbenz[*a*]anthracene; EMSA, electrophoretic mobility shift analysis; HMECs, human mammary epithelial cells; PAHs, polycyclic aromatic hydrocarbons; S–D, Sprague–Dawley.

in vitro treated HMECs. We show that NF-κB/Rel activation occurs prior to malignant transformation, suggesting it plays an early and potentially important role in the progression of breast epithelial cells towards a malignant phenotype.

Materials and methods

Cell growth and treatment conditions

Hs578T tumor cell line was derived from a carcinosarcoma and is epithelial in origin (24). MCF-10F (HMECs) were established from a patient with fibrocystic disease and do not display characteristics of a malignant phenotype (22). These cells represent a non-tumorigenic, immortally transformed cell line. The D3-1 and BP-1 lines were derived by DMBA- and B[*a*]P-mediated transformation of MCF-10F cells, respectively (22), and were cultured as published previously (22). 184 HMEC strain, derived from reduction mammoplasty tissue, and the 184A1 cell line, which emerged from 184 HMECs after exposure to B[*a*]P, were cultured as described (25). These HMECs were arrested in G_0 by exposure for 48 h to medium lacking EGF and containing the anti-EGF receptor antibody, Mab 225, as described previously (26). For IκB-α protein turnover assays, exponentially growing cells were treated with 20 μg/ml emetine (Sigma Chemical Co., St Louis, MO) and cytoplasmic extracts (50 μg/sample) subjected to immunoblot analysis with the IκB-α antibody (sc# 371; Santa Cruz Biotechnology, Santa Cruz, CA), essentially as described previously (12).

Electrophoretic mobility shift analysis (EMSA)

Nuclear extracts were prepared from breast cancer cells essentially as described previously (12). Briefly, cells were washed twice with ice-cold PBS (Ca^{2+} and Mg^{2+} free) containing protease inhibitors [0.5 mM dithiothreitol (DTT), 0.5 mM phenylmethylsulfonyl fluoride (PMSF) and 10 μg/ml leupeptin (LP)]. They were then resuspended in 1 ml of cold hypotonic RSB buffer (10 mM NaCl, 3 mM $MgCl_2$, 10 mM Tris pH 7.4) containing 0.5% NP-40 detergent plus protease inhibitors as above. Following a 15 min incubation on ice, the cells were dounce homogenized until cell lysis occurred. Nuclei were resuspended in two packed nuclear volumes of extraction buffer C (420 mM KCl, 20 mM HEPES pH 7.9, 1.5 mM $MgCl_2$, 0.2 mM EDTA, 20% glycerol) plus protease inhibitors as above, and incubated on ice for 30 min. Protein concentration was determined using the Bio-Rad protein assay, following the manufacturer's directions (Bio-Rad Laboratories, Hercules, CA). The sequence of the NF-κB-containing oligonucleotide from the c-*myc* gene (27) is as follows: 5′-GATCCAAGTCCGGGTTTTCCCCAACC-3′, where the underlined region indicates the core binding element. The sequences of the PU.1- and TCF-1-containing oligonucleotides are as follows, PU.1: 5′-GATCTACTTCTGCTTTTG-3′; TCF-1: 5′-GGGAGACTGAGAACAAAGC-GCTCTCACAC-3′ (28). For labeling of the double-stranded oligonucleotide, which has 5′ overhangs allowing fill-in with DNA polymerase I, a 150–300 ng sample was incubated for 30 min at 37°C in a solution adjusted to a final concentration of 50 mM Tris–HCl pH 7.6, 5 mM $MgCl_2$, 10 mM β-mercaptoethanol, 20 μM each of dATP and dTTP, 50 μCi each of [^{32}P]dCTP and [^{32}P]dGTP, and 5 U of Klenow fragment of DNA polymerase I (New England Biolabs, Beverly, MA). For the binding reaction, ^{32}P-labeled oligonucleotide (20 000–25 000 c.p.m.) was incubated with 5 μg of nuclear extract, 5 μl sample buffer (10 mM HEPES, 4 mM DTT, 0.5% Triton X-100 and 2.5% glycerol), 2.5 μg poly(dI–dC) as non-specific competitor, and the salt concentration adjusted to 100 mM using buffer C. The reaction was carried out at room temperature for 30 min. DNA–protein complexes were subjected to electrophoresis at 11 V/cm and resolved on a 4.5% polyacrylamide gel (using 30% acrylamide/0.8% bisacrylamide) with 0.5× TBE running buffer (90 mM Tris, 90 mM boric acid, 2 mM EDTA pH 8.0). Supershift analyses were performed by incubating with the appropriate antibodies for an additional 1 h after the binding reaction had taken place. For supershift/blocking analysis, either of two antibodies against the p50 subunit were used; these were either kindly provided by K.LeClair (Procept Inc., Cambridge, MA) or purchased (sc-114; Santa Cruz Biotechnology). Antibodies against the p65 and c-Rel subunits were sc-109 and sc-372 (Santa Cruz Biotechnology) and #1226, kindly provided by N.Rice (NCI, Frederick, MD) and sc-070 (Santa Cruz Biotechnology), respectively.

Transfection and transactivation analysis

Wild-type (E8) and mutant (mutE8) NF-κB element–thymidine kinase (TK) promoter–chloramphenicol acetyltransferase (CAT) reporter vectors were constructed as reported previously (27). Briefly, these consisted of two copies of either the wild-type NF-κB element from upstream of the c-*myc* promoter, sequence given above, or versions with the two internal G residues converted to C residues, which significantly reduces NF-κB binding and transactivation (27). Each cell type displayed very large differences in transfection efficiency, and thus optimization of the specific transfection protocol was performed for each individual line. D3-1 cells were transfected by a modified calcium phosphate protocol, as described previously (12). MCF-10F and BP-1 cells were transfected using Lipofectamine reagent (Gibco BRL, Gaithersburg, MD). Cultures of 184 and 184 A1 cells were transfected using Cytofectin (Glen Research, Sterling, VA). All cells were harvested using reporter lysis buffer (Promega, Madison, WI) and CAT assays and luciferase assays were performed as published previously (12). Alternatively, confluent cultures of MCF-10F cells were transiently transfected with the p1.6 Bgl c-*myc* promoter CAT, containing 1.2 kb of upstream and 0.4 kb exon 1 sequences, including the two NF-κB elements (29), using FUGENE transfection reagent (Boehringer Mannheim, Indianapolis, IN), according to the manufacturer's instructions. Vector pEVRF-p65, encoding murine p65 protein (kindly provided by R.Sen, Brandeis University, Waltham, MA), was co-transfected, as indicated. Total DNA transfected was maintained at 4–5 μg. Cells were harvested after 24 h and extracts normalized for protein assayed, as above.

Transfection and immunoblot analysis

Cultures of MCF-10F cells, at 70% confluence, were transiently transfected with 4 μg pEVRF-p65 plus 20 μg pcDNA3 plasmid or with 24 μg pcDNA3 plasmid DNA with 30 μl FUGENE transfection reagent. After 48 h, cells were rinsed with cold PBS, and harvested in lysis buffer (50 mM Tris–HCl pH 8.0, 5 mM EDTA pH 8.0, 150 mM NaCl, 0.5 mM DTT, 2 μg/ml aprotinin, 2 μg/ml leupeptin, 0.5 mM PMSF, 0.5% NP-40). Whole-cell extracts (WCEs) were obtained by sonication, followed by centrifugation at 14 000 r.p.m. for 30 min. Samples (40 μg) of WCEs were subjected to electrophoresis and immunoblot analysis, as above. Blots were probed with rabbit anti-c-Myc antibody (786-4, a gift from S.Hann, Vanderbilt University, Memphis, TN), and mouse anti-β-actin monoclonal antibody (AC-15; Sigma).

Carcinogen treatment of rats

Virgin female S–D rats, fed AIN-76A diet, were handled according to a protocol approved by the Boston University Institutional Animal Care and Use Committee. For analysis of mammary glands from normal animals, five virgin female S–D rats (Charles River Laboratories, Wilmington, MA), 6 weeks of age, were housed in the AAALAC-approved Laboratory Animal Science Center and fed AIN76 diet for 3 weeks. They were killed with CO_2; all 12 mammary glands were combined for each animal, and nuclear extracts prepared as described previously (12). For the time-course analysis, S–D rats from the same supplier were housed in environmentally controlled animal quarters in the Mallory Institute of Pathology, fed AIN-76A diet, and randomly entered into control or DMBA-treated groups of either four or five animals. At 8 weeks of age they were given either a single intragastric dose of 15 mg/kg DMBA dissolved in sesame oil or given the sesame oil vehicle alone. Rats were predesignated to be killed and necropsied at 6 or 24 h, or 1, 3 or 9 weeks after DMBA or oil administration. Rats were palpated weekly for tumor. At necropsy of each control and DMBA-treated rat, all 12 mammary glands were rapidly removed, combined and frozen in liquid nitrogen for storage. At 9 weeks, two rats were found to have non-palpable tumors in one gland each. These tumors were excluded from the mammary gland samples taken for the time-course study. Nuclear extracts were prepared, as described previously (12), and subjected to EMSA.

Results

Activation of NF-κB/Rel occurs prior to tumor formation in mammary glands of rats treated with DMBA

Recently, we have demonstrated that 86% of the mammary tumors induced by DMBA-treatment of S–D rats displayed aberrant activation of NF-κB/Rel compared with the normal mammary glands of the age-matched, vehicle-treated control animals (12). To determine the nature of the NF-κB binding activity in the normal mammary gland, EMSA was performed on nuclear proteins isolated from the mammary glands of five virgin female 9 week old S–D rats and a radiolabelled NF-κB-containing oligonucleotide, as probe (Figure 1A). A major band (band 1) was seen (Figure 1A), which was better resolved on a light exposure (Figure 1B); many extracts also displayed a minor, slower migrating complex (band 2) seen on a longer exposure (Figure 1A and data not shown). To identify the nature of the subunits within these complexes, antibody supershift/blocking EMSA was performed. Addition of a supershifting antibody against the p50 subunit of NF-κB yielded a new

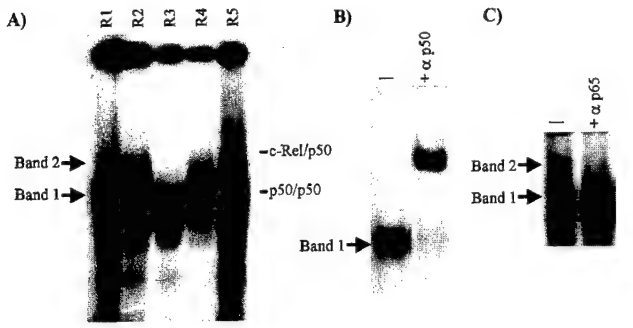

Fig. 1. Nuclear extracts of normal mammary glands of female S–D rats express low levels of NF-κB complexes. (**A**) EMSA was performed using samples (3 μg) of nuclear extracts from mammary glands of five S–D female rats (R1–R5), and an NF-κB oligonucleotide, as probe. Film was exposed for 7 days. The position of the major (band 1) and minor (band 2) complexes are indicated. The positions of the p50 homodimer and p50/c-Rel complexes formed with nuclear extracts of murine WEHI 231 B cells, isolated as described previously (4) and similarly analyzed on the gel, are indicated. (**B**) Samples of Rat 4 nuclear extract (3 μg) were incubated in the absence (–) or presence of 1 μl p50 antibody (sc-114) (α p50) for 60 min and subjected to EMSA using an NF-κB oligonucleotide, as probe. Film was exposed for 6 h. (**C**) Samples of Rat 4 nuclear extract (3 μg) were incubated in the absence (–) or presence of 1 μl p65 antibody sc-372 (α p65) for 60 min and then subjected to EMSA using an NF-κB oligonucleotide, as probe. Film was exposed for 5 days.

band and dramatically reduced formation of the band 1 complex (Figure 1B). Addition of a blocking antibody against p65 ablated formation of band 2 (Figure 1C). Addition of an antibody against c-Rel had no effect on binding (data not shown). From these experiments, we conclude that normal mammary glands express predominantly p50 homodimers with minor amounts of a p65-containing complex. Based on its migration, band 2 likely represents p50/p65 heterodimers.

We performed a time-course experiment to assess the kinetics of activation of NF-κB/Rel in S–D rats as a function of carcinogen treatment (12). S–D rats were administered 15 mg/kg DMBA in sesame oil by intragastric gavage. At this dose, tumors are first detectable after 7 weeks, and numbers increase until ~90% of animals have tumors at 15 weeks (21). Control rats were similarly administered the vehicle alone. Animals were necropsied at 6 and 24 h, and 1, 3 and 9 weeks. For each animal, all 12 mammary glands were excised, combined and nuclear extracts prepared. (At the 9 week time-point, a tumor was observed in one mammary gland of each of two DMBA-treated animals; these were excluded from the remaining glands which were histologically normal.) EMSA analysis was performed using a radiolabelled NF-κB-containing oligonucleotide as probe with extracts from treated or control animals (Figure 2A and B, respectively). A sample of a nuclear extract from an S–D rat mammary tumor, with a typical level of binding, was added to each gel to permit comparison of the relative levels of NF-κB/Rel expression amongst the various samples. As seen previously (12), NF-κB/Rel binding levels were extremely low in mammary gland extracts from control, vehicle-treated rats after a 6 h period (Figure 2B), consistent with data presented in Figure 1A. Similar binding levels were seen with additional control animals, e.g. after various times up to the 9 week period (data not shown). Overall, normal mammary glands exhibited <10% of the binding levels seen in the tumor sample, as judged by densitometry. After 6 h, 24 h or 1 week following DMBA treatment, no increase in NF-κB/Rel binding was detected. However, at 3 weeks, there was clearly significant activation of formation of all complexes in two of the five animals (nos 46 and 47) that were administered DMBA. The binding levels in these animals approached 39 and 48% of the control tumor sample, as judged by densitometry. At 9 weeks, in two of the five animals (nos 53 and 55) induction of higher constitutive levels of NF-κB/Rel was again detected. Interestingly, these rats were the ones discussed above that had developed one mammary tumor each. The higher intensity of binding in these four samples was not due to unequal loading, as judged by EMSA with an Sp1 oligonucleotide (data not shown). Also, no contamination of B lymphocytes, neutrophils, mast or myeloid cells or of T lymphocytes was detected as judged by EMSA with oligonucleotides containing binding sites for PU.1 and TCF-1 (Figures 2C and D, respectively, and data not shown). Thus, these data indicate that activation of NF-κB/Rel binding in the mammary gland can occur 3 weeks post-DMBA administration, preceding tumor formation which is not detectable prior to 7 weeks of treatment with this dose of carcinogen (21) and was not detected at necropsy until 9 weeks in this experiment.

Transformation of MCF-10F cells by the PAHs DMBA and B[a]P increases NF-κB activity

We next sought to determine whether treatment with PAHs *in vitro* would similarly lead to an induction of NF-κB/Rel activity in HMECs. D3-1 and BP-1 cell lines were derived from the non-tumorigenic MCF-10F cell line by 24 h treatment of either DMBA and B[*a*]P, respectively. Both cell lines exhibit malignant characteristics. BP-1 cells exhibit increased anchorage independent growth, increased chemotaxis and chemoinvasiveness. D3-1 cells exhibit increased chemotactic and chemoinvasive capabilities, but to a lesser extent than BP-1 cells (22). Nuclear extracts from D3-1 and BP-1 cells displayed significantly increased NF-κB binding activity compared with the parental MCF-10F cells (inset Figure 3A). Equal loading was confirmed in EMSA using an Oct-1 probe (data not shown). Two bands were seen with the extracts from the D3-1 and BP-1, which co-migrated with bands seen with nuclear extracts from the MCF-10F cells. (The upper band with MCF-10F extract was better seen on a longer exposure.)

To confirm that the binding activity was functional, transient transfection analysis was performed using E8 and mutE8 multimerized NF-κB element-driven TK promoter–CAT reporter constructs. Since transfection efficiency of these lines varied, the activity of wild-type κB construct was normalized to that of the mutE8 activity, which is reflective of basal reporter activity without any contribution from NF-κB. The parental MCF-10F cells showed a minimal induction of E8 activity over the mutE8 of (~1.7 ± 0.6)-fold (Figure 3A). The D3-1 and BP-1 cells showed a significantly higher level of NF-κB activity of (4.1 ± 1.4)-fold and (11.6 ± 0.2)-fold, respectively. Thus, the relative levels of binding and activity correlate directly.

To confirm that the activity of the E8 vector seen in the transformed cell lines was due to NF-κB/Rel binding, co-transfection analysis was performed with an increasing dose of a vector expressing the NF-κB/Rel specific inhibitory protein IκB-α. The activity of the E8 vector in the D3-1 cells was specifically repressed in a dose-dependent manner by IκB-α (Figure 3B). Similarly, co-transfection with 1.4 μg of vector expressing IκB-α reduced NF-κB-specific activity (3.6 ± 0.1)-fold in the BP-1 cells. Thus, the transformed D3-1 and BP-1 cell lines display increased levels of functional NF-κB/Rel than seen in the parental MCF-10F cells.

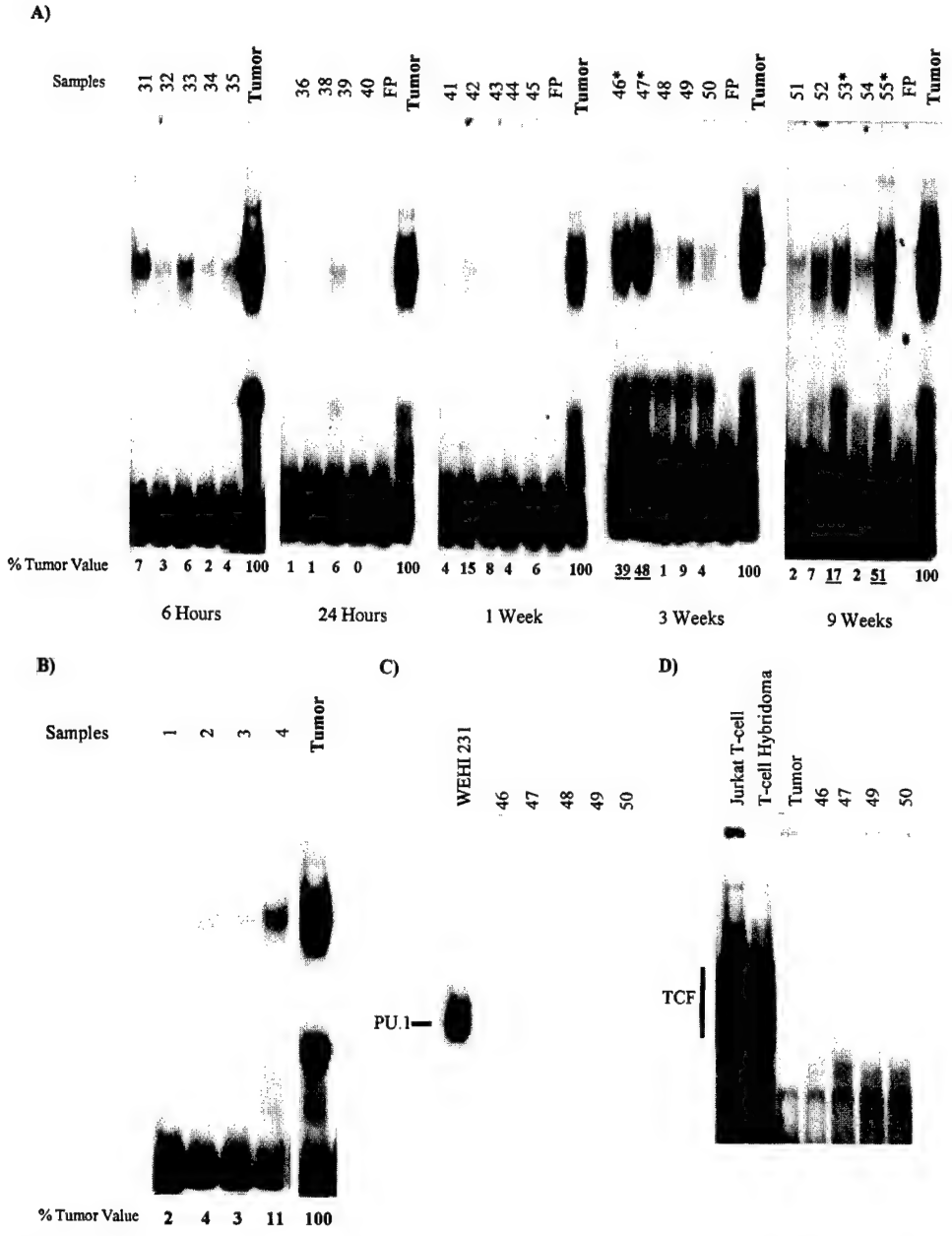

Fig. 2. Nuclear extracts of mammary glands from DMBA-treated S–D rats display high NF-κB/Rel binding activity prior to tumor formation. (A and B) NF-κB EMSA. EMSA was performed using samples (5 μg) of nuclear extracts from mammary glands of rats treated with DMBA (**A**) or representative control 6 h control rats (**B**), and an NF-κB oligonucleotide, as probe. In each panel, a sample (5 μg) of nuclear extract from a DMBA-treated rat mammary tumor (Tumor) was run to allow for comparison between gels, and to serve as a normalization for intensity of binding observed in the various samples. Densitometry analysis was performed to compare the relative level of NF-κB/Rel binding in nuclear extracts from mammary glands from the control or DMBA-treated animals, and intensity values are given as percent of tumor binding intensity (where the tumor intensity was set at 100%). *, animals whose binding intensity were at least one standard deviation above the average intensity of the control animals. (**C**) PU.1 EMSA. EMSA was performed using samples (5 μg) of nuclear extracts from mammary glands of the 3 week DMBA-treated rats (46–50) with the PU.1 oligonucleotide, as probe. As a positive control for binding, nuclear extracts from WEHI 231 B cells were analyzed on the same gel. (**D**) TCF-1 EMSA. Samples (5 μg) of nuclear extracts from mammary glands of the indicated 3 week DMBA-treated rats and a DMBA-induced mammary tumor were subjected to EMSA with the TCF-1 oligonucleotide, as probe (28). As a positive control for binding, nuclear extracts (5 μg) from Jurkat T cells and from an activated T-cell hybridoma were analyzed on the same gel.

Antibody supershift/blocking analysis was performed to identify the NF-κB subunit composition in the various extracts. Addition of an antibody against the p50 subunit to nuclear extracts from MCF-10F cells resulted in a supershift of the both bands, while addition of a blocking antibody against the p65 subunit deleted the upper complex selectively (Figure 4A). Therefore, the upper complex was identified as a p50/p65 complex, also known as classical NF-κB, a potent transactivator (1). Addition of an antibody to the p52 subunit had no effect on binding (data not shown). Thus, based on the faster migration of the bottom band, this complex likely consists of p50/p50 homodimers, which have only minimal transactivation potential. Similar analysis was performed with the D3-1 and BP-1 nuclear extracts (Figure 4B and data not shown). The upper band was eliminated upon addition of the p65 antibody with extracts from both cells, whereas the p50 antibody completely shifted the lower band, and cleared most of the upper band as well (Figure 4B and data not shown).

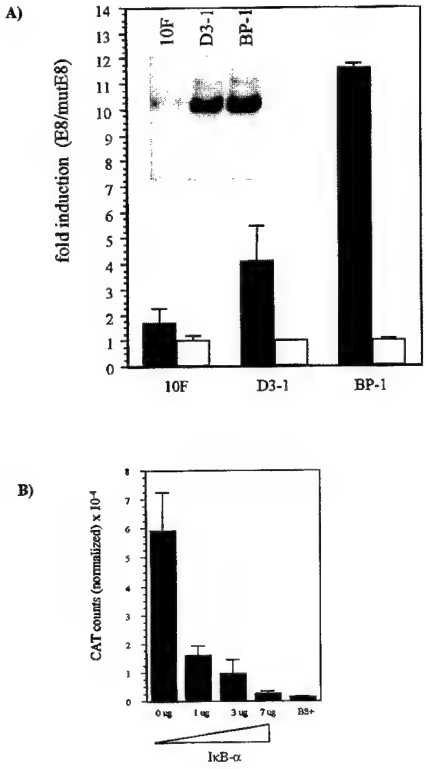

Fig. 3. Carcinogen-transformed D3-1 and BP-1 cells display higher constitutive levels of functional NF-κB than the parental MCF-10F cells. (**A**) Comparison of lines. The MCF-10F cells (10F) and BP-1 cells were transiently transfected by lipofection, in triplicate or duplicate, respectively, with 2 μg E8 or mutE8 reporter construct. Alternatively, D3-1 cells were transfected, in duplicate, using 20 μg of either E8 or mutE8 by the calcium phosphate method. After 24 h (for lipofectamine) or 72 h (for calcium phosphate), extracts were prepared, normalized for protein and assayed for CAT activity. The values for E8 CAT activity are represented as fold induction over mutE8 CAT activity which was set at 1.0 for each cell line. Shown is the representative data from a minimum of two experiments. (Inset) Equal amounts (5 μg) of nuclear extracts from exponentially growing parental MCF-10F cells or transformed D3-1 or BP-1 cells were subjected to EMSA with a radiolabeled oligonucleotide NF-κB element as probe. A representative experiment of two independent assays is shown. (**B**) Activity is inhibited with IκB-α expression. D3-1 cells were transiently transfected, in duplicate, with 15 μg of E8 reporter construct and 0, 1, 3 or 7 μg of PMT2T IκB-α expression vector, in the presence of 2.5 μg TK-luciferase construct for normalization of transfection efficiency. The total amount of plasmid DNA transfected in each sample was adjusted to 25 μg by addition of pBlueScript+ plasmid DNA. Alternatively, 25 μg of pBlueScript DNA was used alone. Lysates were prepared after 72 h and analyzed as described previously (12).

Addition of an antibody against c-Rel did not affect the pattern of migration with either cell extract. Thus, for the D3-1 and BP-1 cells, the upper band consists of the p50/p65 heterodimers, and the lower band consists of the p50/p50 homodimers, respectively. Thus, carcinogen transformation yields a functional binding complex of classical NF-κB at much higher intensity but of similar subunit composition to the parental MCF-10F cells, consistent with the identical patterns of migration.

IκB-α has a shorter half-life in D3-1 and BP-1 than in MCF-10F cells

In B cells, it has been shown that faster turnover of IκB-α proteins is, at least in part, responsible for the higher levels of functional NF-κB in the nucleus (30). Therefore, we next sought to determine if the increase in NF-κB levels in the

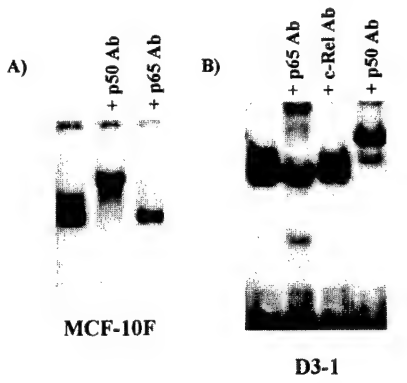

Fig. 4. Supershift analysis reveals classical NF-κB subunits in the binding complex. (**A**) Supershift analysis of MCF10F cells. Following a 30 min incubation of nuclear extracts (5 μg) with the probe, 1 μl of antibody against either the p50 (kindly provided by K.LeClair) or p65 (sc-109) was added as indicated, and the reaction incubated for an additional 1 h and subjected to EMSA as above. (**B**) Supershift analysis of D3-1 cells. Following a 30 min incubation of nuclear extracts (5 μg) with the probe, 1 μl of antibody against the p50 (sc-114), p65 (#1226, kindly provided by N.Rice) or c-Rel (sc-070) was added as indicated, incubated and subjected to EMSA.

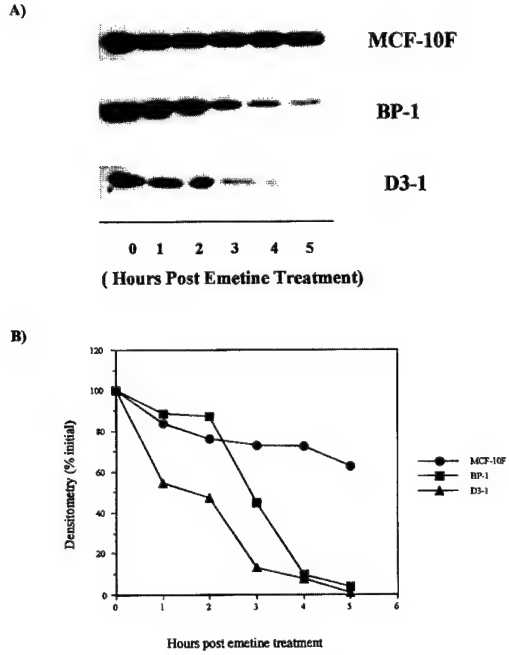

Fig. 5. IκB-α protein in D3-1 and BP-1 cells has a shorter half life than in parental MCF-10F cells. (**A**) MCF-10F, D3-1 and BP-1 cells were incubated in the absence or presence of 20 μg/ml emetine for the indicated periods of time. Cytoplasmic extracts (50 μg protein/lane) were separated by electrophoresis in a 10% SDS–polyacrylamide gel, and subjected to immunoblot analysis for IκB-α protein using SC-371 antibody. These blots are representative of two experiments. (**B**) The immunoblot for IκB-α protein in (A) was quantitated by densitometry, and the data plotted as percent of the original protein value in untreated control cells (0 h). The decay curves were extrapolated by using an exponential best fit analysis.

transformed D3-1 and BP-1 cells could be correlated with changes in stability of the IκB-α protein. Exponentially growing cells were treated with emetine, a specific inhibitor of elongation of polypeptide chain synthesis, for 0–5 h, and cytoplasmic extracts prepared and subjected to immunoblot analysis for IκB-α protein (Figure 5A). The decay of the IκB-α protein in the BP-1 and D3-1 cells appeared more rapid than that observed in the MCF-10F cells. Equal loading of the

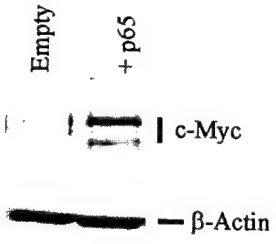

Fig. 6. Ectopic expression of p65 in MCF-10F cells increases c-Myc oncoprotein levels. Cultures of MCF-10F cells, at 70% confluence, were transiently transfected with 4 μg *pEVRF-p65* plus 20 μg *pcDNA3* plasmid or with 24 μg *pcDNA3* plasmid DNA with 30 μl FUGENE transfection reagent. After 48 h, cells were rinsed with cold PBS, and WCEs prepared. Samples (40 μg) were subjected to electrophoresis and immunoblot analysis for c-Myc (786-4, anti-c-Myc antibody), and β-actin (AC-15; Sigma).

lanes was confirmed by probing the same membranes with an antibody to the p65 subunit; this protein appeared to be quite stable even at 5 h post-treatment in all three cell types (data not shown). The resulting autoradiograms were quantified by densitometry and the data plotted in Figure 5B. The half-life of decay of IκB-α protein was determined in the BP-1 and D3-1 cells to be between 2 and 2.5 h, and 1 and 2 h, respectively. In contrast, in the parental MCF-10F cells, a half-life of ~7.8 h was determined. Thus, the chemical transformation of these cells dramatically affects the stability of the IκB-α protein correlating with the higher levels of constitutively active NF-κB associated with the malignant phenotype.

Ectopic p65 expression in MCF-10F cells induces the c-myc oncogene

To begin to assess the potential functional role of the elevated levels of NF-κB activity following transformation of the MCF-10F, we performed transient transfection and measured the effects of increased p65 levels on expression of the c-*myc* oncogene, which contains two NF-κB elements (29). MCF-10F cells, in exponential growth, were transfected in duplicate with 0, 0.5 or 1 μg *pEVRF-p65* vector DNA expressing p65 protein and 1 μg p1.6 Bgl CAT c-*myc* promoter construct. An increase in c-*myc* promoter activity of (18.9 ± 2.3)-fold and (21.3 ± 5.4)-fold was detected with 0.5 and 1.0 μg p65 expression vector, respectively. To verify that p65 expression enhances the endogenous c-*myc* gene, similar transfections were performed. MCF-10F cells were transfected with *pEVRF-p65* vector DNA or with *pcDNA3* plasmid DNA. After 48 h, whole-cell lysates were isolated and subjected to immunoblot analysis for levels of c-Myc and β-actin, as control for equal loading (Figure 6). A significant increase in c-Myc expression was detected upon transfection of the *pEVRF-p65* vector DNA compared with vector DNA alone. In this and two duplicate experiments, a (3.4 ± 0.7)-fold increase was determined by densitometry. In contrast, levels of β-actin remained unchanged (Figure 6). Thus, ectopic expression of the p65 subunit in MCF-10F cells leads to increased c-Myc levels.

HMECs transformed by B[a]P exhibit high levels of NF-κB binding activity even in the premalignant state

To monitor the expression of NF-κB earlier during the transformation process, we compared the normal finite life-span 184 HMEC cell strain with its immortally transformed derivative cell line, 184A1. The 184 HMEC cell strain, derived from reduction mammoplasty tissue, senesces after approximately 80 population doublings. The immortal but non-tumorigenic 184A1 line was established following B[*a*]P treatment of

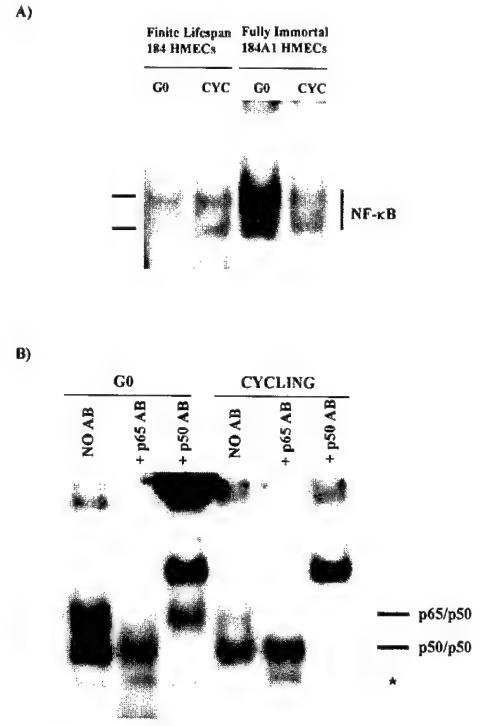

Fig. 7. Dysregulated NF-κB/Rel expression in 184A1 immortalized HMECs. (**A**) 184A1 cells display increased NF-κB binding in quiescence. EMSA was performed with nuclear extracts (5 μg) from finite life-span 184 and fully immortal 184A1 cells following G_0 synchronization upon blockage of EGF receptor signal transduction for 48 h (G_0) or during exponential growth (CYC). Two distinct NF-κB binding complexes were detected. (**B**) Supershift EMSA reveals classical NF-κB in the binding complex of 184A1 cells. Supershift analysis was performed on nuclear extracts (5 μg) harvested from fully immortal 184A1 HMECs in exponential growth, or made quiescent following blockage of EGF receptor signal transduction for 48 h. Following a 30 min incubation of nuclear extracts with the probe, 1 μl of antibody against p50 (sc-114) or p65 (#1226) was added as indicated, and the reaction incubated for an additional 1 h and subjected to EMSA, as above. The upper binding complex is composed of p65/p50 subunits, and lower binding complex is a p50/p50 homodimer. Position of a nonspecific band is indicated by an asterisk (*).

primary cultures of the 184 HMEC strain (25,31). NF-κB binding activity in the finite life-span 184 cells, and the late passage immortal 184A1 cell line was compared. Extracts from both cells gave a similar pattern with two bands detectable (Figure 7A), which co-migrated with the complexes observed in MCF-10F cells (data not shown). The levels of these complexes in the two populations of cycling cells were similar (Figure 7A). The half-life of decay of the IκB-α proteins in these cycling cell populations were also identical; a half-life of ~3.5 h was determined (data not shown). Previously, we had noted that B[*a*]P exposure led to dysregulated gene expression in quiescence (32). Thus, finite life-span and fully immortal cells were made quiescent upon blockage of EGF receptor signal transduction for 48 h, and nuclear extracts used in EMSA (Figure 7A). The levels of binding of finite life-span cells remained unchanged. In contrast, an increase in NF-κB binding activity was evident in the quiescent G_0 immortally transformed 184A1 cells (Figure 7A). In fact, the level was essentially comparable with that found in the D3-1 and BP-1 lines; a commensurate decrease in half-life of decay of IκB-α was determined in these G_0 cells to ~2.5 h (data not shown). Supershift EMSA was performed to identify the subunit components of the complexes in the cycling and quiescent 184A1 HMECs (Figure 7B). In nuclear extracts from 184A1

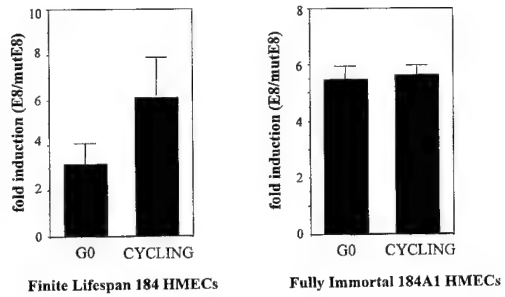

Fig. 8. Transient transfection analysis was performed in both the G_0 and exponential cycling states. Twenty-four hours after plating (110 000 cells/sample), finite life-span 184 and fully immortal 184 A1 cells were transfected, in duplicate, with equivalent amounts of either the E8 or mutE8 plasmid using Cytofectin reagent. Total amount of DNA was normalized to be either 1 or 1.5 μg (equivalent within each experiment) using pBlueScript. Cells were washed in PBS after 5 h and fresh media was added. After 24 h, cells were either given fresh normal medium (CYCLING) or medium minus EGF plus MAb 225 (G_0). Cells were harvested 24 h later in reporter lysis buffer, and assayed for CAT activity. The values for E8 CAT activity are represented as fold induction over mutE8 CAT activity which was set at 1.0 and were normalized for protein levels. Shown is the representative data from a minimum of two experiments.

cells in either growth state, the upper complex was depleted upon addition of an anti-p65 antibody. Addition of an anti-p50 antibody abrogated formation of the bottom complex and reduced the upper complex. Thus, in both cycling and arrested cells, the upper complex is classical NF-κB, composed of a p65 and p50 subunit, while the bottom complex is likely composed of a p50 homodimer. Similar complexes were identified with the 184 cell extracts (data not shown). These findings indicate that NF-κB is dysregulated in the growth-arrested late passage fully immortal 184A1 cells.

To assess the functionality of the increase in NF-κB binding in quiescence, transient transfection analysis was performed (Figure 8). Cells were transfected with E8 and mutE8, as above, and then incubated either in normal medium or medium deprived of EGF receptor signal transduction to make them quiescent. As expected, when the finite life-span 184 HMECs cells were quiescent, the level of E8/mutE8 induction decreased from a 6.1- to a 3.1-fold induction. The fact that the activity decreases most likely reflects the effects that quiescence has on reducing the overall rate of protein synthesis within these cells (26). When the immortally transformed 184A1 HMECs were similarly analyzed, an ~5-fold induction of E8/mutE8 activity was seen in cycling cells, and this induction was maintained even when the cells were made quiescent (Figure 8). This maintenance of E8 activity is most likely due to the increased induction of NF-κB/Rel in the G_0 state, and correlates with the increased binding displayed by EMSA (Figure 7A). Thus, even when growth arrested, NF-κB appears to maintain functionality in the fully immortal cells indicating a dysregulated expression of NF-κB in quiescence. Thus, dysregulation of expression of classical NF-κB can occur significantly prior to malignant transformation of the HMEC in culture.

Discussion

Here we demonstrate that the aberrant activation of NF-κB/Rel, which typifies human and rodent breast cancer, occurs early during the malignant transformation process, and involves de-stabilization of the specific inhibitory protein IκB-α. In S–D rats, activation of NF-κB/Rel occurred in the mammary glands of 40% of the animals 3 weeks after DMBA-treatment, a time-point at which tumor formation was not observed. If not every mammary gland from a DMBA-treated animal has responded, this value potentially represents an underestimation due to the pooling of all 12 mammary glands from individual animals that was performed to facilitate the time course analysis. Furthermore, the observation of NF-κB/Rel activation *in vivo* with this rodent model was extended to cultured HMECs. Carcinogen induced transformation was found to result in elevated levels of NF-κB in the malignantly transformed D3-1 and BP-1 cells compared with their parental, non-malignant MCF-10F cells. This activation of classical NF-κB in the MCF-10F-derived lines correlated with de-stabilization of IκB-α. Furthermore, enhanced expression of p65 in MCF-10F cells led to induction of the c-*myc* oncogene. Lastly, dysregulated expression of NF-κB was seen in the immortal but non-malignant 184A1 cells compared with the finite life-span 184 strain. Given the involvement of NF-κB/Rel factors in control of genes signaling proliferation, cell survival and neoplastic transformation, the early and persistent functional activation of these factors in carcinogen-induced rodent and human mammary systems suggests a potential critical role in the malignant transformation process.

There is mounting evidence for NF-κB/Rel factors mediating signals that induce cell proliferation. Firstly, these factors have been found to transactivate critical genes controlling growth either directly, e.g. c-*myc* (27,29,33), or indirectly, e.g. various interleukins or growth factors (1). Furthermore, constitutive NF-κB/Rel activity has been shown to be essential for proliferation of several cell types, e.g. smooth muscle cells (34), and hepatocytes during liver regeneration after partial hepatectomy or toxic damage (35). In the T lymphoma cell line HuT 78, constitutive NF-κB activation, apparently due to autocrine TNF-α production, was shown to accompany enhanced cellular proliferation (36). Furthermore, we have recently found that ectopic expression of c-Rel subunit permits Hs578T breast cancer cells to overcome TGF-β1-induced growth inhibition (37). Consistent with this role of NF-κB/Rel, the D3-1 and BP-1 cells both proliferate at a faster rate than the parental MCF-10F cells (22), correlating well with the higher NF-κB activity in these cells. Likewise, the late passage 184A1 cells are able to proliferate indefinitely even in the presence of TGF-β1, compared with the parental 184 cells which are TGF-β1-sensitive.

Constitutive or induced activation of NF-κB has been implicated in promoting cell survival by protecting cells from undergoing apoptosis (3). Studies of mice null for the *RelA* gene, encoding the p65 protein, provided the first suggestive evidence (38). Deletion of the p65 subunit is embryonal lethal with liver degeneration due to extensive apoptosis of the hepatocytes (38). Direct evidence for the anti-apoptotic role of NF-κB/Rel was demonstrated in breast cancer cells (12), B-lymphoma cells (3) and in hepatocytes (6): inhibition of constitutive NF-κB/Rel led to cell death by apoptosis. Furthermore, maintenance of NF-κB/Rel activity conferred protection from apoptosis induced by TNF-α or irradiation (8–11), TGF-β1 (7), or B cell receptor signals (4,39). In light of such evidence, the early activation NF-κB/Rel may play a similar role in the mammary gland following DMBA treatment leading to dysregulation of normal control of proliferation and protecting the epithelial cells from apoptosis.

Here we provide evidence that one of the genes regulated by NF-κB/Rel, that may promote epithelial cell proliferation and survival, is the c-*myc* proto-oncogene (40). A drop in

c-*myc* has been found to induce apoptosis of many cell types including breast cancer cell lines (41), while conversely, c-*myc* overexpression is able to promote survival of several cell types, including B cells (40). Furthermore, overexpression of c-*myc* has been implicated in the etiology of breast cancer (42). The regulation of the c-*myc* promoter by NF-κB/Rel was first demonstrated in human breast cancer cells (12). Here, we extend this observation to MCF-10F cells showing that both the c-*myc* promoter and endogenous c-*myc* gene respond to ectopic expression of p65. Interestingly, BP-1 cells overexpress the c-*myc* oncogene (43), and tumors from DMBA treated S–D rats have increased c-*myc* mRNA expression (D.W.Kim and G.E.Sonenshein, unpublished observations). Studies are in progress to determine whether inhibition of NF-κB/Rel activation leads to decreased c-*myc* gene expression and ablates the carcinogen transformation process.

Lastly, aberrant activation of nuclear NF-κB/Rel has been found to correlate with oncogenesis in several different systems, including breast cancer, thyroid carcinoma (44), non-small cell lung carcinoma, colon carcinoma, ovarian carcinoma, prostate cancer (45), Hodgkin's disease (46,47) and various types of lymphomas (13). The results presented here extend this association to carcinogen-induced *in vitro* malignant transformation of HMECs. Furthermore, our findings indicate that the activation of NF-κB/Rel in mammary glands upon carcinogen treatment of rodents is an early event. It was also interesting to note that in our studies with DMBA-treated S–D rats, the two animals studied at 9 weeks which displayed elevated NF-κB/Rel binding activity in the grossly normal mammary glands had non-palpable tumors. Taken together, our results suggest a novel mechanism for carcinogen induction of tumors of the mammary glands, i.e. via the activation of NF-κB/Rel factors. Thus, inhibition of NF-κB may provide a means of intervention at early, as well as later, stages of the transformation process in the mammary gland. Furthermore, the possibility that NF-κB/Rel may serve as a diagnostic marker for pre-malignant mammary glands warrants further investigation. Studies are underway to test directly the role of activation of NF-κB/Rel in neoplastic transformation by enforcing expression of a transactivating subunit of NF-κB/Rel in the mammary glands of transgenic mice.

Acknowledgements

We thank Nancy Rice, Ken LeClair, Uli Siebenlist, Ranjan Sen and Shyr-Te Ju for generously providing antibody reagents, cloned DNA and nuclear extracts. We thank Judith Foster for the use of the densitometer. We thank D.Sloneker for assistance in preparation of this manuscript. This work was supported by grants DAMD17-98-1 (G.E.S.), DAMD17-94-J-4421 (A.E.R., L.J.H.), DAMD 17-98-1-8034 (D.W.K.) from the Department of Army, CA24844 (M.R.S., P.Y.), CA82742 (G.E.S.) from the National Cancer Institute, SC-DPH-3408-699D018 from the Commonwealth of Massachusetts Department of Public Health (M.A.S), from the American Heart Association (D.W.K.) and the Karin Grunebaum Cancer Research Fellowship (D.W.K.), a Graduate Research Student Fellowship from Boston University School of Medicine (D.W.K.), and Contract No. DE-AC03-76sF00098 (M.R.S., P.Y.) from the Office of Energy Research, Office of Health and Biological Research, US Department of Energy, and a grant from the Tea Trade Health Research Association (A.E.R.).

References

1. Siebenlist,U., Franzoso,G. and Brown,K. (1994) Structure, regulation and function of NF-κB. *Ann. Rev. Cell. Biol.*, **10**, 405–455.
2. Verma,I.M., Stevenson,J.K., Schwartz,E.M., Van Antwerp,D. and Miyamoto,S. (1995) Rel/NF-κB/IκB family: intimate tales of association and dissociation. *Genes Dev.*, **9**, 2723–2735.
3. Sonenshein,G.E. (1997) Rel/NF-κB transcription factors and the control of apoptosis. *Semin. Cancer Biol.*, **8**, 113–119.
4. Wu,M., Lee,H., Bellas,R.E., Schauer,S.L., Arsura,M., Katz,D., Fitzgerald,M.J., Rothstein,T.L., Sherr,D.H. and Sonenshein,G.E. (1996) Inhibition of NF-κB/Rel induces apoptosis of WEHI 231 murine B cells. *EMBO J.*, **15**, 4682–4690.
5. Arsura,M., Wu,M. and Sonenshein,G.E. (1996) TGF-β1 inhibits NF-κB/Rel activity inducing apoptosis of B cells:transcriptional activation of IκB-α. *Immunity*, **5**, 31–40.
6. Bellas,R.E., Fitzgerald,M.J., Fausto,N. and Sonenshein,G.E. (1997) Inhibition of NF-kappa B activity induces apoptosis in murine hepatocytes. *Am. J. Pathol.*, **151**, 891–896.
7. Arsura,M., FitzGerald,M.J., Fausto,N. and Sonenshein,G.E. (1997) Nuclear factor-kappa B Rel blocks transforming growth factor beta 1-induced apoptosis of murine hepatocyte cell lines. *Cell Growth Differ.*, **8**, 1049–1059.
8. Beg,A.A., Sha,W.C. and Baltimore,D. (1996) An essential role for NF-kappa B in preventing TNF-alpha-induced cell death. *Science*, **274**, 782–784.
9. Wang,C.Y., Mayo,M.W. and Baldwin,A.S.J. (1996) TNF- and cancer therapy-induced apoptosis: potentiation by inhibition of NF-kappaB. *Science*, **274**, 784–787.
10. VanAntwerp,D.J., Martin,S.J., Kafri,T., Green,D.R. and Verma,I.M. (1996) Suppression of TNF-alpha-induced apoptosis by NF-kappaB. *Science*, **274**, 787–789.
11. Liu,Z.G., Hsu,H.L., Goeddel,D.V. and Karin,M. (1996) Dissection of TNF receptor 1 effector functions: JNK activation is not linked to apoptosis while NF-kappaB activation prevents cell death. *Cell*, **87**, 565–576.
12. Sovak,M.A., Bellas,R.E., Kim,D.W., Zanieski,G.J., Rogers,A.E., Traish,A.M. and Sonenshein,G.E. (1997) Aberrant nuclear factor-kappaB/Rel expression and the pathogenesis of breast cancer. *J. Clin. Invest.*, **100**, 2952–2960.
13. Luque,I. and Gelinas,C. (1997) Rel/NF-κB and IκB factors in oncogenesis. *Semin. Cancer Biol.*, **8**, 103–111.
14. Morris,J.J. and Seifter,E. (1992) The role of aromatic hydrocarbons in the genesis of breast cancer. *Med. Hyp.*, **38**, 177–184.
15. Dusich,K., Sigurson,F., Hall,W.N. and Dean,A.G. (1980) Cancer rates in a community exposed to low levels of creosote components in municipal water. *Minn. Med.*, **63**, 803–806.
16. Manz,A., Berger,J., Dwyer,J.H., Flesch-Janys,D., Nagel,S. and Waltsgott,H. (1991) Cancer mortality among workers in chemical plant contaminated with dioxin. *Lancet*, **338**, 959–964.
17. Willett,W. (1989) The search for the causes of breast and colon cancer. *Nature*, **338**, 389–394.
18. Wolff,M.S., Toniolo,P.G., Lee,E.W., Rivera,M. and Dublin,N. (1993) Blood levels of organochlorine residues and risk of breast cancer. *J. Natl Cancer Inst.*, **85**, 648–652.
19. Falck,F.J., Ricci,A.J., Wolff,M.S., Godbold,J. and Deckers,P. (1992) Pesticides and polychlorinated biphenyl residues in human breast lipids and their relation to breast cancer. *Arch. Env. Health*, **47**, 143–146.
20. Wassermann,M., Nogueira,D.P., Tomatis,L., Mirra,A.P., Shibata,H., Arie,G., Cucos,S. and Wassermann,D. (1976) Organochlorine compounds in neoplastic and adjacent apparantly normal breast tissue. *Bull. Environ. Contam. Toxicol.*, **15**, 478–484.
21. Rogers,A.E. and Conner,B.H. (1990) Dimethylbenzanthracene-induced mammary tumorigenesis in ethanol-fed rats. *Nutr. Res.*, **10**, 915–928.
22. Calaf,G. and Russo,J. (1993) Transformation of human breast epithelial cells by chemical carcinogens. *Carcinogenesis*, **14**, 483–492.
23. Dipple,A., Khan,Q.A., Page,J.E., Ponten,I. and Szeliga,J. (1999) DNA reactions, mutagenic action and stealth properties of polycyclic aromatic hydrocarbon carcinogens (review). *Int. J. Oncol.*, **14**, 103–111.
24. Hackett,A.J., Smith,H.S., Springer,E.L., Owens,R.B., Nelson-Rees,W.A., Riggs,J.L. and Gardner,M.B. (1977) Two syngeneic cell lines from human breast tissue: the aneuploid mammary epithelial (Hs578T) and the diploid myoepithelial (Hs578Bst) cell lines. *J. Natl Cancer Inst.*, **58**, 1795–1806.
25. Stampfer,M.R. and Yaswen,P. (1993) Culture systems for study of human mammary epithelial cell proliferation, differentiation and transformation. *Cancer Surv.*, **18**, 7–34.
26. Stampfer,M.R., Pan,C.H., Hosoda,J.J.J.B., Mendelsohn,J. and Yaswen,P. (1993) Blockage of EGF receptor signal transduction causes reversible arrest of normal and immortal human mammary epithelial cells with synchronous reentry into the cell cycle. *Exp. Cell, Res.*, **208**, 175–188.
27. Duyao,M.P., Buckler,A.J. and Sonenshein,G.E. (1990) Interaction of an NF-κB-like factor with a site upstream of the c-*myc* promoter. *Proc. Natl Acad. Sci. USA*, **87**, 4727–4731.

28. van de Wetering,M., Oosterwegel,M., Dooijes,D. and Clevers,H. (1991) Identification and cloning of TCF-1, a T lymphocyte-specific transcription factor containing a sequence-specific HMG box. *EMBO J.*, **10**, 123–132.
29. Duyao,M.P., Kessler,D.J., Spicer,D., Bartholomew,C., Cleveland,J., Siekevitz,M. and Sonenshein,G.E. (1992) Transactivation of the c-*myc* promoter by the HTLV-1 *tax* gene. *J. Biol. Chem.*, **267**, 16288–16291.
30. Miyamoto,S., Chiao,P. and Verma,I. (1994) Enhanced IκB degradation is responsible for constitutive NF-κB activity in mature B-cell lines. *Mol. Cell. Biol.*, **14**, 3276–3282.
31. Stampfer,M.R., Bodnar,A., Garbe,J., Wong,M., Pan,A., Villeponteau,B. and Yaswen,P. (1997) Gradual phenotypic conversion associated with immortalization of cultured human mammary epithelial cells. *Mol. Biol. Cell*, **8**, 2391–2405.
32. Campisi,J., Gray,H.E., Pardee,A.B., Dean,M. and Sonenshein,G.E. (1984) Cell-cycle control of c-*myc* but not c-*ras* expression is lost following chemical transformation. *Cell*, **36**, 241–247.
33. La Rosa,F.A., Pierce,J.W. and Sonenshein,G.E. (1994) Differential regulation of the c-*myc* oncogene promoter by the NF-κB/Rel family of transcription factors. *Mol. Cell Biol.*, **4**, 1039–1044.
34. Bellas,R.E., Lee,J.S. and Sonenshein,G.E. (1995) Expression of a constitutive NF-κB-like activity is essential for proliferation of cultured bovine vascular smooth muscle cells. *J. Clin. Invest.*, **96**, 2521–2527.
35. Taub,R. (1996) Liver regeneration 4: transcriptional control of liver regeneration. *FASEB J.*, **10**, 413–427.
36. O'Connell,M.A., Cleere,R., Long,A., O'Neill,L.A. and Kelleher,D. (1995) Cellular proliferation and activation of NF-kappaB are induced by autocrine production of tumor necrosis factor alpha in the human T lymphoma line HuT 78. *J. Biol. Chem.*, **270**, 7399–7404.
37. Sovak,M.A., Arsura,M., Zanieski,G., Kavanagh,K.T. and Sonenshein,G.E. (1999) The inhibitory effects of transforming growth factor-beta1 on breast cancer cell proliferation are mediated through regulation of aberrant NF-kappaB/Rel expression. *Cell Growth Differ.*, **10**, 537–544.
38. Beg,A.A., Sha,W., Bronso,R., Ghosh,S. and Baltimore,D. (1995) Embryonic lethality and liver degeneration in mice lacking the RelA component of NF-κB. *Nature*, **376**, 167–170.
39. Giri,D.K. and Aggarwal,B.B. (1998) Constitutive activation of NF-kappaB causes resistance to apoptosis in human cutaneous T cell lymphoma HuT-78 cells. Autocrine role of tumor necrosis factor and reactive oxygen intermediates. *J. Biol. Chem.*, **273**, 14008–14014.
40. Wu,M., Arsura,M., Bellas,R.E., FitzGerald,M.J., Lee,H., Schauer,S.L., Sherr,D.H. and Sonenshein,G.E. (1996) Inhibition of c-*myc* expression induces apoptosis of WEHI 231 murine B cells. *Mol. Cell. Biol.*, **16**, 5015–5025.
41. Thompson,E.B. (1998) The many roles of c-Myc in apoptosis. *Annu. Rev. Physiol.*, **60**, 575–600.
42. Pavelic,Z.P., Steele,P. and Presler,H.D. (1991) Evaluation of c-*myc* proto-oncogene in primary human breast carcinomas. *Anticancer Res.*, **11**, 1421–1427.
43. Russo,J., Yang,Z., Hu,Y.-F., Bove,B.A., Huang,Y., Silva,I.D.C.G., Tahin,Q., Wu,Y., Higgy,N., Zekri,A. and Russo,I.H. (1998) Biological and molecular basis of human breast cancer. *Frontiers Biosci.*, **3**, 944–960.
44. Visconti,R., Cerutti,J., Battista,S., Fedele,M., Trapasso,F., Zeki,K., Miano,M.P., Nigris,F.D., Casalino,L., Curcio,F., Santoro,M. and Fusco,A. (1997) Expression of the neoplastic phenotype by human thyroid carcinoma cell line requires NF-kappaB p65 protein expression. *Oncogene*, **15**, 1987–1994.
45. Sumitomo,M., Tachibana,M., Nakashima,J., Murai,J., Miyajima,A., Kimura,F., Hayakawa,M. and Nakamura,H. (1999) An essential role for nuclear factor kappa B in preventing TNF-alpha-induced cell death in prostate cancer cells. *J. Urol.*, **161**, 674–679.
46. Wood,K.M., Roff,M. and Hay,R.T. (1998) Defective IkappaBalpha in Hodgkin cell lines with constitutively active NF-kappaB. *Oncogene*, **16**, 2131–2139.
47. Bargou,R.C., Leng,C., Krappmann,D., Emmerich,F., Mapara,M.Y., Bommert,K., Royer,H.D., Scheidereit,C. and Dorken,B. (1996) High-level nuclear NF-kappaB and Oct-2 is a common feature of cultured Hodgkin/Reed-Sternberg cells. *Blood*, **87**, 4340–4347.

Received April 8, 1999; revised January 21, 2000; accepted January 31, 2000

Oncogene (2000) 19, 5498–5506

www.nature.com/onc

The RelA NF-κB subunit and the aryl hydrocarbon receptor (AhR) cooperate to transactivate the c-*myc* promoter in mammary cells

Dong W Kim[1], Lee Gazourian[1], Shafat A Quadri[2], Raphaëlle Romieu-Mourez[1], David H Sherr[2,3] and Gail E Sonenshein*[,1,3]

[1]*Department of Biochemistry and the Program in Research on Women's Health, Boston University School of Medicine, Boston, Massachusetts, MA 02118, USA;* [2]*Department of Environmental Health, and the Program in Research on Women's Health, Boston University Schools of Medicine and Public Health, Boston, Massachusetts, MA 02118, USA*

NF-κB/Rel transcription factors regulate many genes involved in control of cellular proliferation, neoplastic transformation, and apoptosis, including the c-*myc* oncogene. Recently, we have observed that levels of NF-κB and aryl hydrocarbon receptor (AhR), which mediates malignant transformation by environmental carcinogens, are highly elevated and appear constitutively active in breast cancer cells. Rel factors have been found to functionally interact with other transcription factors. Here we demonstrate a physical and functional association between the RelA subunit of NF-κB and AhR resulting in the activation of c-*myc* gene transcription in breast cancer cells. RelA and AhR proteins were co-immunoprecipitated from cytoplasmic and nuclear extracts of non-malignant MCF-10F breast epithelial and malignant Hs578T breast cancer cells. In transient co-transfection, RelA and AhR gene products demonstrated cooperation in transactivation of the c-*myc* promoter, which was dependent on the NF-κB elements, and in induction of endogenous c-Myc protein levels. A novel AhR/RelA-containing NF-κB element binding complex was identified by electrophoretic mobility shift analysis of nuclear extracts from *RelA* and *AhR* co-transfected Hs578T cells. Thus, the RelA and AhR proteins functionally cooperate to bind to NF-κB elements and induce c-*myc* gene expression. These findings suggest a novel signaling mechanism whereby the Ah receptor can stimulate proliferation and tumorigenesis of mammary cells. *Oncogene* (2000) **19,** 5498–5506.

Keywords: NF-κB; RelA; AhR; c-*myc* oncogene; breast cancer

Introduction

NF-κB/Rel is a family of dimeric transcription factors characterized by the presence of a Rel homology region (RHR) of about 300 amino acids in length, which controls multiple functions including dimerization, DNA binding, and nuclear localization. Classical NF-κB is a heterodimer composed of p65 (or RelA) and p50 (or NFκB1) subunits (Grimm and Baeuerle, 1993). The RelA subunit has potent transactivation potential, while the p50 subunit has only modest transactivation ability *in vivo* (Grimm and Baeuerle, 1993; Ballard *et al.*, 1992; La Rosa *et al.*, 1994). Many genes are regulated by NF-κB (Grilli *et al.*, 1991; Grimm and Baeuerle, 1993). For example, we demonstrated that the c-*myc* oncogene is potently transactivated by NF-κB/Rel factors (La Rosa *et al.*, 1994). In most cells, other than B lymphocytes, NF-κB/Rel proteins are sequestered in the cytoplasm bound to one of the specific inhibitory proteins termed IκBs of which IκB-α is the paradigm. A variety of agents can induce NF-κB/Rel, including oxidative stress (Grimm and Baeuerle, 1993; Verma *et al.*, 1995). Activation of NF-κB involves phosphorylation and degradation of IκB, which allows for translocation of an active NF-κB complex into the nucleus where it can bind to NF-κB responsive elements (Verma *et al.*, 1995). However, we recently demonstrated that breast cancer cell lines and primary breast cancer specimens are typified by aberrant constitutive activation of NF-κB (Sovak *et al.*, 1997).

We have postulated that one mechanism leading to constitutive NF-κB activation may be oxidative stress induced by activation of cytochrome P450 enzymes, some of which are regulated by the aryl hydrocarbon receptor (AhR) (Nebert *et al.*, 1990, 1991). The AhR is a cytosolic protein complexed with heat shock protein (Hsp90) and an immunophilin-like molecule, ARA-9/XAP-2/AIP (Carver and Bradfield, 1997; Jain *et al.*, 1994; Perdew and Bradfield, 1996; Ma and Whitlock, 1996; Meyer *et al.*, 1998), and c-Src (Enan and Matsumura, 1996). Acute activation can occur with multiple agents, including classes of carcinogenic environmental chemicals (e.g. dioxins, polycyclic aromatic hydrocarbons (PAH), and planar polychlorinated biphenyls (PCBs)). Upon activation, the receptor translocates to the nucleus, binds specific response elements (XREs), and induces transcription of a number of genes, including those encoding the P450 enzymes CYP1A1, CYP1A2, and CYP1B1. As predicted from the working model, we have recently found high levels of constitutively active AhR in PAH-induced rat mammary tumors (Trombino *et al.*, 2000), that coincide with constitutively active NF-κB (Sovak *et al.*, 1997).

The recent work of Tian *et al.* (1999) suggests a second pathway linking AhR and NF-κB activities. In particular, they demonstrated a physical association between the AhR and the RelA subunit of NF-κB in murine hepatoma cells, and transcriptional down-

*Correspondence: GE Sonenshein, Department of Biochemistry, Boston University Medical School, 715 Albany St., Boston, Massachusetts, MA 02118, USA
[3]These authors contributed equally to this manuscript
Received 19 April 2000; revised 18 September 2000; accepted 22 September 2000

regulation by AhR-NF-κB subunit complexes of an NF-κB element driven construct. To test for this additional regulatory mechanism in human breast epithelial and tumor cell lines, the potential for AhR and NF-κB subunits to associate and regulate an NF-κB-regulated gene promoter, i.e. c-*myc*, was examined. We report that the RelA and AhR proteins co-precipitate in untransfected or *RelA*- and *AhR*-transfected human mammary epithelial cell (HMEC) lines. In contrast to the previous report by Tian and coworkers (1999), however, we find RelA and AhR cooperate to positively transactivate the c-*myc* gene, apparently via direct binding to NF-κB elements. These findings suggest a new mechanism whereby aberrant constitutive NF-κB/AhR expression can promote activation of the c-*myc* gene and thereby proliferation and neoplastic transformation.

Results

RelA and AhR are associated in HMECs

To assess the association of the RelA subunit of NF-κB with AhR in breast epithelial cells, co-immunoprecipitation studies were performed. Total cell, nuclear, and cytoplasmic extracts were prepared from malignant Hs578T breast cancer cells, which have been found to express both RelA (Sovak *et al*., 1997), and AhR proteins. Samples of the nuclear (50 μg) and cytoplasmic (100 μg) fractions were treated with either a goat antibody against AhR (Figure 1a, lanes 2,3) or a goat IgG fraction, as control (Figure 1a, lanes 4,5). Immune complexes were isolated using protein A-Sepharose and subjected to electrophoresis, along with a sample of total cell lysate (Figure 1a, lane 1). The resulting immunoblot was probed with a rabbit polyclonal antibody for expression of the 65 kDa RelA subunit. In the total cell lysate, RelA-specific antibody recognized a protein of the expected molecular weight (65 kDa). The AhR antibody co-precipitated RelA protein from either cytoplasmic or nuclear extracts (Figure 1a), with somewhat greater amounts seen with the cytoplasmic sample. In contrast, the control goat IgG failed to co-precipitate detectable levels of RelA protein. To confirm this association we performed the inverse experiment of immunoprecipitating nuclear (100 μg protein) or cytoplasmic (200 μg protein) extracts with a rabbit antibody against RelA and then immunoblotting for AhR using a goat antibody. The RelA antibody co-precipitated AhR protein from either cytoplasmic or nuclear extracts (Figure 1b). In contrast, the control rabbit IgG failed to co-precipitate detectable levels of AhR protein. As seen above, somewhat greater amounts of complexes were detected in the cytoplasm. These findings suggest that endogenous AhR is associated with RelA in both the nucleus and the cytoplasm of Hs578T cells; although, the majority of the complexes, as judged from this and two duplicate experiments (0.80 ± 0.07), are present in the cytoplasm.

We next sought to assess the ability of RelA to associate with the AhR in non-malignant MCF-10F HMECs. To this end, MCF-10F cells were transfected with a vector expressing the *T7-pcDNA3-AhR* vector encoding T7-tagged AhR. Alternatively, cells were transfected with the parental *T7-pcDNA3* DNA, as control. Total cell lysates were prepared, and either immunopreciptated with a RelA-specific antibody or an aliquot run directly on the gel. The resulting

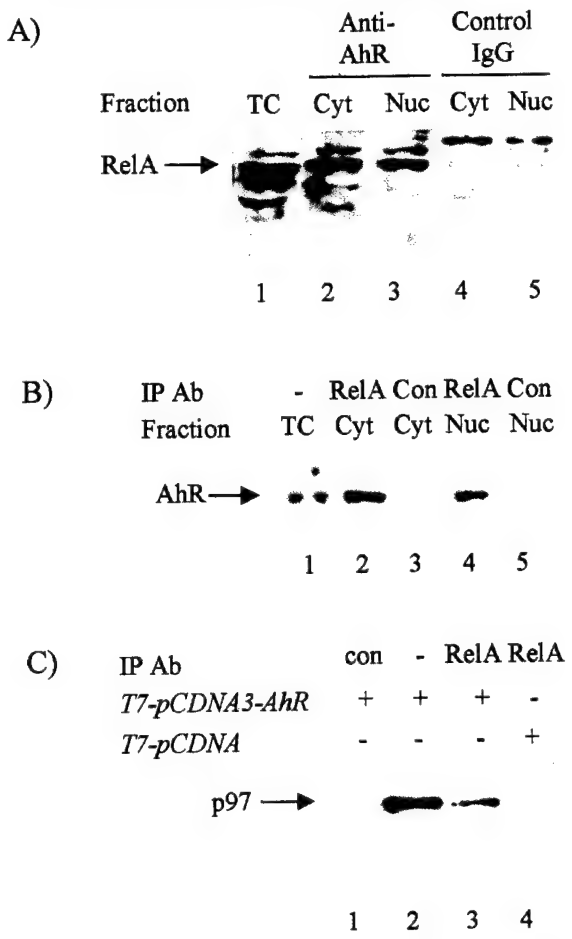

Figure 1 AhR and RelA are associated in Hs578T and MCF-10F cells. (**a**) Cytosolic (100 μg from 1 mg total) or nuclear (50 μg from 128 μg total) proteins from Hs578T cells were immunoprecipitated using 5 μg/ml of either a polyclonal goat anti-AhR antibody (lanes 2,3) or a control goat IgG (lanes 4,5). Of 30 μl of resulting antibody-protein A-sepharose eluates, 20 μl were subjected to immunoblot analysis with RelA-specific antibody (Cyt: cytosolic immunoprecipitate; Nuc: nuclear immunoprecipitate). Total cell lysate (30 μg protein) was analysed as a positive control (lane 1) (TC: total cell lysate). The position of the 65 kDa RelA protein is indicated. (**b**) Cytosolic (200 μg from 1.5 mg total) or nuclear (100 μg from 330 μg total) proteins from Hs578T cells were immunoprecipitated using 5 μg/ml of either a polyclonal rabbit RelA-specific antibody (sc-372) (lanes 2,4) or a control rabbit IgG (lanes 3,5). Of 50 μl of resulting antibody-protein A-sepharose eluates, 30 μl were subjected to immunoblot analysis with polyclonal goat anti-AhR antibody (sc-8088) (Cyt: cytosolic immunoprecipitate; Nuc: nuclear immunoprecipitate). Total cell lysate (40 μg protein) was analysed as a positive control (lane 1) (TC: total cell lysate). The position of the AhR protein is indicated. (**c**) Total cell proteins (100 μg) from *T7-pcDNA3-AhR*- or *T7-pcDNA3*-transfected MCF-10F cells were immunoprecipitated using 5 μg/ml of either normal rabbit IgG as a negative control (lane 1) or RelA-specific antibody (lanes 3,4). The resulting antibody-protein A-sepharose eluates were subjected to immunoblot analysis with T7 epitope-specific antibody, as described above. Total cell lysate (30 μg protein) was analysed as a positive control (lane 2). The 97–100 kDa T7-AhR product is indicated

immunoblot was probed with a T7 epitope-specific antibody. A protein of the size expected for T7-tagged AhR, i.e. 97–100 kDa, was recognized in total cell extracts from cells transfected with the *T7-pcDNA3-AhR* vector (Figure 1c, lane 2). Similarly a 97 kDa AhR protein was detected following co-precipitation with RelA-specific antibody (lane 3), whereas no protein was detected following 'immunoprecipitation' with control rabbit IgG (lane 1). No anti-T7 antibody-reactive protein was detected in extracts from cells transfected with the parental vector (lane 4). Furthermore, AhR protein was not detected in T7-AhR-specific immunoblots of *T7-pcDNA3*-transfected MCF-10F cell extracts precipitated with a p50-specific antibody (data not shown). Similar results were obtained with transfected Hs578T cells (not shown). Overall, these results indicate that the RelA, but not p50, and the AhR are physically associated within Hs578T and MCF-10F cells.

*RelA and AhR cooperate to activate the c-*myc *promoter in non-malignant MCF-10F cells*

To determine whether AhR and NF-κB/Rel can function cooperatively, we examined the effects of *AhR* and *RelA* co-transfection on the c-*myc* promoter, a transcriptional target of classical NF-κB (La Rosa *et al*., 1994). Since we have found that endogenous AhR levels decrease in cells as the cultures reach confluence (SAQ and DHS, unpublished observations), all transfections were performed with confluent cultures. In addition, in order to maximize conditions for observing RelA-AhR transcriptional cooperation, we first titered the dose of expression vector transfected such that minimal augmentation of reporter activity would be observed. Addition of 1 μg of the *pEVRF-p65* expression plasmid increased the transcriptional activity of the p1.6 Bgl promoter ~20-fold (data not shown), consistent with the potent role of RelA in transactivation of the c-*myc* promoter (La Rosa *et al*., 1994). When the level of RelA expression plasmid was lowered eightfold to 0.125 μg, a 2.4±0.5-fold increase in transactivation of the murine c-*myc* promoter was observed (Figure 2a). This amount (0.125 μg) was selected for future transfections. Minimal transcriptional activity was observed when MCF-10F cells were transfected with p1.6 Bgl alone (Figure 2a). This is consistent with the observation that c-*myc* gene transcription is minimal in cells at confluence. Transfection of 2 or 4 μg of AhR alone had no effect on the transcriptional activity of the p1.6 Bgl promoter. However, when 0.125 μg *pEVRF-p65* were co-transfected with 2 μg *pcDNA3-AhR* expression plasmid, a 6.2±0.3-fold induction of c-*myc* promoter activity was seen. Upon co-transfection of 0.125 μg *pEVRF-p65* with 4 μg *pcDNA3-AhR* expression plasmid the fold induction was 8.0±0.2. Using the latter conditions, an average fold induction in three separate experiments of 5.6±2.1-fold ($P<0.01$) was obtained. Thus, RelA and AhR cooperate to significantly increase c-*myc* promoter activity in MCF-10F cells.

We next asked whether the increase in transactivation of the c-*myc* promoter was mediated by the NF-κB elements located upstream of the promoter and/or within exon 1 (URE and IRE, respectively) (Duyao *et al*., 1990; Kessler *et al*., 1992b). A transfection experiment, similar to that described above, was performed using the p1.6 Bgl double mutant (p1.6 Bgl dbl mut) reporter plasmid, in which the URE and IRE NF-κB sites have been mutated so that the promoter can no longer be transcriptionally activated by classic NF-κB (Duyao *et al*., 1992; Kessler *et al*., 1992a; La Rosa *et al*., 1994). In the absence of exogenous RelA or AhR, the p1.6 bgl double mutant displayed about one half of the activity of the wild type p1.6 Bgl reporter (Figure 2a). This modest decrease in activity of the mutant *vs* wild type p1.6 Bgl reporter construct is consistent with the low levels of RelA/p50 complexes present in the MCF-10F cells (Sovak *et al*., 1997). Ectopically expressed RelA in *pEVRF-p65* transfected cells was unable to transactivate the mutant construct, consistent with our previous findings (La Rosa *et al*., 1994). Furthermore, co-transfection with 4 μg *pcDNA3-AhR* and 0.125 μg *pEVRF-p65* did not significantly affect the activity of the mutated c-*myc* promoter (Figure 2a). Taken together these findings indicate that RelA and AhR function cooperatively to transactivate the c-*myc* promoter via binding at the URE and/or IRE NF-κB elements.

*RelA and AhR activate the c-*myc *promoter in Hs578T cells*

We next asked whether RelA and AhR can activate the c-*myc* promoter in a human malignant breast cancer cell line by performing similar co-transfection analyses with Hs578T cells. In these cells the basal activity of the p1.6 Bgl promoter was notably higher than observed in transfected MCF-10F cells (Figure 2b). This result likely reflects the higher transfection efficiency of Hs578T cells (20–30% *vs* 5% for MCF-10F cells), and potentially the higher endogenous levels of nuclear NF-κB/Rel proteins in these malignant cells (Sovak *et al*., 1997). Interestingly, the activity of the p1.6 Bgl reporter plasmid increased in a dose-dependent fashion with transfection of increasing levels of AhR expression plasmid alone. Following transfection with 4 μg of *pc-DNA3-AhR*, CAT activity was 2.1±0.4-fold higher than basal levels. This result may be due to the effect of relatively high levels of constitutively active endogenous RelA protein present in these cells (see below). When a suboptimal dose (0.25 μg) of *pEVRF-p65* plasmid alone was added, no apparent change in p1.6 Bgl activity was seen. However, co-transfection of both the RelA and AhR expression plasmids resulted in induction of a higher level of c-*myc* promoter activity than was seen following transfection of either plasmid alone (Figure 2b). Specifically, a 3.1±0.3-fold induction of the c-*myc* promoter activity was observed following co-transfection with 4 μg *pc-DNA3-AhR* and 0.25 μg *pEVRF-p65* expression plasmids. The fact that the cooperative effects seen following AhR and RelA plasmid co-transfections in Hs578T cells were not as great as those seen in co-transfected MCF-10F cells may have been due to the higher level of background activity in the former cells, as well as the modest induction of reporter activity following transfection with 4 μg AhR expression plasmid alone in Hs578T cells.

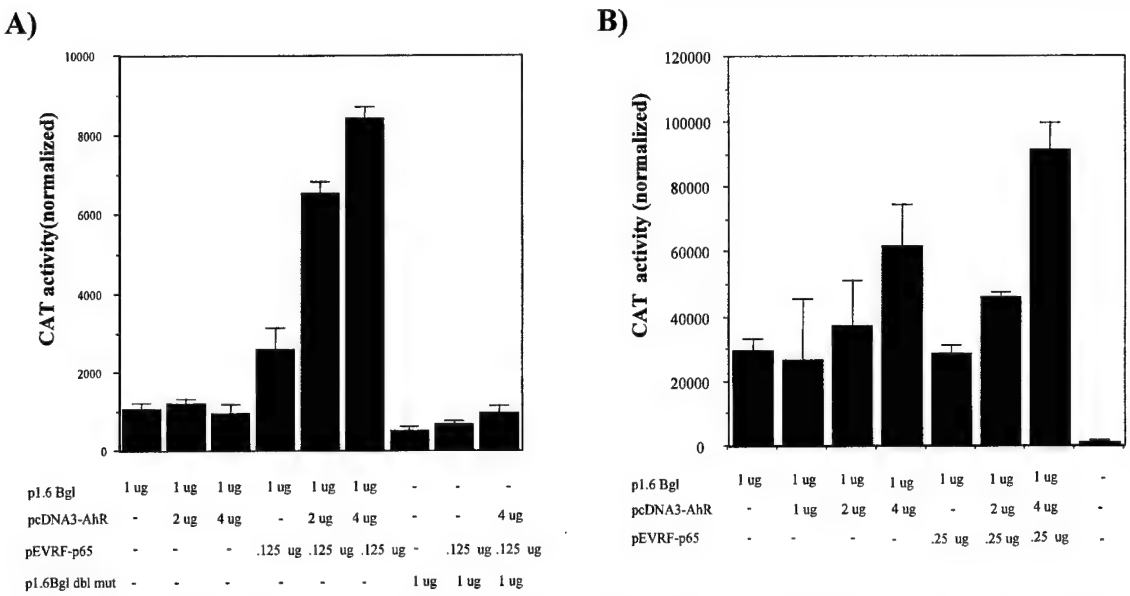

Figure 2 RelA and AhR cooperate to transactivate the wildtype p1.6 Bgl, but not the p1.6 Bgl dbl mut, c-*myc* promoter construct. (**a**) Confluent MCF-10F cells (~200 000 cells in 35 mm^2 dishes) were transiently transfected, in duplicate, with either 1 μg p1.6 Bgl or p1.6 Bgl dbl mut, and 0, 2, or 4 μg *pcDNA3-AhR* (murine AhR) expression vector in the absence or presence of 0.125 μg *pEVRF-p65* (RelA expression) plasmid using 7 μl FUGENE reagent. In each transfection, 1 μg of TK-luciferase plasmid was added as an internal control for normalization of transfection efficiency. Total DNA transfected was maintained at 6 μg by addition *pcDNA3* plasmid (parent vector for *pcDNA3-AhR*). Transfected cells were harvested after 24 h in reporter lysis buffer, and analysed for CAT and luciferase activity. CAT activities are presented normalized for transfection efficiency, using the luciferase activity. (**b**) Confluent Hs578T breast cancer cells were transiently transfected, in duplicate, with 1 μg of p1.6 Bgl plus 0, 1, 2, or 4 μg of *pcDNA3-AhR*, in the absence or presence of 0.25 μg of *pEVRF-p65* plasmid using 5 μl of FUGENE reagent. In each transfection, 0.5 μg of TK-luciferase plasmid was added and total DNA was maintained at 6 μg by addition of the appropriate amounts of *pcDNA3* plasmid. After 24 h, cells were harvested and analysed for CAT and luciferase activities and protein levels. Values were normalized to protein levels because the TK-luciferase activity was not appreciable in these cells at confluence

AhR/RelA complexes bind to the URE NF-κB element

To determine whether the AhR and RelA proteins are able to associate with the NF-κB binding elements in the c-*myc* gene, electrophoretic mobility shift assays (EMSA) were performed using an oligonucleotide containing the NF-κB upstream regulatory element (URE) as probe. To enhance AhR and RelA expression, nuclear extracts from transfected Hs578T cells were used. (Hs578T cells were selected rather than MCF-10F cells because of the better transfection efficiency obtained with this line.) Confluent cultures of Hs578T cells were transfected using FUGENE with *pcDNA3-AhR* vector DNA in the absence or presence of *pEVRF-p65* RelA expression plasmid. As an additional control, cells were transfected with empty parental *pcDNA3* vector alone. Nuclear extracts, prepared 24 h post-transfection, were then used in EMSA. Since an AhR/RelA complex might not bind DNA with the same affinity as typical NF-κB complexes, a lower dI:dC concentration was used to reduce the likelihood of competing away a specific binding complex. In control cells transfected with only parental *pcDNA3*, a major band migrating with the mobility of classic NF-κB was detected (labeled as band 1 in Figure 3a). No change in the binding pattern was seen upon transfection with *pcDNA3-AhR*. When nuclear extracts from cells co-transfected with *pEVRF-p65* and *pcDNA3-AhR* expression plasmids were used, both the putative classic NF-κB band and a novel upper band (labeled 'N') were seen (Figure 3a). The intensity of band 1 increased. Equal loading of the lanes was confirmed in EMSA for an Oct-1 probe (data not shown). Addition of fourfold or 20-fold molar excess wild type URE oligonucleotide successfully competed away complexes represented in both bands, whereas addition of similar amounts of mutant URE oligonucleotide, having the same two G to C conversions as in the p1.6 Bgl dbl mut construct (Duyao *et al*., 1992), failed to compete (Figure 3b).

To determine the identity of the subunits found in the two specific binding complexes, supershift EMSA was performed using polyclonal rabbit antibodies raised against either RelA or the AhR. Addition of the AhR antibody specifically ablated band N without significantly changing the migration pattern of band 1 (Figure 4a). Antibody alone plus probe did not yield a similar complex (Figure 4c). Furthermore, the AhR antibody had no affect on binding of nuclear proteins to an Oct-1 sequence (data not shown). Addition of the RelA-specific antibody (sc-372X) clearly ablated formation of both band 1 and band N (Figure 4b,c). Addition of a second RelA-specific antibody #1226 (kindly provided by N Rice) similarly reduced formation of both band 1 and band N (data not shown). In contrast, addition of an antibody against the p50 subunit reduced band 1 and ablated a minor band below (Figure 4b). An equivalent amount of a rabbit polyclonal antibody against an irrelevant protein

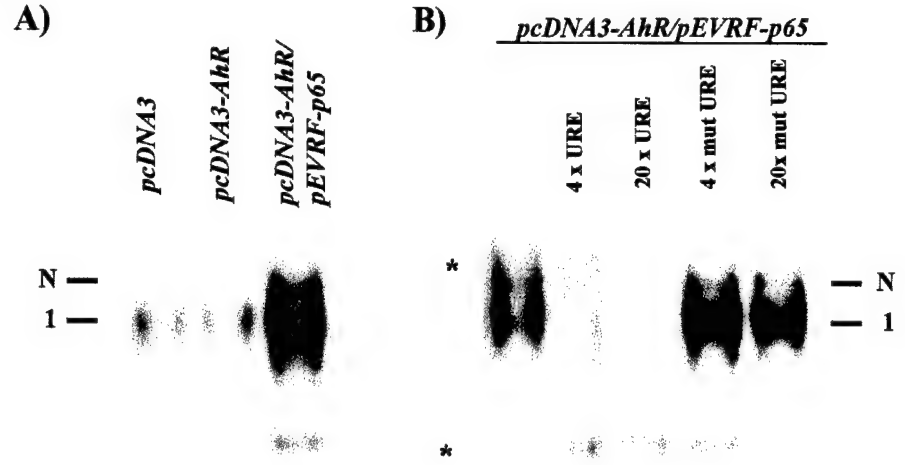

Figure 3 Expression of RelA and AhR yields a novel URE NF-κB element binding complex. (**a**) Co-transfection with AhR and RelA expression vectors leads to formation of a novel complex. Confluent cultures (100 mm^2 dishes) of Hs578T cells were transfected with either 52 μg *pcDNA3* empty vector, or 50 μg *pcDNA3-AhR* in the absence or presence of 2 μg *pEVRF-p65* expression plasmid using 70 μl FUGENE reagent. After 24 h, nuclear proteins were isolated using the method of Dignam *et al.* (1983), and subjected to EMSA for NF-κB binding. N indicates position of a new complex; 1, indicates position of a previously observed major complex. (**b**) Competition EMSA confirms the specificity of the major bands. Nuclear extracts of Hs578T cells co-transfected with *pcDNA3-AhR* and *pEVRF-p65* were pre-incubated with either 4- or 20-fold molar excess unlabeled wildtype (URE) or mutant (mt URE) URE prior to the 30 min incubation reaction with the radiolabeled URE. Two nonspecific bands were identified and marked with an asterisk (*)

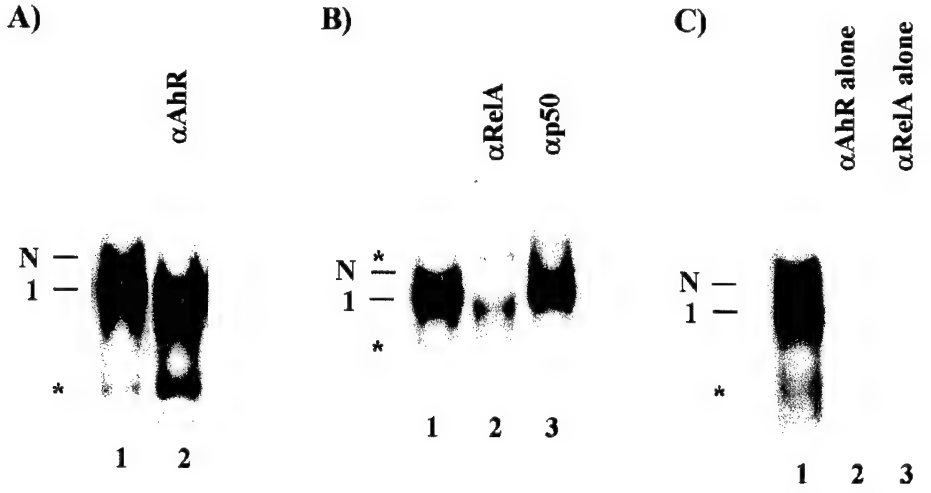

Figure 4 Novel NF-κB binding complex contains AhR and RelA protein. Nuclear extracts from the AhR and RelA expression vector co-transfected cells, prepared as described above in Figure 3, were incubated with the URE probe. Following a 30 min binding reaction, antibodies were added as indicated, the reactions incubated for an additional 1 h, and subjected to EMSA. Alternatively as control, antibodies were added to the probe in the absence of extract, and the mixture incubated as above, and subjected to EMSA. (**a**) Extracts were incubated in the absence (lane 1) or presence of 1 μl AhR-specific antibody (BioMol #SA-210) (lane 2) and subjected to EMSA. Specific binding complexes are indicated as band 1 and band N, as above; nonspecific bands are marked with an asterisk (*). (**b**) Extracts were incubated in the absence (lane 1) or presence of either 1 μl RelA-specific antibody (sc-372X) (lane 2) or 1 μl p50-specific antibody (sc-114) (lane 3), and processed as above. (**c**) Extract was incubated in the absence of antibody and EMSA performed, as above (lane 1). Alternatively either 1 μl AhR-specific antibody (BioMol #SA-210) (lane 2) or 1 μl RelA-specific antibody (sc-372X) (lane 3) was incubated with the probe alone, and subjected to EMSA

(YY1, sc-281-X) failed to alter binding to the URE (data not shown). Thus, band 1 contains RelA and p50 proteins, and most likely represents binding of classical NF-κB heterodimers (RelA/p50). Based on its migration, the minor lower band likely consists of p50 homodimers. Finally, band N contains both RelA and AhR proteins.

*AhR and RelA induce the endogenous c-*myc *gene*

To verify that the affects of AhR and RelA can be seen on chromosomal c-*myc* genes, co-transfection analysis was performed. Cultures of MCF-10F cells at 70% confluence were transfected with *pEVRF-p65* or *T7-pcDNA3-AhR* vector DNA alone or in combination.

Whole cell extracts were prepared and subjected to immunoblot analysis for c-Myc and β-actin protein, which confirmed equal loading (Figure 5). Using densitometry of this and a duplicate experiment, an increase in c-Myc level of 3.1 ± 0.00-fold and 2.75 ± 0.05-fold, respectively upon expression of RelA or AhR alone compared to control vector DNA was measured. An increase in c-Myc expression of 9.5 ± 3.2-fold was observed upon co-transfection of both *pEVRF-p65* and *T7-pcDNA3-AhR* vector DNAs into MCF-10F cells. Thus, while increases in the level of c-Myc protein were seen upon transfection of MCF-10F cells with either vector alone, a greater induction was seen upon transfection of the combination of *pEVRF-p65* and *T7-pcDNA3-AhR* vector DNAs. These results confirm the ability of RelA and AhR to cooperate in activation of the c-*myc* gene.

Discussion

Here we show the physical and functional association of the RelA subunit of NF-κB and AhR in transactivation of the c-*myc* gene in breast epithelial cells. Specifically, RelA and AhR were physically associated in malignant Hs578T breast cancer. Using transfection analysis, RelA and AhR cooperated to transactivate the c-*myc* promoter in non-malignant MCF-10F mammary epithelial cells and to a lesser extent Hs578T cells. Furthermore, RelA and AhR enhanced endogenous c-Myc protein levels in MCF-10F cells. As judged by transfection and mobility shift analyses, the RelA and AhR proteins formed a novel complex that bound to the wild type but not mutant NF-κB element of the c-*myc* gene. We postulate it is this complex, binding via the NF-κB element, that transactivated the c-*myc* promoter. Co-transfection of vectors that express AhR and RelA proteins with a wild type c-*myc* promoter-reporter construct, but not with a promoter construct mutated in the NF-κB binding URE and IRE sites, led to increased levels of c-*myc* promoter transactivation. In contrast, cooperation between AhR and RelB or c-Rel subunits of NF-κB/Rel in transactivation of the c-*myc* gene was not observed in similar transfection analysis (data not shown). Furthermore, the novel transcription factor complex did not appear to contain the p50 subunit. Consistent with these findings, RelA but not p50 was found to specifically interact with the AhR in murine hepatoma cells (Tian *et al*., 1999). Thus, based on the relative mobility in EMSA, and the identified presence of both RelA and AhR in the novel complex, our results suggest that the RelA and AhR bind the URE as a heterotypic dimer composed of one subunit of each protein.

Recently, we demonstrated that rodent and human mammary tumors are typified by aberrant activation of NF-κB/Rel (Sovak *et al*., 1997) and overexpression of AhR (Trombino *et al*., 2000). These tumors are often also characterized by overexpression of c-*myc* (Berns *et al*., 1992; Borg *et al*., 1992; Pavelic *et al*., 1991; DWK and GES, unpublished observations). While in some tumors c-*myc* genes were present in large copy numbers, in other cases overexpression of c-Myc protein was seen without gene amplification (Pavelic *et al*., 1991). The ability of AhR to cooperate with RelA to transactivate promoters through NF-κB elements suggests a novel mechanism for regulation of c-*myc* gene expression.

RelA protein interactions with other transcription factors have been found to lead either to induction (Bassuk *et al*., 1997; Shen and Stavnezer, 1998) or repression (Wissink *et al*., 1997; Ferrier *et al*., 1999) of gene transactivation. In most cases, transcription complex-DNA association involves binding sites for both NF-κB and the partner transcription factor, which are in close proximity to one another (Shen and Stavnezer, 1998; Dickinson *et al*., 1999). However, neither a consensus XRE, which would bind AhR/ARNT complexes, nor an AhR binding half site (5′-CGTC-3′) (Dickinson *et al*., 1999) are present in close proximity to either the URE or the IRE NF-κB elements in the murine c-*myc* gene. In addition, a 10- or 50-fold molar excess of cold XRE did not compete successfully for AhR/RelA-URE binding (data not shown), suggesting that DNA domains typically bound by an AhR/ARNT complex are not required for AhR/RelA-URE binding. Consistent with this observation, competition EMSA with oligonucleotides mutated at additional bases within the core NF-κB element failed to successfully compete for binding (data not shown).

Our findings differ significantly from those reported by Tian and coworkers (1999) who observed repression of RelA transactivation by AhR in a murine cell line. Several explanations may be given for these differences. Tian *et al*. (1999) used a multimerized consensus NF-κB element (5′-GGCAGGGGAATTCCCC-3′) construct in their studies, while we employed a c-*myc* promoter construct. Of note, the core sequence of the consensus binding element differs significantly from that found in the two NF-κB elements within the c-*myc* gene (Duyao *et al*., 1990; Kessler *et al*., 1992b). Interestingly, no new binding complex was seen with the NF-κB consensus element (Tian *et al*., 1999), whereas EMSA with the c-*myc* URE NF-κB element revealed a novel AhR/RelA-containing band, consistent with the functional cooperation in cells co-transfected with AhR and RelA expression vectors. If DNA binding is sequence specific, then only a subset of NF-κB element-containing genes may be affected by

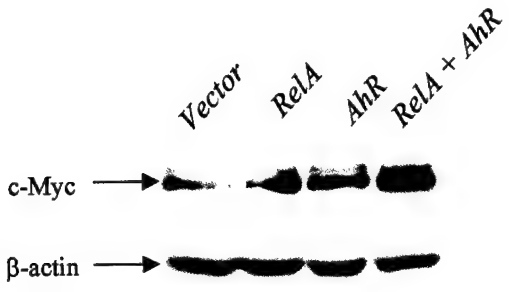

Figure 5 RelA and AhR cooperate to induce the endogenous c-*myc* gene in MCF-10F cells. Cultures of MCF-10F cells, at 70% confluence, were transiently transfected with 4 μg *pEVRF-p65* or 20 μg *T7-pcDNA3-AhR* DNA alone or in combination with 30 μl FUGENE transfection reagent. Total transfected DNA was maintained at 24 μg by addition of *pcDNA3* plasmid. Alternatively, cells were transfected with *pcDNA3* plasmid DNA alone (Vector). After 48 h, cells were harvested and samples of whole cell extracts (40 μg) subjected to immunoblot analysis for c-Myc (786-4) and β-actin (AC-15) proteins

AhR/RelA binding. Furthermore, the c-*myc* promoter likely contains elements capable of binding other potential cooperating transcription factors. Important differences also reside within the cell types used, i.e. murine hepatoma and COS-7 cells *vs* human mammary cell lines. Interestingly, NF-κB failed to transactivate the c-*myc* promoter in normal mouse hepatocytes (Bellas and Sonenshein, 1999), while it effectively induced the promoter in breast cancer cells (Sovak *et al.*, 1997), suggesting that binding to overlapping elements within the c-*myc* gene ablated the ability of NF-κB to bind in hepatocytes.

Different subunits of the NF-κB/Rel family have been shown to interact with members of other protein families (Bassuk *et al.*, 1997; Shen and Stavnezer, 1998; Wissink *et al.*, 1997; Ferrier *et al.*, 1999; Dickinson *et al.*, 1999; Stein *et al.*, 1993; Raj *et al.*, 1996; Kalkoven *et al.*, 1996; Na *et al.*, 1999). In many of these cases, the associations are fairly specific for the RelA subunit, e.g., with glucocorticoid and progesterone receptors (Wissink *et al.*, 1997; Kalkoven *et al.*, 1996) and the YB-1 protein (Raj *et al.*, 1996). In contrast, Stat6 (Shen and Stavnezer, 1998), C/EBP (Stein *et al.*, 1993), and retinoid X receptor (Na *et al.*, 1999) functionally interact with both RelA and p50. Therefore, it is not unusual that only cooperation between AhR and RelA was detected in HMECs. Interestingly, a similar functional interaction of RelA with the progesterone receptor was noted in that p50 and c-Rel subunits failed to affect the transcriptional activity of the activated PR on a progesterone responsive element construct (Kalkoven *et al.*, 1996). The Rel homology region (RHR) is known to be important both for dimerization of NF-κB/Rel subunits (Grimm and Baeuerle, 1993), as well as for interaction with many of these other proteins (Wissink *et al.*, 1997; Stein *et al.*, 1993). While some AhR domains involved in AhR binding to proteins, such as ARNT, hsp90, and the immunophilin-like ARA-9 protein have been evaluated (Perdew and Bradfield, 1996; Meyer *et al.*, 1998; Okey *et al.*, 1994; Carver *et al.*, 1998), those required for AhR dimerization with other proteins, e.g. Rb (Ge and Elferink, 1998), have not been defined. The exact domains mediating the interactions between AhR/RelA and binding of the putative heterodimeric complex to the c-*myc* promoter are under investigation.

The human c-*myc* gene has been found to contain consensus XRE elements. Since our efforts were focused on the potential effects of AhR/RelA interactions, a c-*myc* promoter construct that does not contain these elements was used to reduce complications with effects of AhR alone. Finally, it should be noted that c-*myc* promoter activation following transfection with AhR- and RelA-encoding plasmids and AhR-RelA dimerization in the nuclei of non-transfected cells occurred in the absence of exogenous AhR ligands. These results suggest constitutive AhR activity in mammary tumor cell lines. This hypothesis is strongly supported by constitutive nuclear AhR expression (Chang and Puga, 1998; Singh *et al.*, 1996), and constitutive AhR-mediated transcriptional activity (Chang and Puga, 1998; Ma and Whitlock, 1996) in mouse hepatoma, monkey kidney, and human epithelial carcinoma cell lines. Furthermore, we have recently demonstrated constitutive nuclear AhR expression and high levels of an AhR-regulated gene, *CYP1B1*, in rat mammary tumors (Trombino *et al.*, 2000). While these results support a role for constitutive AhR activation in tumorigenesis, organ defects observed in $AhR^{-/-}$ mice suggest a role for developmentally regulated AhR activation in organogenesis (Hushka *et al.*, 1998; Fernandez-Salguero *et al.*, 1995; Lahvis and Bradfield, 1998; Abbott *et al.*, 1999; Robles *et al.*, 2000). The endogenous signals that induce AhR activity, and the extent to which these AhR activities are modulated by exogenous AhR ligands remain to be elucidated.

Materials and methods

Cell growth and treatment conditions

MCF-10F is a human mammary epithelial cell line established from a patient with fibrocystic disease, which does not display malignant characteristics (Calaf and Russo, 1993). The Hs578T tumor cell line was derived from a mammary carcinosarcoma and is epithelial in origin (Hackett *et al.*, 1977).

Synthesis of AhR expression construct

Full length *AhR* cDNA was PCR amplified using the pMu-AhR plasmid (kindly provided by Dr C Bradfield, University of Wisconsin, Madison, WI, USA) as template, with the following primers carrying *Xba*I restriction sites: sense 5′-CTA GTC TAG ACC ATG AGC AGC GGC GCC AAC-3′; anti-sense 5′-CTA GTC TAG AAA GCT TAG TAT CGA ATT-3′. The *AhR* cDNA was amplified with Pfu Turbo polymerase (Stratagene, La Jolla, CA, USA). The PCR product was gel purified and subcloned into the *Xba*I site of the *T7-pcDNA3* plasmid constructed by linking the DNA coding for the 11 amino acid leader peptide of the T7 major capsid protein (digested out from the pTOPE pET translation vector (Novagen, Madison, WI, USA) to the *Bam*HI site of *pcDNA3* (Invitrogen, Carlsbad, CA, USA). Proper *AhR* and *T7-pcDNA3* directional cloning was confirmed by restriction analysis and DNA sequencing.

Transfection and immunoprecipitation analysis

Cells were transfected in 100 mm^2 culture plates with 5 μg of *T7-pcDNA3-AhR* or *T7-pcDNA3* mixed with 6 μl FUGENE transfection reagent (Boehringer Mannheim, Indianapolis, IN, USA), according to the manufacturer's instructions. After 36 h, cells were rinsed with cold PBS. For total cell lysates, transfected or untransfected cells were lysed in 1 ml immunoprecipitation buffer (50 mM Tris-HCl, pH 8.0; 150 mM NaCl; 2 μg/ml leupeptin; 2 μg/ml aprotonin; 5 μg/ml phenylmethylsulfonyl fluoride) containing 1% IGEPAL CA-630 detergent (Sigma Chemical Co., St. Louis, MO, USA) for 20 min on ice, and centrifuged at 14 000 r.p.m. for 10 min. Alternatively, cytosolic and nuclear fractions were prepared essentially as described (Pollenz *et al.*, 1994). Aliquots were incubated for 1 h with 5 μg/ml polyclonal rabbit anti-RelA/p65 antibody, normal rabbit IgG, polyclonal goat anti-AhR antibody or normal goat IgG (all antibodies from Santa Cruz Biotechnology, Santa Cruz, CA, USA), and immunoprecipitates collected and washed using protein A-sepharose beads. Eluted proteins were subjected to electrophoresis and immunoblot analysis, as described previously (Yamaguchi *et al.*, 1997a,b). Blots were probed with HRP-anti-T7-epitope tag antibody (Novagen), anti-RelA antibody (sc-372, Santa Cruz Biotechnology), or polyclonal goat anti-AhR antibody (sc-8088, Santa Cruz Biotechnology) for 1 h at room temperature. After thorough washing, the membranes were treated for another 45 min with goat anti-rabbit-HRP antibody for RelA-specific

immunoblotting or with anti-goat IgG-HRP antibody for AhR-specific immunoblotting. Membranes were developed by chemiluminesence (Du Pont NEN Research Products Co., Boston, MA, USA) after washing three times with TBS containing 0.05% Tween (Sigma).

Transfection and immunoblot analysis

Cultures of MCF-10F cells, at 70% confluence, were transiently transfected with 4 μg *pEVRF-p65* or 20 μg *T7-pcDNA3-AhR* DNA alone or in combination with 30 μl FUGENE transfection reagent. Total DNA transfected was maintained at 24 μg by addition of *pcDNA3* plasmid. After 48 h, cells were rinsed with cold PBS, and harvested in lysis buffer (50 mM Tris-HCl, pH 8.0; 5 mM EDTA, pH 8.0; 150 mM NaCl; 0.5 mM DTT; 2 μg/ml aprotinin; 2 μg/ml leupeptin; 0.5 mM PMSF; 0.5% NP40). Whole cell extracts (WCE) were obtained by sonication, followed by centrifugation at 14 000 r.p.m. for 30 min. Samples (40 μg) of WCEs were subjected to electrophoresis and immunoblot analysis, as above. Blots were probed with rabbit anti-c-Myc antibody (786-4, a gift from S Hann, Vanderbilt University, Memphis, TN, USA), and mouse anti-β-actin monoclonal antibody (AC-15, Sigma).

Promoter activity analysis

Confluent cultures of MCF-10F or Hs578T cells were transiently transfected using FUGENE transfection, as above, with wild type p1.6 Bgl c-*myc* promoter CAT or a mutant c-*myc* promoter CAT reporter, termed p1.6 Bgl dbl mut vector, described previously (Duyao *et al*., 1992). These constructs contain -1141 to $+513$ bp of the murine c-*myc* promoter/exon1/upstream sequences, including the two NF-κB elements in either wild type or mutant versions, driving a chloramphenicol acetyl transferase (CAT) reporter gene (Duyao *et al*., 1992), and does not contain XREs. Vectors *pcDNA3-AhR*, encoding murine AhR (Dolwick *et al*., 1993) and *pEVRF-p65*, encoding murine RelA protein (kindly provided by R Sen, Brandeis University, Waltham, MA, USA) were co-transfected, as indicated. In each transfection, 1 μg of TK-luciferase plasmid was added as an internal control for normalization of transfection efficiency. Total DNA transfected was maintained at 6 μg by addition of *pcDNA3* plasmid (parent vector for *pcDNA3-AhR*). Transfected cells were harvested after 24 h in reporter lysis buffer, and analysed for CAT and luciferase activity, as described previously (Sovak *et al*., 1997; Dolwick *et al*., 1993).

EMSA

Nuclear extracts were prepared from breast cancer cells by a modification of the method of Dignam *et al*. (1983), and oligonucleotides probes radiolabeled essentially as we have described previously (Sovak *et al*., 1997). The sequence of the URE NF-κB-containing oligonucleotide from the c-*myc* gene (Duyao *et al*., 1990) is as follows: 5′-GATCCAAGTCCGG-GTTTTCCCCAACC-3′, where the underlined region indicates the core binding element. The mutant URE has a two G to C base pair conversion, indicated in bold, blocking the NF-κB/Rel binding (Duyao *et al*., 1990): 5′-GATCCAA-GTCC**GCCTTTTCCCC**AA CC-3′. A slight modification of the usual NF-κB binding reaction (Sovak *et al*., 1997) was used. ^{32}P-labeled oligonucleotide (20 000–25 000 c.p.m.) was incubated with 2.5 μg of nuclear extract, 5 μl sample buffer (10 mM HEPES, 4 mM DTT, 0.5% Triton X-100, and 2.5% glycerol), 0.1 μg poly dI-dC as nonspecific competitor, and the salt concentration adjusted to 100 mM using buffer C. The reaction was carried out at room temperature for 30 min, and DNA/protein complexes were separated, as previously described (Sovak *et al*., 1997). Where indicated, antibodies were added after the binding reaction and the mixture incubated for 1 additional hour. Antibodies used include: anti-RelA subunit, sc-372X from Santa Cruz Biotechnology and #1226, kindly provided by N Rice (NCI, Frederick, MD, USA); anti-p50 subunit, sc-114 from Santa Cruz Biotechnology; anti-AhR, #SA-210 from BioMol (Plymouth Meeting, PA, USA).

Acknowledgments
We thank Nancy Rice, S Hann, R Sen and C Bradfield for generously providing antibody, and cloned DNAs, respectively. Darin Sloneker is acknowledged for assistance in preparation of the manuscript. This work was supported by grants from the Department of Army DAMD 17-98-1-8034 (DW Kim), and DAMD 17-98-1 (GE Sonenshein), the Association pour la Recherche sur le Cancer (R Romieu-Mourez), the Fondation Bettencourt-Schueller (R Romieu-Mourez), and the NIH RO1 ES06086 (DH Sherr) and RO1 CA 82742 (GE Sonenshein) and a Superfund Basic Research Grant #1P42ES 07381 (DH Sherr).

References

Abbott BD, Schmid JE, Pitt JA, Buckalew AR, Wood CR, Held GA and Diliberto JJ. (1999). *Toxicol. Appl. Pharmacol.*, **155,** 62–70.
Ballard DW, Dixon EP, Peffer NJ, Bogerd H, Doerre S, Stein B and Greene WC. (1992). *Proc. Natl. Acad. Sci. USA*, **89,** 1875–1879.
Bassuk AG, Anandappa RT and Leiden JM. (1997). *J. Virol.*, **71,** 3563–3573.
Berns EM, Klijn JG, van Putten WL, van Staveren IL, Portengen H and Foekens JA. (1992). *Cancer Res.*, **52,** 1107–1113.
Bellas RE and Sonenshein GE. (1999). *Cell. Growth Differ.*, **10,** 287–294.
Borg A, Baldetorp B, Ferno M, Olsson H and Sigurdsson H. (1992). *Int. J. Cancer*, **51,** 687–691.
Calaf G and Russo J. (1993). *Carcinogenesis*, **14,** 483–492.
Carver LA and Bradfield CA. (1997). *J. Biol. Chem.*, **272,** 11452–11456.
Carver LA, LaPres JJ, Jain S, Dunham EE and Bradfield CA. (1998). *J. Biol. Chem.*, **273,** 33580–33587.
Chang CY and Puga A. (1998). *Mol. Cell. Biol.*, **18,** 525–535.
Dickinson LA, Trauger JW, Baird EE, Dervan PB, Graves BJ and Gottesfeld JM. (1999). *J. Biol. Chem.*, **274,** 12765–12773.
Dignam JD, Lebovitz RM and Roeder RG. (1983). *Nucleic Acids Res.*, **11,** 1475–1489.
Dolwick KM, Swanson HI and Bradfield CA. (1993). *Proc. Natl. Acad. Sci. USA*, **90,** 8566–8570.
Duyao MP, Buckler AJ and Sonenshein GE. (1990). *Proc. Natl. Acad. Sci. USA*, **87,** 4727–4731.
Duyao MP, Kessler DJ, Spicer DB, Bartholomew C, Cleveland J, Siekevitz M and Sonenshein GE. (1992). *J. Biol. Chem.*, **267,** 16288–16291.
Enan E and Matsumura F. (1996). *Biochem. Pharmacol.*, **52,** 1599–1612.
Fernandez-Salguero P, Pineau T, Hilber DM, McPhail T, Lee SS, Kimura S, Nebert DW, Rudikoff S, Ward JM and Gonzalez FJ. (1995). *Science*, **268,** 722–726.
Ferrier R, Nougarede R, Doucet S, Kahn-Perles B, Imbert J and Mathieu-Mahul D. (1999). *Oncogene*, **18,** 995–1005.
Ge NL and Elferink CJ. (1998). *J. Biol. Chem.*, **273,** 22708–22713.

Grilli M, Chiu J and Lenardo M. (1991). *Intl. Rev. Cytol.*, **143,** 1–62.
Grimm S and Baeuerle PA. (1993). *Biochem. J.*, **290,** 297–308.
Hackett AJ, Smith HS, Springer EL, Owens RB, Nelson-Rees WA, Riggs JL and Gardner MB. (1977). *J. Natl. Cancer. Inst.*, **58,** 1795–1806.
Hushka LJ, Williams JS and Greenlee WF. (1998). *Toxicol. Appl. Pharmacol.*, **152,** 200–210.
Jain S, Dolwick KM, Schmidt JV and Bradfield CA. (1994). *J. Biol. Chem.*, **269,** 31518–31524.
Kalkhoven E, Wissink S, van der Saag PT and van der Burg B. (1996). *J. Biol. Chem.*, **271,** 6217–6224.
Kessler DJ, Duyao MP, Spicer DB and Sonenshein GE. (1992a). *J. Exp. Med.*, **176,** 787–792.
Kessler DJ, Spicer DB, La Rosa FA and Sonenshein GE. (1992b). *Oncogene*, **7,** 2447–2453.
Lahvis GP and Bradfield CA. (1998). *Biochem. Pharmacol.*, **56,** 781–787.
La Rosa FA, Pierce JW and Sonenshein GE. (1994). *Mol. Cell. Biol.*, **4,** 1039–1044.
Ma Q and Whitlock Jr. JP. (1996). *Mol. Cell. Biol.*, **16,** 2144–2150.
Meyer BK, Pray-Grant MG, Vanden Heuvel JP and Perdew GH. (1998). *Mol. Cell. Biol.*, **18,** 978–988.
Na SY, Choi JE, Kim HJ, Jhun BH, Lee YC and Lee JW. (1999). *J. Biol. Chem.*, **274,** 28491–28496.
Nebert DW, Petersen DD and Fornace Jr. AJ. (1990). *Environ. Health Perspect.*, **88,** 13–25.
Nebert DW, Petersen DD and Puga A. (1991). *Pharmacogenetics*, **1,** 68–78.
Okey AB, Riddick DS and Harper PA. (1994). *Toxicol. Lett.*, **70,** 1–22.
Pavelic ZP, Steele P and Presler HD. (1991). *Anticancer Res.*, **11,** 1421–1427.
Perdew GH and Bradfield CA. (1996). *Biochem. Mol. Biol. Int.*, **39,** 589–593.
Pollenz RS, Sattler CA and Poland A. (1994). *Mol. Pharmacol.*, **45,** 428–438.
Raj GV, Safak M, MacDonald GH and Khalili K. (1996). *J. Virol.*, **70,** 5944–5953.
Robles R, Morita Y, Mann KK, Perez GI, Yang S, Matikainen T, Sherr DH and Tilly JL. (2000). *Endocrinology*, **141,** 450–453.
Shen CH and Stavnezer J. (1998). *Mol. Cell. Biol.*, **18,** 3395–3404.
Singh SS, Hord NG and Perdew GH. (1996). *Arch. Biochem. Biophys.*, **329,** 47–55.
Sovak MA, Bellas RE, Kim DW, Zanieski GJ, Rogers AE, Traish AM and Sonenshein GE. (1997). *J. Clin. Invest.*, **100,** 2952–2960.
Stein B, Cogswell PC and Baldwin Jr. AS. (1993). *Mol. Cell. Biol.*, **13,** 3964–3974.
Tian Y, Ke S, Denison MS, Rabson AB and Gallo MA. (1999). *J. Biol. Chem.*, **274,** 510–515.
Trombino AF, Near RI, Matulka RA, Yang S, Hafer LJ, Toselli PA, Kim DW, Rogers AE, Sonenshein GE and Sherr DH. (2000). *Breast Cancer Research and Treatment*, **63,** 117–131.
Verma IM, Stevenson JK, Schwartz EM, Van Antwerp D and Miyamoto S. (1995). *Genes Develop.*, **9,** 2723–2735.
Wissink S, van Heerde ED, Schmitz ML, Kalkhoven E, van der Burg B, Baeuerle PA and van der Saag PT. (1997). *J. Biol. Chem.*, **272,** 22278–22284.
Yamaguchi K, Matulka RA, Shneider AM, Toselli P, Trombino AF, Yang S, Hafer LJ, Mann KK, Tao XJ, Tilly JL, Near RI and Sherr DH. (1997a). *Toxicol. Appl. Pharmacol.*, **147,** 190–203.
Yamaguchi K, Near RI, Matulka RA, Shneider A, Toselli P, Trombino AF and Sherr DH. (1997b). *J. Immunol.*, **158,** 2165–2173.

Oncogene (2001) 20, 1287–1299

www.nature.com/onc

ORIGINAL PAPERS

Her-2/neu overexpression induces NF-κB via a PI3-kinase/Akt pathway involving calpain-mediated degradation of IκB-α that can be inhibited by the tumor suppressor PTEN

Stefania Pianetti[1], Marcello Arsura[1,3], Raphaëlle Romieu-Mourez[1], Robert J Coffey[2] and Gail E Sonenshein*[,1]

[1]*Department of Biochemistry and the Program in Research on Women's Health, Boston University Schools of Medicine, Boston, Massachusetts, MA 02118, USA;* [2]*Vanderbilt University, Nashville, Tennessee, TN 37232, USA*

The Nuclear Factor (NF)-κB family of transcription factors controls expression of genes which promote cell growth, survival, and neoplastic transformation. Recently we demonstrated aberrant constitutive activation of NF-κB in primary human and rat breast cancer specimens and in cell lines. Overexpression of the epidermal growth factor receptor (EGFR) family member Her-2/neu, seen in approximately 30% of breast cancers, is associated with poor prognosis. Previously, Her-2/neu has been shown to signal via a phosphatidylinositol 3 (PI3)-kinase to Akt/protein kinase B (PKB) pathway. Since this signaling pathway was recently shown to activate NF-κB, here we have tested the hypothesis that Her-2/neu can activate NF-κB in breast cancer. Overexpression of Her-2/neu and EGFR-4 in Ba/F3 cells led to constitutive PI3- and Akt kinase activities, and induction of classical NF-κB (p50/p65). Similarly, a tumor cell line and tumors derived from MMTV-Her-2/neu transgenic mice displayed elevated levels of classical NF-κB. Engagement of Her-2/neu receptor downregulated the level of NF-κB. NF-κB binding and activity in the cultured cells was reduced upon inhibition of the PI3- to Akt kinase signaling pathway via ectopic expression of kinase inactive mutants, incubation with wortmannin, or expression of the tumor suppressor phosphatase PTEN. Inhibitors of calpain, but not the proteasome, blocked IκB-α degradation. Inhibition of Akt did not affect IKK activity. These results indicate that Her-2/neu activates NF-κB via a PI3- to Akt kinase signaling pathway that can be inhibited via the tumor suppressor PTEN, and is mediated by calpain rather than the IκB kinase complex. *Oncogene* (2001) **00**, 1287–1299.

Keywords: breast cancer; EGF receptor; transgenic mice; NF-κB; IκB-α; calpain

Introduction

NF-κB/Rel is a family of dimeric transcription factors characterized by the presence of a Rel homology region (RHR) of about 300 amino acids in length, which controls multiple functions including dimerization and nuclear localization. Classical NF-κB is a heterodimer composed of p65 (or RelA) and p50 (or NFκB1) subunits (Grimm and Baeuerle, 1993). The RelA subunit has potent transactivation ability, while the p50 subunit has only modest transactivation potential *in vivo*, but binds very avidly to an NF-κB element (Ballard *et al.*, 1992; Grimm and Baeuerle, 1993; La Rosa *et al.*, 1994). Many genes are regulated by NF-κB (Grimm and Baeuerle, 1993). For example, we demonstrated that the c-*myc* oncogene is potently transactivated by NF-κB/Rel factors (Duyao *et al.*, 1992; Kessler *et al.*, 1992; La Rosa *et al.*, 1994). In most cells, other than B lymphocytes, NF-κB/Rel proteins are sequestered in the cytoplasm bound to one of the specific inhibitory proteins termed IκBs of which IκB-α is the paradigm. During activation of NF-κB by such extracellular stimuli as TNF and IL-1, phosphorylation of IκB-α by the IκB kinase complex targets the inhibitor protein for degradation via the proteasome pathway. The IκB kinase complex contains two IκB kinases, IKKα (or IKK-1) and IKKβ (or IKK-2). Activation of the IκB kinase complex is mediated via phosphorylation of either IKKα or IKKβ (DiDonato *et al.*, 1997; Mercurio *et al.*, 1997; Regnier *et al.*, 1997; Woronicz *et al.*, 1997). IκB-α is then recruited in the IκB kinase complex, where it is phosphorylated by the functional IKKα/IKKβ heterodimer at serine residues at positions 32 and 36 (reviewed in Mercurio and Manning, 1999). This phosphorylation is followed by ubiquitination and rapid degradation through the proteasome pathway (Brown *et al.*, 1995; Chen *et al.*, 1996; DiDonato *et al.*, 1996). This pathway is not universal, however, and proteasome-mediated degradation of IκBα has been ruled out recently in the case of NF-κB induction by oxidative stress and in its constitutive expression in early mature B cells (Fields *et al.*, 2000; Miyamoto *et al.*, 1998; Schoonbroodt *et al.*,

*Correspondence: GE Sonenshein, Department of Biochemistry, Boston University Medical School, 715 Albany Street, Boston, MA 02118, USA
[3]Current address: Department of Pharmacology, University of Tennessee, Memphis, TN 38163, USA
Received 20 October 2000; revised 5 January 2001; accepted 9 January 2001

2000). In these cases, degradation of IκB-α by calpain has been implicated.

Several years ago, we (Sovak *et al.*, 1997) and others (Nakshatri *et al.*, 1997) demonstrated that breast cancer cell lines and primary breast cancer specimens are typified by aberrant constitutive activation of NF-κB. Specifically, human breast tumor cell lines, and the majority of primary human breast tumor tissue samples and mammary tumors induced upon carcinogen treatment of female Sprague-Dawley rats were found to constitutively express high levels of nuclear NF-κB/Rel. In contrast, untransformed breast epithelial cells and normal rat mammary glands contained the expected low basal levels. The Her-2/neu (or c-erbB-2) oncogene, the second member of the epidermal growth factor (EGF) receptor family (EGFR-2), encodes a transmembrane tyrosine kinase receptor. Overexpression of Her-2/neu, which has been seen in approximately 30% of breast cancers, is associated with poor overall survival (Hortobagyi *et al.*, 1999). In particular, it has been found associated with increased metastatic potential and resistance to chemotherapeutic agents. Transgenic mice overexpressing Her-2/neu develop focal mammary tumors after a long latency, whereas, multi-focal tumors appeared after a significantly reduced time frame upon overexpression of both Her-2/neu and TGF-α, a ligand for this EGFR member (Guy *et al.*, 1992; Muller *et al.*, 1996). Recent work has implicated the phosphatidylinositol 3 (PI 3)-kinase and serine/threonine kinase Akt/protein kinase B (PKB) in Her-2/neu signaling (Adam *et al.*, 1998; Ignatoski *et al.*, 2000). PI3-kinase has been shown to play an important role in proliferation and cell survival induced by many cytokines (Miyajima *et al.*, 1999). The tumor suppressor PTEN is a multifunctional phosphatase, which is capable of dephosphorylating products of PI3-kinase (Di Cristofano and Pandoli, 2000). PI3-kinase signaling is mediated via activation of the serine/threonine kinase Akt/protein kinase B (PKB) (Kennedy *et al.*, 1997). PI3-kinase signaling has also been linked to the induction of NF-κB (Arsura *et al.*, 2000; Beraud *et al.*, 1999). For example, we showed that PI3-kinase signaled NF-κB activation via IKKα in Ras-transformed rat liver epithelial cells (Arsura *et al.*, 2000). Furthermore, Akt was recently shown to activate NF-κB via the IKK complex in response to TNF or PDGF stimulation (Ozes *et al.*, 1999; Romashkova and Makarov, 1999). Thus, here we have examined the role of Her-2/neu in mediating induction of NF-κB in breast cancer. We demonstrate NF-κB induction in breast cancer cell lines and primary mouse tumors. Furthermore, activation occurs via a PI3-kinase to Akt pathway that can be repressed by the tumor suppressor PTEN. Surprisingly, this activation does not appear to be mediated via the IKK complex proteasome pathway but rather our results implicate calpain in the basal degradation of IκB-α.

Results

Overexpression of Her-2/neu + EGFR-4 induces NF-κB

To determine whether overexpression of Her-2/neu can lead to induction of NF-κB, we characterized Ba/F3 clones stably expressing either EGFR-1 (Ba/F3-1), EGFR-2 (Her-2/neu) (Ba/F3-2), or combinations of EGFR-1 + Her-2/neu (Ba/F3-1 + 2), and Her-2/neu + EGFR-4 (Ba/F3-2 + 4). Ba/F3 cells transfected with the empty vector LXSN DNA were employed as control (termed parental Ba/F3 here). We first confirmed the previously observed basal tyrosine phosphorylation activity of the Her-2/neu + EGFR-4 receptor signaling using immunoblotting (Riese *et al.*, 1996). Whole cell extracts (WCEs) were prepared from the four clones, as well as from parental Ba/F3 cells. Samples were subjected to an immunoblot assay with an antibody specific for phosphotyrosine Her-2/neu (Figure 1a). As expected, tyrosine phosphorylation of the Her-2/neu protein was observed in Ba/F3-2 + 4 cells overexpressing Her-2/neu + EGFR-4 proteins. In addition, low levels of activity were seen in Ba/F3-1 cells, expressing EGFR-1. Equal loading was confirmed by immunoblot analysis of the same filter for Akt protein levels. Thus, as seen previously (Riese *et al.*, 1996), overexpression of the Her-2/neu + EGFR-4 receptors in Ba/F3 leads to elevated kinase activity and resultant basal phosphorylation of Her-2/neu.

To assess NF-κB/Rel binding levels, nuclear extracts were prepared from the Ba/F3 lines and used in EMSA. An oligonucleotide containing the NF-κB element upstream of the c-*myc* promoter, which binds all Rel family members (La Rosa *et al.*, 1994) was used as probe. Nuclear extracts from the parental Ba/F3 cells and from the Ba/F3-2 cells displayed low levels of two NF-κB binding complexes (Figure 1b). Higher levels of band 1 were seen in the Ba/F3-1, Ba/F3-1 + 2 and Ba/F3-2 + 4 lanes. Interestingly, an increased level of band 2 was observed predominantly in the Ba/F3-2 + 4 cell extract, and to a lesser extent in the Ba/F3-1 lane (better seen with a longer exposure). Equal loading was confirmed by analysis for the ubiquitously expressed Sp1 protein (Figure 1b, bottom panel). Similar profiles were seen previously in wild-type Ba/F3 cells and bands 1 and 2 were identified as p50 homodimers, and classical NF-κB (p50/p65), respectively (Besancon *et al.*, 1998; Jeay *et al.*, 2000). To confirm the identity of the subunits within the Ba/F3-2 + 4 cells, supershift EMSA was performed (Figure 1c). Addition of an antibody that preferentially recognizes p50 in a homodimer complex, eliminated band 1 and reduced band 2. Addition of an antibody against p65 selectively reduced band 2. Taken together, these results indicate that band 1 contains p50 homodimers and band 2 is a heterodimer of p50/p65 or classical NF-κB. Thus, overexpression of the Her-2/neu + EGFR-4 receptors in Ba/F3 cells leads to elevated basal phosphorylation of Her-2/neu and to activation of classical NF-κB.

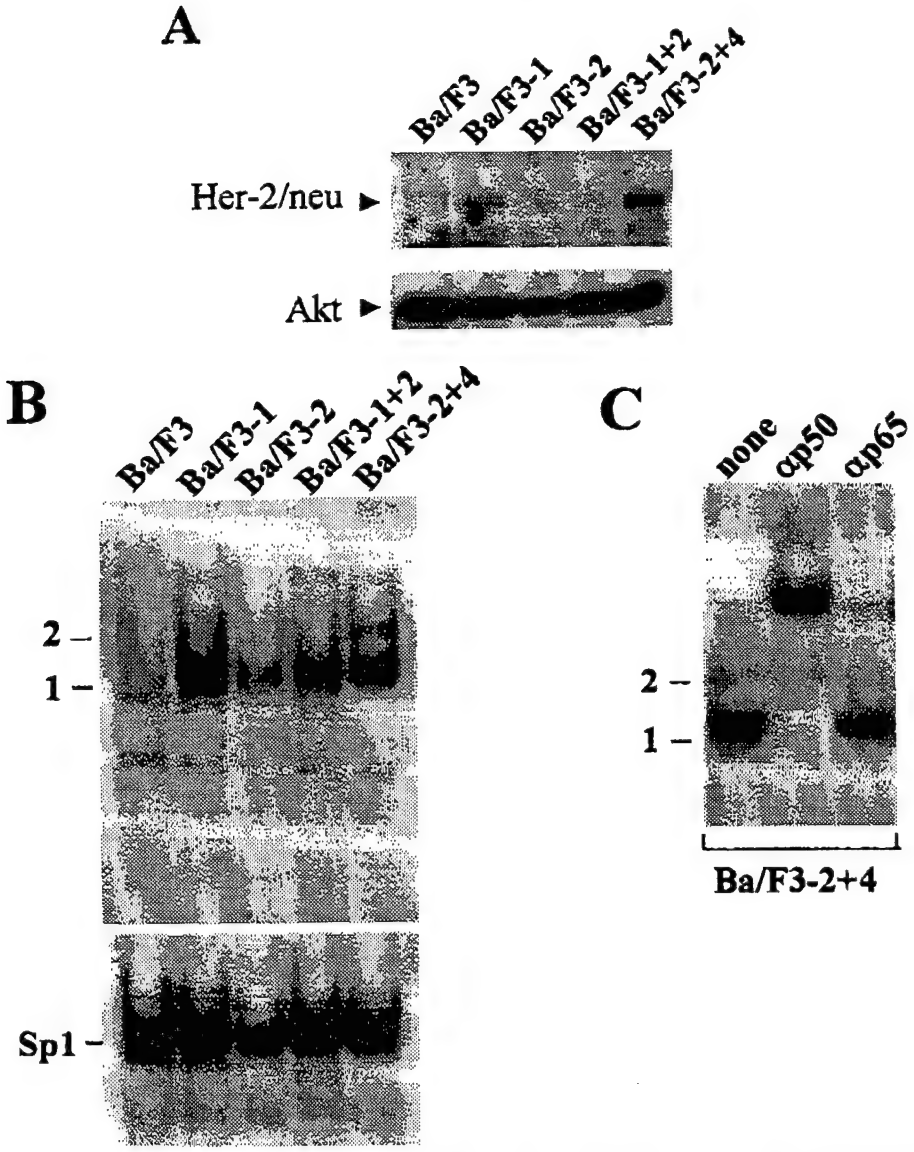

Figure 1 NF-κB activation in Ba/F3 cells expressing various EGF receptors. (a) Tyrosine phosphorylation of Her-2/neu is highest in Her-2/neu + erbB-4 double recombinant Ba/F3 clones. Total proteins were isolated with RIPA buffer from Ba/F3 clones, and samples (60 μg) were analysed by immunoblotting with an anti-phosphotyrosine Her-2/neu antibody (top panel), and an AKT antibody, as control for equal loading (bottom panel). Ba/F3 cell lines derived by transfection with vector LXSN DNA only, Ba/F3; vectors expressing EGFR, Ba/F3-1; Her-2/neu, Ba/F3-2; EGFR + Her-2/neu, Ba/F3-1+2; Her-2/neu + erbB-4, Ba/F3-2+4. (b) HER-2/neu + erbB-4 double recombinant Ba/F3 cells display elevated levels of NF-κB/Rel binding levels. Nuclear extracts were prepared from the Ba/F3 clones and used in EMSA with an oligonucleotide containing the URE NF-κB element upstream of the c-*myc* promoter, as probe (top panel) or with an Sp1 oligonucleotide, as a loading control (bottom panel). (c) Her-2/neu + erbB-4 double recombinant Ba/F3 cells express classical NF-κB. Supershift EMSA was performed with nuclear extracts from the Her-2/neu + erbB-4 transfected Ba/F3-2+4 cells in the absence (none) or presence of antibodies specific for NF-κB subunit: p50, sc-114 (αp50), or p65, sc-372 (αp65). The two major complexes, labeled bands 1 and 2, were identified as p50 homodimers and p50/p65, respectively

Activation of NF-κB occurs via a PI3-kinase signaling pathway

Her-2/neu has been shown to signal via PI3-kinase, which has been implicated in NF-κB induction (Arsura *et al.*, 2000). To test for involvement of this pathway, we employed wortmannin, a potent PI3-kinase inhibitor (Arcaro and Wymann, 1993). Ba/F3-2+4 cells were incubated for 24 h in the presence of 100 nM wortmannin, that had been dissolved in DMSO, or the equivalent amount of carrier solution. Wortmannin treatment resulted in a significant decrease in NF-κB binding compared to treatment with DMSO alone (Figure 2a). Equal loading of Sp1 confirmed the

selectivity of the observation. Since one of the important downstream targets of PI3-kinase is Akt, we next tested for phosphorylation of this kinase (Figure 2b). A significant decrease in Akt phosphorylation was noted upon 24 h treatment with 100 nM wortmannin. Densitometry indicated wortmannin-treated cells displayed 60% of the Akt phosphorylation seen in control cells. Thus, NF-κB activation in the Ba/F3-2+4 cells appears to be mediated via a PI3-kinase to Akt signaling pathway.

MMTV-Her-2/neu tumor cell line expresses elevated levels of classical NF-κB

The NF639 cell line was established from a mammary tumor that arose in the MMTV-Her-2/neu transgenic mouse (Elson and Leder, 1995). To test for NF-κB activation, EMSA was performed using nuclear extracts from these cells compared to non-tumorigenic MCF-10F HMECs, which express only low basal levels of classical NF-κB (Sovak *et al.*, 1997) (Figure 3). The level of binding was significantly higher in the NF639 line compared to MCF-10F cells. The specificity of the complexes was confirmed using competition assays and IκB-α-GST protein, a specific inhibitor of NF-κB DNA binding. Successful competition was observed with the NF639 cell extracts upon addition of excess oligonucleotide containing wild-type but not mutant URE NF-κB elements (Figure 3). Furthermore, addition of IκB-α GST fusion protein, greatly reduced formation of bands 1 and 2. Bands 1 and 2 in the human MCF-10F line have been identified as p50 homodimer and p50/p65 classical NF-κB, respectively (Kim *et al.*, 2000). Addition of an antibody against the p50 subunit greatly reduced bands 1 and 2, while addition of an antibody against p65 selectively reduced band 2. In contrast, addition of an antibody against c-Rel subunit had no detectable effect on these specific complexes, while a p52 specific antibody caused a slight reduction in band 1. Thus, antibody supershift analysis identified band 2 in the NF639 nuclear extract as consisting of heterodimers of p50 and p65, while band 1 contains p50 and possibly some p52 protein, as well.

Using transient transfection analysis of wild-type vs mutant NF-κB element driven CAT reporter constructs (E8 vs mutE8), we previously demonstrated that MCF-

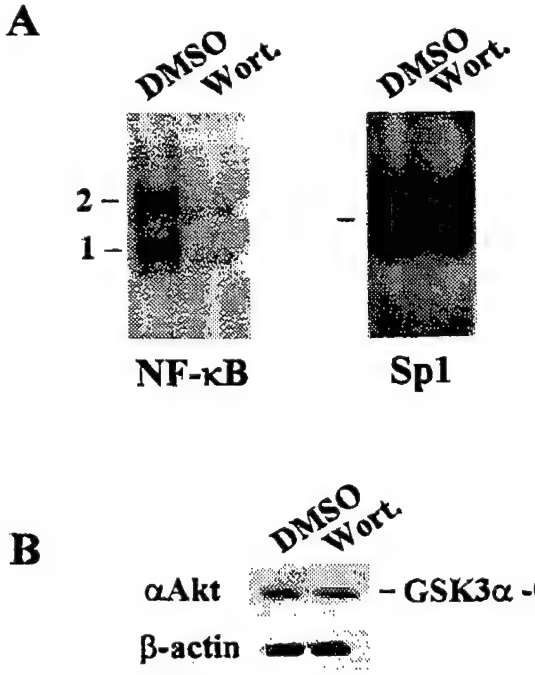

Figure 2 Wortmannin reduces NF-κB binding and phosphorylation of Akt. Her-2/neu+erbB-4 transfected Ba/F3-2+4 cells were incubated for 24 h in the presence of PI3-kinase inhibitor wortmannin (100 nM) dissolved in DMSO or the equivalent volume of DMSO alone. (a) Nuclear extracts were isolated and samples (5 μg) subjected to EMSA for NF-κB (left panel) and Sp1 (right panel), as loading control. (b) Total proteins were isolated with lysis buffer. Samples (60 μg) were immunoprecipitated overnight with a phospho-Akt antibody immobilized on agarose beads, and bound proteins used in a kinase assay with 1 μg GSK3α-GST protein as substrate. Phosphorylated GSK3α was identified by immunoblotting. Alternatively, samples (60 μg) were subjected to immunoblotting for β-actin, as a control for equal protein loading

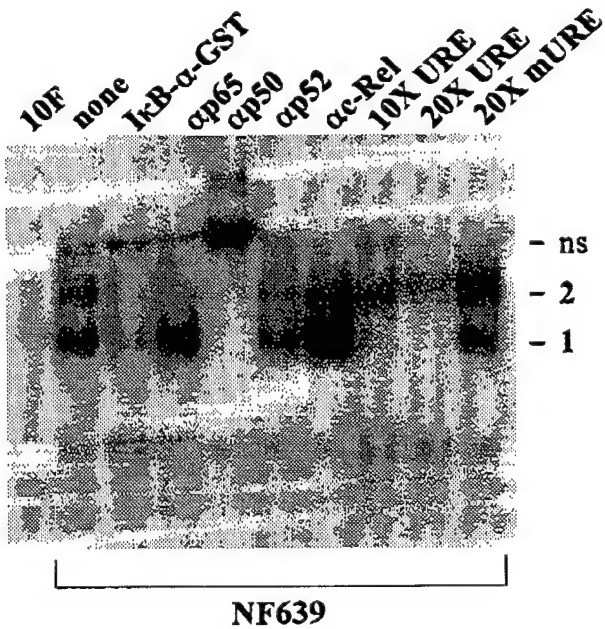

Figure 3 MMTV- Her-2/neu mammary tumor derived cell line NF639 expresses classical NF-κB. Samples of NF639 cell nuclear extracts (5 μg) were incubated overnight at 4°C in the absence (none), or the presence of 1 μg IκB-α-GST protein, or 1 ul antibody against the p65, p50, p52, or c-Rel NF-κB subunits, as indicated. Alternatively, a nuclear extract from MCF-10F (10F) cells was used. EMSA for NF-κB was performed, as described in Materials and methods. To test for specificity of binding, the binding reaction with the NF639 cell nuclear extract was incubated with 10× or 20× excess unlabeled wild-type (URE) or mutant URE oligonucleotide (mURE), as indicated. The positions of two specific complex, labeled bands 1 and 2, as well as, a non-specific complex (ns), are as indicated. (All lanes are from the same gel)

10F cells display very little NF-κB transactivation capability, consistent with the low levels of binding seen (Kim *et al*., 2000). In particular, MCF-10F cells showed a minimal induction of E8 activity over the mutE8 of approximately 1.7-fold ± 0.6. Transient transfection analysis of the NF639 cells was performed similarly using the E8 and mutE8 TK promoter-CAT reporter vectors. A ninefold ± 0.4 higher level of activity was obtained with E8 compared with mutE8 vector. Thus, the NF639 cells display elevated levels of NF-κB binding and transactivation potential.

MMTV-Her-2/neu mouse mammary tumors express elevated levels of NF-κB

We next asked whether mouse mammary tumors driven by MMTV-Her-2/neu express constitutive nuclear NF-κB. Nuclear extracts were prepared from several tumors and from histologically normal mammary glands from the same animals. As seen previously in the rat (Sovak *et al*., 1997; Kim *et al*., 2000), a normal mammary gland expresses only low levels of NF-κB (Figure 4a and data not shown). Tumors displayed elevated levels of NF-κB (Figure 4a), consistent with the EMSA of the NF639 line seen above (Figure 3). Two specific complexes were apparent, as judged by competition analysis with excess unlabeled oligonucleotide, which were labeled bands 1 and 2 (Figure 4b). Antibody supershift analysis identified bands 1 and 2 as p50 homodimers and p50/p65 heterodimers, respectively, consistent with the studies on the NF639 line (Figure 4b). EMSA with oligonucleotides containing binding sites for PU.1, and TCF-1 indicate the NF-κB binding in the tumor sample nuclear extracts was not likely due to contamination of B lymphocytes, neutrophils, mast or myeloid cells, or of T lymphocytes, respectively. Thus, mammary tumors from MMTV-Her-2/neu mice, as well as the cell lines derived from these tumors, express constitutive nuclear NF-κB.

Inhibition of the PI3-kinase to Akt signaling pathway reduces NF-κB levels

We next sought to determine the involvement of the PI3-kinase/Akt signaling pathway in the activation of NF-κB in the NF639 line. We first tested whether specific inhibition of the pathway affects NF-κB binding. NF639 cells were transiently transfected with vectors expressing either a kinase inactive version of PI3-kinase (PI3KΔ85) or of Akt (AktΔK), which function as dominant negatives. Alternatively vectors expressing either wild-type (Akt) or a membrane form of Akt, which is constitutively active (AktM) were similarly transfected to determine whether increasing the level of this kinase will enhance activation of NF-κB in the NF639 line. The transfection efficiency of the NF639 cells was approximately 60% as judged by green fluorescent protein (data not shown). Expression of either the dominant negative PI3-kinase or Akt caused a significant reduction in NF-κB binding (Figure 5a), implicating this pathway in activation of this transcription factor in the NF639 MMTV-Her-2/neu cells. Expression of Akt had only marginal effects

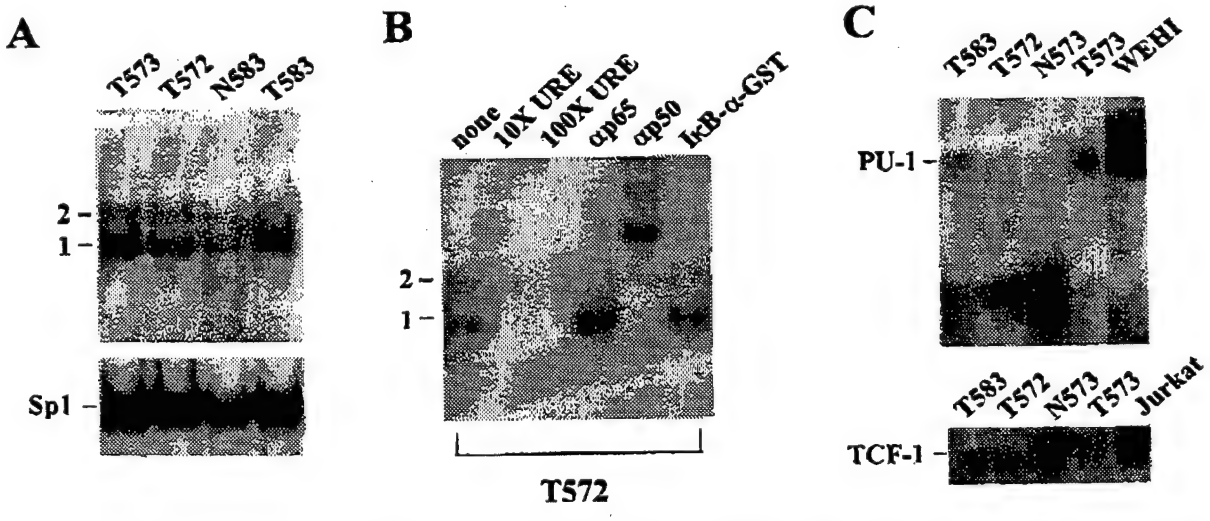

Figure 4 MMTV-Her-2/neu tumors display elevated NF-κB binding. Nuclear extracts were prepared from the indicated histologically normal mammary glands (N) and breast tumors (T) from MMTV-Her-2/neu mice. (a) NF-κB EMSA. Samples of nuclear extracts (5 μg) were subjected to EMSA for NF-κB and Sp1, as loading control. (b) Antibody supershift. Samples of nuclear extracts (5 μg) from the T572 tumor were incubated overnight at 4°C in the absence (none) or the presence of 1 ul antibody against the p65 or p50 NF-κB subunits, or 1 μg IκB-α-GST protein, as indicated. EMSA for NF-κB was performed, as described in Materials and methods. To test for specificity of binding, samples were incubated with 10× or 100× excess unlabeled wild-type (URE). The positions of two specific complexes are as indicated. (c) PU.1 and TCF-1 EMSA. Samples of nuclear extracts (5 μg) were subjected to EMSA for PU.1 and TCF-1. Where indicated, samples (5 μg) of nuclear extract of WEHI 231 B cells (WEHI) and Jurkat T cells (Jurkat) were added as controls for positive binding

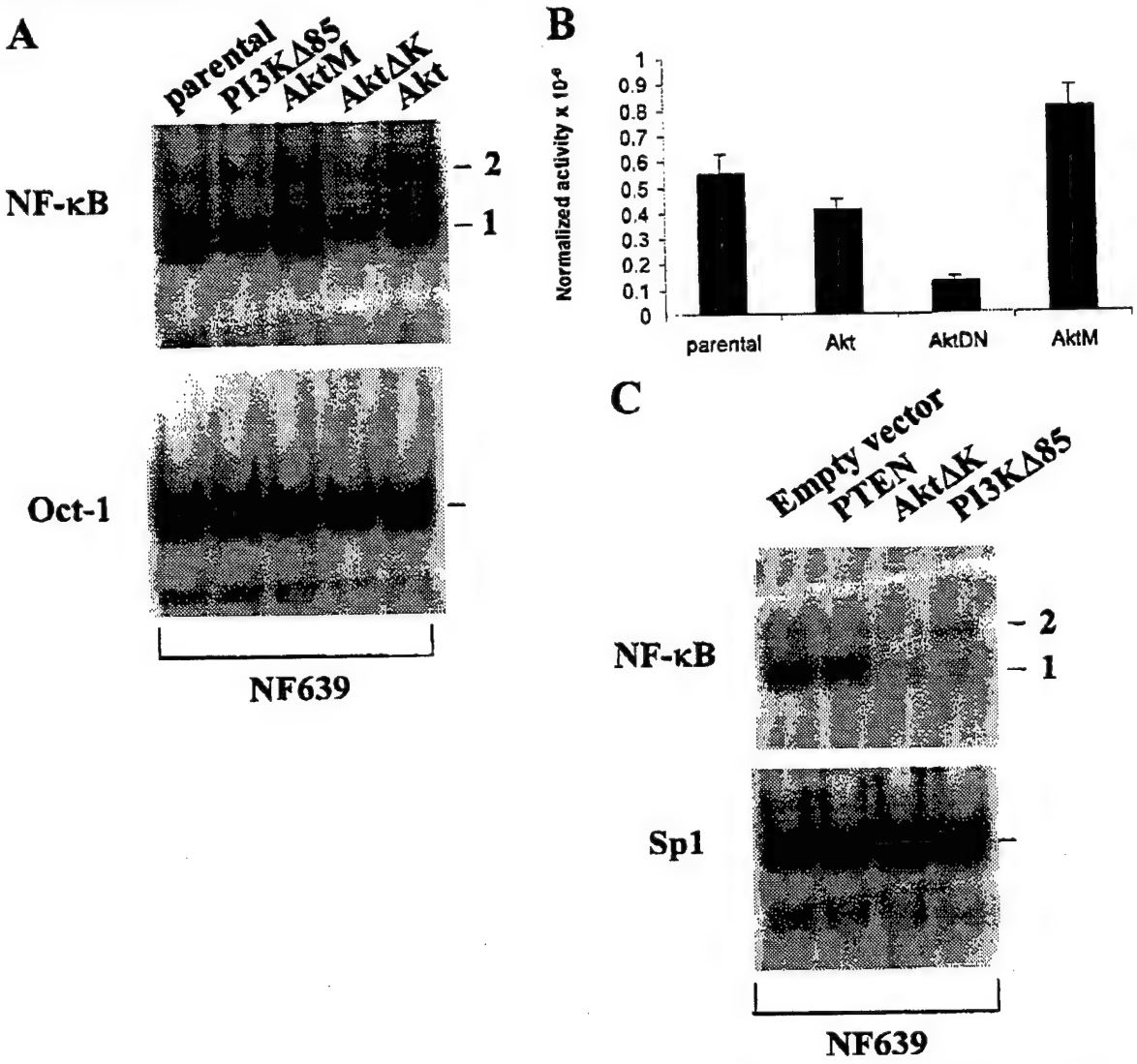

Figure 5 Inhibition of PI 3-kinase and Akt reduce NF-κB activity. (a) Cultures (P100) of NF639 cells were transfected with 9 μg of SRα, parental vector or of vectors: PI3KΔ85 (dead kinase), AktM (membrane kinase), AktΔK (dead kinase), Akt (wt Akt). After 48 h, nuclear extracts were prepared and samples (5 μg) used in EMSA with oligonucleotides containing elements for NF-κB or Oct-1, as control for equal loading. Positions of the two major NF-κB bands and the one Oct-1 complex, are as indicated. (b) Cultures (P35) of NF639 cells were transfected, in triplicate, with 1 μg NF-κB-element driven luciferase construct in the presence of 2 μg either pCMV empty vector (parental), or of vectors: AktΔK (AktDN), Akt, or AktM, and 1 μg SV40βgal. After 36 h, extracts were prepared and samples, normalized for β-galactosidase activity, were assayed for luciferase activity. The average values are presented +/− the standard deviation. (c) Cultures of NF639 cells were transfected, as in part (a), with either pCMV empty vector, or the indicated expression constructs. After 24 h, nuclear extracts were prepared and samples (5 μg) used in EMSA with oligonucleotides containing elements for NF-κB or Sp1, as control for equal loading

on NF-κB binding, while expression of the myristylated AktM form led to increased NF-κB binding (Figure 5a). Equal loading was confirmed via EMSA for the Oct-1 protein (Figure 5a). We next assessed the effects of these vectors on NF-κB activity, using co-transfection analysis of an NF-κB element driven luciferase construct (Figure 5b). Expression of the dominant negative Akt caused an over 80% reduction in NF-κB activity while expression of the constitutively active myristylated AktM form resulted in elevated NF-κB activity, and the wild-type Akt had little effect on activity or binding (Figure 5b). Thus, the changes in NF-κB binding were paralleled by changes in activity. Taken together, these findings indicate a PI3-kinase/Akt pathway plays a role in the constitutive activation of NF-κB in the MMTV-c-neu NF639 cells.

The PTEN lipid phosphatase, which is the most highly mutated tumor-suppressor gene in breast cancer, has been shown to functionally down-modulate PI3-kinase activity (reviewed in Di Cristofano and

Pandolfi, 2000). Thus we next asked whether PTEN expression affects NF-κB binding. NF639 cells were transfected with a PTEN expression vector or with the dominant negative PI3-kinase and Akt expression vectors for comparison and EMSA performed. As seen in Figure 5c, expression of PTEN reduced the level of NF-κB binding, although, to a lesser extent than seen with the kinase inactive PI3-kinase and Akt proteins. Equal loading was confirmed by analysis for Sp1 binding. Thus, PTEN reduces the activation of NF-κB seen in the Her-2/neu transformed NF639 line.

Engagement of the Her-2/neu receptor reduces NF-κB levels

Anti-neu antibody treatment of breast cancer cells *in vitro* has been found to cause a reversion of transformed phenotype (Drebin *et al*., 1985; Pegram *et al*., 1998). Since NF-κB has been implicated in regulation of genes that control transformed phenotype of breast cancer cells, including c-*myc* (Duyao *et al*., 1992; Kessler *et al*., 1992; La Rosa *et al*., 1994), we next evaluated the effects of this treatment on NF-κB. NF639 cells were incubated with an antibody that recognizes rat Her-2/neu (αneu) for 24 h, and nuclear extracts subjected to EMSA for NF-κB and Sp1, as a control for equal loading. As seen in Figure 6a, the anti-Her-2/neu antibody caused a significant reduction in NF-κB binding. To verify the efficacy of the antibody treatment on the Akt signaling pathway, extracts were subjected to an Akt kinase assay. Whole cell extracts were immunoprecipitated with a monoclonal anti-Akt, which preferentially recognizes phosphorylated protein. GSK3α-GST was then used as substrate with the resulting immunoprecipitated Akt, and phosphorylated material identified by immunoblot analysis for phosphorylated GSK3α-GST protein (Figure 6b). Treatment with the Her-2/neu antibody resulted in a decrease in phosphorylated GSK3α-GST, demonstrating receptor engagement causes decreased Akt kinase activity. Immunoblotting of the WCE for β-actin demonstrated the specificity of the decrease in Akt kinase activity (Figure 6b). Overall, these results confirm the ability of anti-Her-2/neu treatment to reduce NF-κB levels in breast cancer cells, and suggest involvement of Akt.

IKK pathway is not involved in the NF-κB induction by Her-2/neu

To explore the role of the IκB kinase/proteasome pathway, NF639 cells were incubated in the presence of either 40 μg/ml of MG132, a specific inhibitor of the proteasome pathway or carrier DMSO, as control. After 30 min, cycloheximide was added and WCEs prepared at the times indicated and subjected to immunoblotting for IκBα expression (Figure 7a). Addition of MG132 had only a very modest affect on decay of IκB-α. To verify the effectiveness of the MG132, the blot was probed for expression of the cyclin-dependent kinase inhibitor $p27^{Kip1}$ protein, which

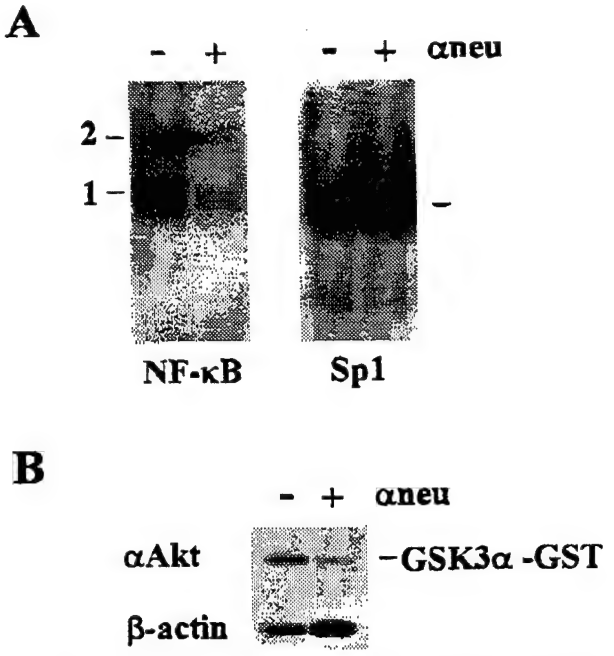

Figure 6 Engagement of the Her-2/neu receptor reduces NF-κB binding. Cultures (P100) of NF639 cells were incubated in the absence or presence of 1 μg anti-HER-2/neu (αneu) antibody for 24 h and nuclear and whole cell extracts prepared. (a) EMSA. Samples of nuclear extracts (5 μg) were subjected to EMSA for NF-κB and Sp1, as loading control. (b) Akt kinase assay. Samples of whole cell extracts (80 μg) were incubated with an Akt antibody, and the resulting immunoprecipitated Akt protein subjected to kinase assay using GSK3α-GST, as substrate (as described in the legend to Figure 2). Phosphorylated GSK3α was identified by immunoblotting. Samples (80 μg) of the whole cell extracts were analysed for β-actin, as control

is degraded via the proteasome (Tam *et al*., 1997) (Figure 7b). Turnover of p27 protein was completely ablated by the addition of MG132. Similarly, addition of MG132 blocked turnover of the c-Myc protein (data not shown), which is also mediated by the proteasome (Gregory and Hann, 2000). Thus, basal turnover of IκB-α largely does not appear to be mediated by the proteasome in NF639 cells.

To further assess the potential role of the proteasome, NF639 were transfected with a Ser32/36 to Ala double mutant version of human IκB-α (A32/36). This protein cannot be phosphorylated and subsequently degraded by the proteasome pathway. Decay of the A32/36 double mutant protein was followed using a human-specific IκB-α antibody (Figure 7c). The rate of decay was quite similar to that of the endogenous IκB-α seen above, suggesting again that decay is mediated via a non-proteasome pathway.

We next assessed the role of the IKK kinase complex in basal NF-κB expression. NF639 were transiently transfected with the vector expressing AktΔK to inhibit Akt or with the parental vector, and analysed for effects on IKKα and IKKβ activity. Alternatively cells were transfected with vectors expressing AktM or wild-type Akt. Extracts were prepared, and samples (200 μg)

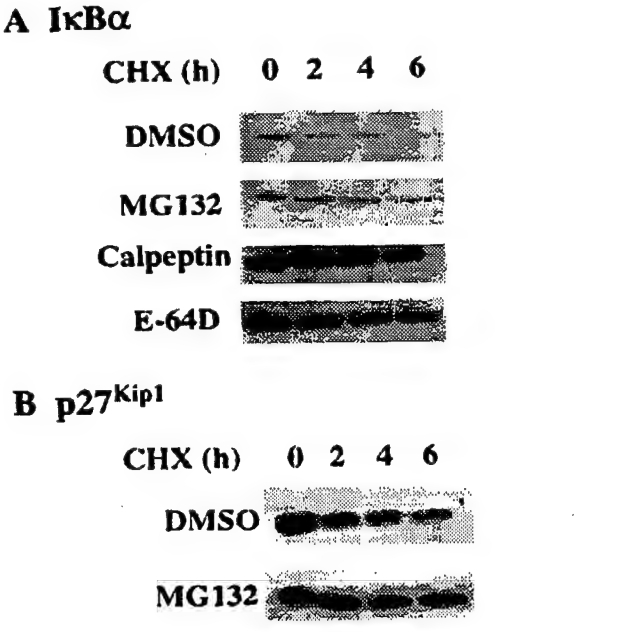

Figure 7 Inhibition of calpain blocks IκBα degradation in NF639 cells. NF639 cells were incubated either with DMSO alone, or with 40 μg/ml MG132, E64-D, or calpeptin for 30 min. Following addition of 50 μg/ml cycloheximide (CHX), WCEs were prepared at the times indicated, and samples (40 μg) subjected to immunoblot analysis for either IκBα (C-21) (a) or $p27^{Kip1}$ (M197) (b). (c) NF639 cells were transfected with 2 μg $pRC_{\beta actin}$ double mutant human IκBα (A32/36) vector. After 36 h, cultures were incubated with 40 μg/ml MG132 for 30 min. Following addition of 50 μg/ml cycloheximide extracts were prepared at the times indicated and subjected to immunoblot analysis using an antibody specific for human IκB-α (C-15). The position of the human IκB-α is as indicated (hIκB-α). A minor slower migrating non-specific band is also seen

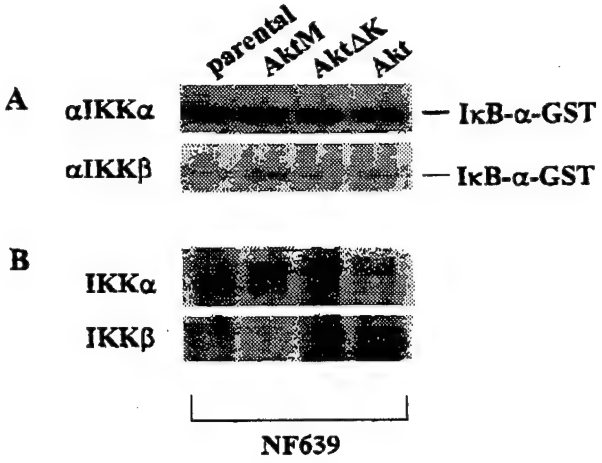

Figure 8 IKK kinase complex is inactive in MMTV-Her-2/neu NF639 cells. (a) Total proteins were isolated from NF639 cells, and samples (200 μg) immunoprecipitated with antibodies against either IKKα or IKKβ, as indicated. Two-thirds of the preparations were subjected to a kinase assay using 1 μg IκB-α-GST protein, as substrate. (b) The remainders of the preparations were immunoblotted for either IKKα or IKKβ to verify immunoprecipitation

immunoprecipitated with antibodies against either IKKα or IKKβ. The resulting immunoprecipitated proteins were used in a kinase assay with IκB-α-GST as substrate. Expression of AktΔK, which dramatically decreased NF-κB levels above, caused no significant reduction in activity of either IKKα or IKKβ (Figure 8a). In fact, a minor increase of 1.2±0.1-fold was seen in this and a duplicate experiment. Thus, inhibition of Akt does not alter IKK kinase activity in the NF639 cells. Expression of the AktM, which caused a slight increase in NF-κB levels above (Figure 5), resulted in a slight increase in IKK activity (Figure 8a). No difference in IKK activity was noted in the NF639 cells transfected with parental Akt expression vector. Essentially equal amounts of IKK proteins were present in the extracts as verified by immunoblotting (Figure 8b). Thus, activation of the IKKα and IKKβ components of the IKK kinase complex does not appear able to account for the constitutive basal NF-κB binding seen in the MMTV-Her-2/neu NF639 cell line, consistent with the failure of the proteasome inhibitor to substantially affect IκB-α turnover.

Recent work has demonstrated a role for calpain in IκB-α turnover in B cells, which constitutively express NF-κB (Fields *et al*., 2000; Miyamoto *et al*., 1998). Thus, we next investigated the involvement of calpain in IκB-α degradation in the NF639 line using the inhibitors calpeptin and E-64D. While both inhibitors are specific for calpain, the E-64D does not enter cells as well and has been found to be less effective than calpeptin (Fields *et al*., 2000; Miyamoto *et al*., 1998). NF639 cells were incubated in the presence of 40 μg/ml calpeptin or E-64D, or carrier DMSO as control. Calpeptin essentially completely prevented the decay of IκB-α (Figure 7a). Treatment with E-64D also ablated the rate of IκB-α decay, but was somewhat less effective, consistent with the findings of others. Thus, inhibition of calpain ablates IκB-α turnover, indicating the activation of NF-κB that occurs as a result of overexpression of Her-2/neu is mediated, at least in part, by calpain.

Discussion

In this study we show that overexpression of Her-2/neu leads to constitutive induction of NF-κB mediated through a PI3-kinase/Akt kinase pathway that signaled degradation of IκB-α via calpain. The activation of NF-κB could be inhibited by the phosphatase PTEN. Constitutive nuclear NF-κB was observed in Ba/F3 cells overexpressing Her-2/neu + EGFR4, as well as in

cell lines derived from MMTV-Her-2/neu mouse mammary gland tumors and in primary tumor specimens. Inhibition of PI3-kinase by either wortmannin treatment or by ectopic expression of a kinase inactive variant reduced NF-κB levels. Consistent with these findings, negative or positive modulation of Akt kinase activity either repressed or induced NF-κB activity, respectively. Previously, our laboratory demonstrated aberrant NF-κB/Rel activation typifies primary human breast cancers (Sovak *et al.*, 1997). Here we begin to provide a mechanism for the aberrant expression of these factors in cancers with overexpression of Her-2/neu. Furthermore, our findings implicate the calcium sensitive cysteine protease calpain family in breast cancer progression through the constitutive activation of NF-κB.

Overexpression of Her-2/neu in breast cancer correlates with a poor prognosis due to enhanced metastatic potential and resistance to chemotherapy (Hortobagyi *et al.*, 1999; Slamon *et al.*, 1987; Yu *et al.*, 1998). The transmembrane receptor encoded by the Her-2/neu oncogene has intrinsic kinase activity even in the absence of ligand that activates receptor-mediated signal transduction. Consistent with these observations, here we detected intrinsic tyrosine activation of Her-2/neu in Ba/F3 overexpressing Her-2/neu+EGFR4, as well as in NF639 cells (data not shown). Recently overexpression of Her-2/neu in immortalized HMECs has been found to result in growth factor independence, acquisition of anchorage-independent growth capacity and ability to induce invasion in a manner similar to breast cancer cells (Ignatoski *et al.*, 2000). NF-κB has been implicated in the regulation of a wide spectrum of genes, including those that mediate transformation (e.g., c-*myc*) (La Rosa *et al.*, 1994; Kessler *et al.*, 1992; Duyao *et al.*, 1992; Kim *et al.*, 2000) and metastasis (e.g., metalloproteinases) (reviewed in Grimm and Baeuerle, 1993). Thus, it is likely that aberrant NF-κB activity plays an important role in the transformed phenotype displayed in cells with overexpression of Her-2/neu.

Overall our work has implicated NF-κB in the neoplastic development of mammary and liver epithelial tumors (Sovak *et al.*, 1997; Arsura *et al.*, 2000). We first reported aberrant elevated levels of NF-κB binding in over 85% of mammary tumors in the Sprague-Dawley rat after exposure to 7,12-dimethylbenz(*a*)anthracene (DMBA) (Sovak *et al.*, 1997). More recently NF-κB activation was observed within 3 weeks of DMBA treatment when tumors had not yet developed, suggesting that it is an early event in tumor formation (Kim *et al.*, 2000). Furthermore, we showed that in Ras- and Raf-transformed rat liver cells, NF-κB levels are enhanced, promoting cell survival, transformed phenotype, and resistance to TGF-β1 treatment (Arsura *et al.*, 2000). The induction of NF-κB by Ras was mediated by two pathways involving both Raf and PI3-kinase leading to the activation of the IKK complex (Arsura *et al.*, 2000). Importantly, many other tumors have recently been shown to display constitutive activation of NF-κB (reviewed in Rayet and Gelinas, 1999), including the human cutaneous T-cell lymphoma HuT-78 (Giri and Aggarwal, 1998), Hodgkin's lymphomas (Bargou *et al.*, 1997), melanoma (Shattuck *et al.*, 1994) pancreatic adenocarcinoma (Wang *et al.*, 1999), primary adult T-cell leukemia (Mori *et al.*, 1999), and head and neck squamous cell carcinoma (Duffey *et al.*, 1999). Furthermore, the Tax transforming protein produced by the human T-cell leukemia virus type 1 induces NF-κB activity (Mercurio *et al.*, 1997; Sun *et al.*, 1994) through activation of both IKK1 and IKK2 (Geleziunas *et al.*, 1998; Sumitomo *et al.*, 1999b). Moreover, NF-κB induction has been found to inhibit TNF-α-induced cell death of breast, prostate, and bladder cancer cells (Geleziunas *et al.*, 1998; Sumitomo *et al.*, 1999a) (reviewed in Rayet and Gelinas, 1999). Interestingly, TNF-α activation of NF-κB in primary patient samples overexpressing Her-2/neu was reported to occur via a PI3-kinase/Akt/IKK pathway recently by Zhou *et al.* (2000). Here, we have shown that enhanced basal levels of NF-κB are displayed by specimens of Her-2/neu induced primary mouse breast tumors compared to normal mammary gland, as well as in a cell line derived from one of these tumors. No effect of inhibition of Akt on IKK kinase activity nor substantial involvement of the proteasome in turnover of IκB-α could be detected in the NF639 cell line. Thus, the constitutive activation of NF-κB upon overexpression of Her-2/neu in this mouse mammary tumor cell line appears to be mediated via a non-IKK/proteasome pathway that involves calpain, similar to findings with mature early B cells (Fields *et al.*, 2000). The IKK activity seen in the tumor cells by Zhou *et al.* (2000) may have resulted from the *in vitro* exposure to TNF-α. Alternatively, the differences may relate to involvement of different cell types in the two studies. Work is in progress to evaluate the sites of phosphorylation and the role of the PEST domain of IκB-α in its turnover in these cells.

The PTEN lipid phosphatase, which has been shown to modulate PI3-kinase activity and PIP-3 levels, is lost in a variety of tumors (Li *et al.*, 1997; Di Cristofano *et al.*, 1998; Whang *et al.*, 1998). In quiescent untransformed cells, PIP-3 levels are very low, and rapidly increase upon stimulation by growth factors, through activation of PI3-kinase. Accumulation of PIP-3 allows the recruitment and activation of Akt via phosphorylation. Overexpression of PTEN in glioma and breast cancer has been reported to result in the inactivation of Akt and the induction of anoikis, a specific apoptotic pathway initiated by cell detachment from the extracellular matrix (Lu *et al.*, 1999). Furthermore, PI3-kinase and Akt regulation of NF-κB has been implicated in survival of cells transformed by Ras (Madrid *et al.*, 2000). In our study, ectopic expression of PTEN in the NF639 cells reduced the activity of Akt and the levels of NF-κB binding. Based on our previous work (Sovak *et al.*, 1997; Wu *et al.*, 1996), this drop in NF-κB likely plays a critical role in induction of apoptosis.

Anti-Her-2/neu antibodies have been shown to be potent growth inhibitors. The human monoclonal

antibody (Herceptin) is currently in use in adjuvant therapy for women with overexpression of Her-2/neu. The systemic administration of the antibodies in combination of cytotoxic chemotherapy in these patients has been shown to increase the length of time of recurrence and the sensitivity to chemotherapy (Ross and Fletcher, 1998). We have then shown that treatment of NF639 cells with anti-neu antibodies decreased NF-κB binding levels, through the inhibition of Akt activation. Thus, it is tempting to speculate that repression of NF-κB is one of the significant targets of these antibodies, and thus agents that inhibit NF-κB may provide additional adjuvant therapy reagents in the treatment of breast disease.

Materials and methods

Cell growth and treatment conditions

MCF-10F human mammary epithelial cells (HMECs) were established from a patient with fibrocystic disease and do not display characteristics of a malignant phenotype. They represent a non-tumorigenic, immortally transformed cell line (Calaf and Russo, 1993), and were cultured as we have published previously (Sovak *et al.*, 1999). The MMTV-c-neu transgene cell line NF639, derived from mammary gland tumors (kindly provided by P Leder, Harvard Medical School, Boston, MA, USA), was cultured as described previously (Elson and Leder, 1995). Ba/F3 cells transfected to express EGFR-1 (Ba/F3-1), Her-2/neu or EGFR-2 (Ba/F3-2), EGFR-1 and Her-2/neu (Ba/F3-1+2), and Her-2/neu and EGFR-4 (Ba/F3-2+4) were kindly provided by David Stern (Yale University, New Haven, CN, USA) (Riese *et al.*, 1996). The parental cells and isolated clones were grown in RPMI supplemented with 10% fetal bovine serum, conditioned medium from WEHI 3 cells, and antibiotics, as described previously (Riese *et al.*, 1996). Where indicated cells were treated with the PI3-kinase inhibitor 100 nM wortmannin (Sigma Chemical Co., St Louis, MO, USA) in DMSO or DMSO alone as control, or with 1 μg anti-neu antibody (Ab-4, Calbiochem, San Diego, CA, USA). Alternatively, the proteasome inhibitor MG132, or calpain inhibitor calpeptin (Calbiochem), or E-64D (Peptide International) dissolved in DMSO, or a similar dilution of DMSO as control, was added. For half-life studies, 50 μg/ml cycloheximide was added, and whole cellular extracts prepared and subjected to immunoblot analysis, as described below.

Electrophoretic mobility shift analysis

Nuclear extracts were prepared from breast cancer cells by a modification of the method of Dignam *et al.* (1983). Briefly, cells were washed twice with ice cold PBS (Ca^{2+} and Mg^{2+} free) containing protease inhibitors (0.5 mM dithiothreitol (DTT), 0.5 mM phenylmethylsulfonyl fluoride (PMSF) and 10 ug/ml leupeptin (LP)). They were then resuspended in 1 ml of cold hypotonic RSB buffer (10 mM NaCl, 3 mM $MgCl_2$, 10 mM Tris pH 7.4) containing 0.5% NP-40 detergent plus protease inhibitors as above. Following a 10 min incubation on ice, the cells were Dounce homogenized until cell lysis occurred. Nuclei were resuspended in two packed nuclear volumes of extraction buffer C (420 mM KCl, 20 mM HEPES pH 7.9, 1.5 mM $MgCl_2$, 0.2 mM EDTA, 20% glycerol) plus protease inhibitors as above, and incubated on ice for 30 min. Protein concentration was determined using the Bio-Rad protein assay, following the manufacturer's directions (Bio-Rad Laboratories, Hercules, CA, USA). The sequence of the URE NF-κB-containing oligonucleotide from the c-*myc* gene (Duyao *et al.*, 1990) is as follows: 5′-GATCCAAGTCCGGGTTTTCCCCAACC-3′, where the underlined region indicates the core binding element. The mutant URE has a two G to C base pair conversion, indicated in bold, which blocks NF-κB/Rel binding: 5′-GATCCAAGTCCGCCTTTTCCCCAACC-3′. The Octomer-1 (Oct-1) oligonucleotide has the following sequence: 5′-TGTCGAATGCAAATCACTAGAA-3′. The sequence of the Sp1 oligonucleotide is 5′-ATTCGATCGGGGCGGGGC-GACC-3′. The sequences of the PU.1- and TCF-1-containing oligonucleotides are as follows, PU.1: 5′-GATC-TACTTCTGCTTTTG-3′; TCF-1: 5′-GGGAGACTGAGAA-CAAAGCGCTCTCACAC-3′ (van de Wetering *et al.*, 1991). Oligonucleotides were end labeled with large Klenow fragment of DNA polymerase and [^{32}P]dNTPs. The electrophoretic mobility shift assay (EMSA) was performed using approximately 4 ng of labeled oligonucleotide (40 000 d.p.m.), 5 μg of nuclear extract, 5 μl of sample buffer (10 mM HEPES pH 7.5, 4 mM DTT, 0.5% Triton X-100, and 2.5% glycerol), 2.5 μg poly dI-dC as nonspecific competitor and adjusted to 100 mM with KCl in a final volume of 25 μl. This mixture was incubated at room temperature for 30 min. Complexes were resolved in a 4.5% polyacrylamide gel using 1 × TBE running buffer (90 mM Tris, 90 mM boric acid, 2 mM EDTA pH 8.0). For antibody supershift analysis, the binding reaction was performed in the absence of the probe, the appropriate antibody was added and the mixture incubated for 16 h at 4°C. The probe was then added and the reaction incubated an additional 30 min at 25°C and the complexes resolved by gel electrophoresis, as above. Antibodies used include: anti-RelA subunit: sc-372X, anti-p50 subunit: sc-114, anti-p52 subunit: sc-7386, and anti-c-Rel subunit: sc-71 (all from Santa Cruz Biotechnology Inc, Santa Cruz, CA, USA). For the IκB-α blocking assays, 1 μg of IκB-α-glutathione-S-transferase (GST) fusion protein was added to the binding reaction, as described for the antibody supershift analysis.

Transfection analysis

Twenty-four hours after plating at 30% confluence in P100 dishes, NF639 cells were incubated with 8 μg DNA in 10 μl FuGENE Reagent, according to manufacturer's instructions (Roche Molecular Biochemicals, Indianapolis, IN, USA). After 24 or 48 h, cells were harvested, nuclear fraction isolated and subject to EMSA analysis as described above. The SR-αΔp85 (dead kinase) PI3-kinase construct has been described elsewhere (Kotani *et al.*, 1994). AKT, AKTΔK (dead kinase), and AktM (myristylated membrane kinase) were cloned in a cytomegalovirus (CMV) promoter-driven expression vector and were kindly provided by Z Luo (Boston Medical School, Boston, MA, USA). The PTEN plasmid was cloned in pCMV5, and was kindly provided by JE Dixon (University of Michigan, Ann Arbor, MI, USA). Wild-type (E8) and mutant (mutE8) NF-κB element-thymidine kinase (TK) promoter-chloramphenicol acetyltransferase (CAT) reporter vectors were constructed as reported previously (Duyao *et al.*, 1990). Briefly, these consisted of two copies of either the wild-type or mutant NF-κB element from upstream of the c-*myc* promoter, sequences given above. Twenty-four hours after plating at 30% confluence in P35 dishes, NF639 cells were transfected, in triplicate, with 4 μg DNA in 4 μl FuGENE Reagent. After 24 h, cells were harvested and equal amounts of protein

subjected to CAT assays, as we have described previously (Sovak *et al.*, 1997). Alternatively, cells were co-transfected with an NF-κB-element driven luciferase construct (Rawadi *et al.*, 1999), kindly provided by Georges Rawadi (Hoechst-Marion-Roussel, Romainville, France) in the presence of parental or Akt expression vectors and luciferase activity measured as described previously (Dolwick *et al.*, 1993). Standard deviation was obtained using the Student's *t*-test. The $pRC_{\beta actin}$ containing double mutant human IκB-α (A32/36) was kindly provided by Michael Karin (University of California, San Diego, CA, USA).

Immunoblot analysis

Ba/F3 cells were rinsed with cold PBS, and harvested in lysis buffer (50 mM Tris-HCl pH 8.0, 5 mM EDTA pH 8.0, 150 mM NaCl, 0.5 mM DTT, 2 μg/ml aprotinin, 2 μg/ml LP, 0.5 mM PMSF, 0.5% NP40). Whole cell extracts (WCEs) were obtained by sonication, followed by centrifugation at 14 000 r.p.m. for 30 min. WCEs, in the amount indicated in each experiment, were subjected to electrophoresis in a 10% polyacrylamide-SDS gel, transferred to PVDF membrane (Millipore, Bedford, MA, USA) and immunoblotting, as previously described (Arsura *et al.*, 1997). Antibodies used were: C-21, mouse IκB-α; C-15, human-specific IκB-α; M197, p27Kip1 (all from Santa Cruz Biotechnology).

Akt kinase assay

The Akt kinase assay, was performed following the directions of Akt Kinase Assay Kit (#9840, New England Biolabs, Beverly, MA, USA). Briefly samples (80 μg) of WCEs were immunoprecipitated with an agarose conjugated anti-Akt antibody (#9279, New England Biolabs) at 4°C overnight. The immunoprecipitate was resuspended in kinase buffer and the assay performed at 30°C for 45 min, using 1 μg of GSK3α-GST fusion protein as substrate in the presence of 10 μM ATP. The resulting products were resolved in a 10% polyacrylamide-SDS gel and subjected to immunoblotting, as above, using phosphospecific GSK-3α antibody (#9331, New England Biolabs).

Isolation of MMTV-c-neu mammary gland tumor and normal mammary gland proteins

MMTV-neu tumors and histologically normal mammary gland tissue surrounding the tumor (Muller *et al.*, 1996) were frozen in liquid nitrogen, and powdered using mortar and pestle. For isolation of nuclear proteins, the powders (1 gm tissue/ml) were resuspended in homogenization buffer (10 mM HEPES pH 7.9, 10 mM KCl, 0.1 mM EDTA, 0.1 mM EGTA, 50 mM sucrose, 1 mM DTT, 0.5 mM PMSF, 5 μg/ml LP, 5 μg/ml aprotinin), and homogenized with a Dounce. The concentration of KCl was then adjusted to 100 mM and the samples were centrifuged at 4000 r.p.m. for 15 min at 4°C. The pellets were then resuspended in 100 μl extraction buffer (10 mM HEPES pH 7.9, 400 mM NaCl, 0.1 mM EDTA, 0.1 mM EGTA, 20% glycerol, 1 mM DTT, 0.5 mM PMSF, 5 μg/ml LP, 5 μg/ml aprotinin), and incubated at 4°C for 30 min with gentle agitation. The samples were then centrifuged at 15 000 r.p.m. at 4°C for 15 min, and the supernatant (nuclear extract) recovered.

Immunoprecipitation and IKK kinase assay

NF639 cells were washed with cold PBS and WCEs prepared in PD buffer (40 mM Tris pH 8.0, 500 mM NaCl, 6 mM EDTA, 6 mM EGTA, 10 mM β-glycerophosphate, 10 mM NaF, 10 mM PNPP, 300 μM Na_3VO_4, 1 mM benzamidine, 2 μM PMSF, 10 μg/ml aprotinin, 1 μg/ml LP, 1 μg/ml pepstatin, 1 mM DTT, 0.1% NP-40). Samples (200 μg) were precleared with protein A-Sepharose beads (Amersham Pharmacia Biotech, Piscataway, NJ, USA) for 1 h at 4°C. The precleared samples were subjected to immunoprecipitation in 500 μl PD buffer. Antibody (1 μl) against either IKKα (Sc7182) or IKKβ (Sc7607, both from Santa Cruz Biotechnology Inc) was added to the mixture and the reaction incubated overnight at 4°C with gentle agitation. The following day, 100 μl protein A-Sepharose beads were added and the samples incubated for 1 h at 4°C. The samples were then washed three times in PD buffer. Two-thirds of the immunoprecipitate were subjected to a kinase assay essentially as published previously (Mercurio *et al.*, 1997). Briefly, samples were resuspended in 20 μl of kinase buffer C [20 mM HEPES pH 7.7, 2 mM $MgCl_2$, 10 μM ATP, 3 μCi [γ-^{32}P]ATP, 10 mM β-glycerophosphate, 10 mM NaF, 10 mM PNPP, 300 μM Na_3VO_4, 1 mM benzamidine, 2 μM PMSF, 10 μg/ml aprotinin, 1 μg/ml LP, 1 μg/ml pepstatin, 1 mM DTT], and incubated at 30°C for 45 min in the presence of 200 ng IκB-α-GST fusion protein, as substrate. The kinase reaction was stopped by addition of 2×SDS-polyacrylamide gel electrophoresis sample buffer, subjected to polyacrylamide-SDS gel analysis and visualized by autoradiography. The remaining immunoprecipitated fraction was subjected to immunoblot analysis, as described above.

Acknowledgments
We thank N Rice, C Rich, J Foster, W Ogawa, J Dixon, F Mercurio, ZG Rawadi and M Karin for generously providing antibody or cloned DNA. We thank D Stern, P Leder, W Muller and M Michelman for generously providing the Ba/F3 and MMTV-c-neu cell lines. We thank D Sloneker for assistance in preparation of this manuscript. This work was supported by grants from the Department of Army DAMD 17-98-1 (GE Sonenshein), and the NIH/NCI CA 82742 (GE Sonenshein), CA78616 (M Arsura), the Charlotte Geyer Foundation (M Arsura), and the Association pour la Recherche sur le Cancer (R Romieu-Mourez) and Fondation Bettencourt-Schueller (R Romieu-Mourez).

References

Adam L, Vadlamudi R, Kondapaka SB, Chernoff J, Mendelsohn J and Kumar R. (1998). *J. Biol. Chem.*, **273**, 28238–28246.

Arcaro A and Wymann MP. (1993). *Biochem. J.*, **296**, 297–301.

Arsura M, FitzGerald MJ, Fausto N and Sonenshein GE. (1997). *Cell Growth Differ.*, **8**, 1049–1059.

Arsura M, Mercurio F, Oliver A, Thorgeirsson SS and Sonenshein GE. (2000). *Mol. Cell. Biol.*, **20**, 5381–5391.

Ballard DW, Dixon EP, Peffer NJ, Bogerd H, Doerre S, Stein B and Greene WC. (1992). *Proc. Natl. Acad. Sci. USA*, **89**, 1875–1879.

Bargou RC, Emmerich F, Krappmann D, Bommert K, Mapara MY, Arnold W, Royer HD, Grinstein E, Greiner A, Scheidereit C and Dorken B. (1997). *J. Clin. Investig.*, **100**, 2961–2969.

Beraud C, Henzel WJ and Baeuerle PA. (1999). *Proc. Natl. Acad. Sci. USA*, **96**, 429–434.

Besancon F, Atfi A, Gespach C, Cayre YE and Bourgeade MF. (1998). *Proc. Natl. Acad. Sci. USA*, **95**, 8081–8086.

Brown K, Gerstenberger S, Carlson L, Franzoso G and Siebenlist U. (1995). *Cell*, **84**, 853–862.

Calaf G and Russo J. (1993). *Carcinogenesis*, **14**, 483–492.

Chen ZJ, Mercurio F, Rosette C, Wu-Li J, Suyang H, Ghosh S and Karin M. (1996). *Mol. Cell. Biol.*, **16**, 1295–1304.

Di Cristofano A and Pandolfi PP. (2000). *Cell*, **100**, 387–390.

Di Cristofano A, Pesce B, Cordon-Cardo C and Pandolfi PP. (1998). *Nat. Genet.*, **19**, 348–355.

DiDonato J, Hayakawa A, Rothwarf DM, Zandi E and Karin M. (1997). *Nature*, **388**, 548–554.

DiDonato JF, Mercurio F, Rosette C, Wu-Li J, Suyang H, Ghosh S and Karin M. (1996). *Mol. Cell. Biol.*, **16**, 1295–1304.

Dignam JD, Lebovitz RM and Roeder RG. (1983). *Nucleic Acids Res.*, **11**, 1475–1489.

Dolwick KM, Swanson HI and Bradfield CA. (1993). *Proc. Natl. Acad. Sci. USA*, **90**, 8566–8570.

Drebin JA, Link VC, Stern DF, Weinberg RA and Greene MI. (1985). *Cell*, **41**, 695–706.

Duffey DC, Chen Z, Dong G, Ondrey FG, Wolf JS, Brown K, Siebenlist U and Van Waes C. (1999). *Cancer Res.*, **59**, 3468–3474.

Duyao MP, Buckler AJ and Sonenshein GE. (1990). *Proc. Natl. Acad. Sci. USA*, **87**, 4727–4731.

Duyao MP, Kessler DJ, Spicer DB, Bartholomew C, Cleveland J, Siekevitz M and Sonenshein GE. (1992). *J. Biol. Chem.*, **267**, 16288–16291.

Elson A and Leder P. (1995). *J. Biol. Chem.*, **279**, 26116–26122.

Fields E, Seufzer BJ, Oltz EM and Miyamoto S. (2000). *J. Immunol.*, **164**, 4762–4267.

Geleziunas R, Ferrell S, Lin X, Mu Y, Cunningham Jr ET, Grant M, Connelly MA, Hambor JE, Marcu KB and Greene WC. (1998). *Mol. Cell. Biol.*, **18**, 5257–5262.

Giri DK and Aggarwal BB. (1998). *J. Biol. Chem.*, **273**, 14008–14014.

Gregory MA and Hann SR. (2000). *Mol. Cell. Biol.*, **20**, 2423–2435.

Grimm S and Baeuerle PA. (1993). *Biochem. Journal*, **290**, 297–308.

Guy CT, Webster MA, Schaller M, Parson TJ, Cardiff RD and Muller WJ. (1992). *Proc. Natl. Acad. Sci. USA*, **89**, 10578–10582.

Hortobagyi GN, Hung M-C and Buzdar AU. (1999). *Semin. Oncol.*, **26**, 11–20.

Ignatoski KM, Maehama T, Markwart SM, Dixon JE, Livant DL and Ethier SP. (2000). *Brit. J. Cancer*, **82**, 666–674.

Jeay S, Sonenshein GE, Postel-Vinay M-C and Baixeras E. (2000). *Molec. Endocrinol.*, **14**, 650–661.

Kennedy SG, Wagner AJ, Conzen SD, Jordan J, Bellacosa A, Tsichlis PN and Hay N. (1997). *Genes Dev.*, **11**, 701–713.

Kessler DJ, Duyao MP, Spicer DB and Sonenshein GE. (1992). *J. Exp. Med.*, **176**, 787–792.

Kim DW, Sovak MA, Zanieski G, Nonet G, Romieu-Mourez R, Lau AW, Hafer LJ, Yaswen P, Stampfer M, Russo J, Rogers AE and Sonenshein GE. (2000). *Carcinogenesis*, **21**, 871–879.

Kotani K, Yonezawa K, Hara K, Ueda H, Kitamura Y, Sakaue H, Ando A, Chavanieu A, Calas B, Grigorescu F, Nishiyama M, Waterfield MD and Kasuga M. (1994). *EMBO J.*, **13**, 2313–2321.

La Rosa FA, Pierce JW and Sonenshein GE. (1994). *Mol. Cell. Biol.*, **4**, 1039–1044.

Li J, Yen C, Liaw D, Bose PKS, Wang SI, Puc J, Miliaresis C, Rodgers L, McCombie R, Bigner SH, Giovanella BC, Ittmann M, Tycko B, Hibshoosh H, Wigler MH and Parsons R. (1997). *Science*, **275**, 1943–1947.

Lu Y, Lin Y-Z, LaPushin R, Cuevas B, Fang X, Yu SX, Davies MA, Khan H, Furui T, Mao M, Zinner R, Hung M-C, Steck P, Siminovitch K and Mills GB. (1999). *Oncogene*, **18**, 7034–7045.

Madrid LV, Wang C-Y, Guttridge DC, Schottelius AJG, Baldwin Jr AS and Mayo MW. (2000). *Mol. Cell. Biol.*, **20**, 1626–1638.

Mercurio F and Manning A. (1999). *Curr. Opinion Cell. Biol.*, **11**, 226–232.

Mercurio F, Zhu H, Murray BW, Shevchenko A, Bennett BL, Li JW, Young DB, Barbosa M, Mann M, Manning A and Rao A. (1997). *Science*, **278**, 860–865.

Miyajima A, Ito Y and Kinoshita T. (1999). *Int. J. Hematol.*, **69**, 137–146.

Miyamoto S, Seufzer BJ and Shumway SD. (1998). *Mol. Cell. Biol.*, **18**, 19–29.

Mori N, Fujii M, Ikeda S, Yamada Y, Tomonaga M, Ballard DW and Yamamoto N. (1999). *Blood*, **93**, 2360–2368.

Muller WJ, Arteaga CL, Muthuswamy PM, Siegel PM, Webster MA, Cardiff RD, Meise KS, Li F, Halter SA and Coffey RJ. (1996). *Mol. Cell. Biol.*, **16**, 5726–5736.

Nakshatri H, Bhat-Nakshatri P, Martin DA, Goulet Jr J and Sledge GW. (1997). *Mol. Cell. Biol.*, **17**, 3629–3639.

Ozes ON, Mayo LD, Gustin JA, Pfeffer SR, Pfeffer LM and Donner BD. (1999). *Nature*, **401**, 82–85.

Pegram MD, Lipton A, Hayes DF, Weber BL, Baselga JM, Tripathy D, Baly D, Baughman SA, Twaddell T, Glaspy JA and Slamon DJ. (1998). *J. Clin. Oncol.*, **16**, 2659–2671.

Rawadi G, Zugaza JL, Lemercier B, Marvaud JC, Popoff M, Bertoglio J and Roman-Roman S. (1999). *J. Biol. Chem.*, **274**, 30794–30798.

Rayet B and Gelinas C. (1999). *Oncogene*, **18**, 6938–6947.

Regnier CH, Song HY, Gao X, Goeddel DV, Cao Z and Rothe M. (1997). *Science*, **278**, 866–869.

Riese II DJ, Kim ED, Elenius K, Buckley S, Klagsbrun M, Plowman GD and Stern DF. (1996). *J. Biol. Chem.*, **271**, 20047–20052.

Romashkova JA and Makarov SS. (1999). *Nature*, **410**, 86–90.

Ross JS and Fletcher JA. (1998). *Oncologist*, **3**, 237–252.

Schoonbroodt S, Ferriera V, Best-Belpomme M, Boelaert JR, Legrand-Poels S, Korneer M and Piette J. (2000). *J. Immunol.*, **164**, 4292–4300.

Shattuck RL, Wood LD, Jaffe GJ and Richmond A. (1994). *Mol. Cell. Biol.*, **14**, 791–802.

Slamon DJ, Clark GM, Wong SG, Levin WJ, Ullrich A and McGuire WL. (1987). *Science*, **235**, 177–182.

Sovak MA, Arsura M, Zanieski GJ, Kavanagh KT and Sonenshein GE. (1999). *Cell Growth Diff.*, **10**, 537–544.

Sovak MA, Bellas RE, Kim DW, Zanieski GJ, Rogers AE, Traish AM and Sonenshein GE. (1997). *J. Clin. Invest.*, **100**, 2952–2960.

Sumitomo M, Tachibana M, Nakashima J, Murai M, Miyajima A, Kimura F, Hayakawa M and Nakamura H. (1999a). *J. Urol.*, **161**, 674–679.

Sumitomo M, Tachibana M, Ozu C, Asakura H, Murai M, Hayakawa M, Nakamura H, Takayanagi A and Shimizu N. (1999b). *Hum. Gene Ther.*, **10**, 37–47.

Sun SC, Elwood J, Beraud C and Greene WC. (1994). *Mol. Cell. Biol.*, **14**, 7377–7384.

Tam SW, Theodoras AM and Pagano M. (1997). *Leukemia*, **11**, Suppl 3, 363–366.

van de Wetering M, Oosterwegel M, Dooijes D and Clevers H. (1991). *EMBO J.*, **10**, 123–132.

Wang W, Abbruzzese JL, Evans DB, Larry L, Cleary KR and Chiao PJ. (1999). *Clin. Cancer Res.*, **5**, 119–127.

Whang YE, Wu X, Suzuki H, Reiter RE, Tran C, Vessella RL, Said JW, Isaacs WB and Sawyers CL. (1998). *Proc. Natl. Acad. Sci. USA*, **95**, 5246–5250.

Woronicz JD, Gao X, Cao Z, Rothe M and Goeddel DV. (1997). *Science*, **278**, 866–869.

Wu M, Lee H, Bellas RE, Schauer SL, Arsura M, Katz D, FitzGerald MJ, Rothstein TL, Sherr DH and Sonenshein GE. (1996). *EMBO J.*, **15**, 4682–4690.

Yu D, Jing T, Liu B, Yao J, Tan M, McDonnell TJ and Hung MC. (1998). *Mol. Cell.* **2**, 581–591.

Zhou BP, Hu MC, Miller SA, Yu Z, Xia W, Lin SY and Hung MC. (2000). *J. Biol. Chem.*, **275**, 8027–8031.

Journal of Cellular Biochemistry

February 23, 2001

Dr. Gail E. Sonenshein
Department of Biochemistry
Boston University School of Medicine
715 Albany Street
Boston, MA 02118
FAX: 617-638-5339

Dear Dr. Sonenshein:

We are pleased to advise you that your revised manuscript, **JCB #01S-013**, entitled: **"Green tea extracts decrease carcinogen-induced mammary tumor burden in rats and rate of breast cancer cell proliferation in culture"** is acceptable for publication in **Journal of Cellular Biochemistry.**

Your manuscript has been forwarded to the publisher, John Wiley & Sons, Inc. They will contact you regarding page proofs, reprints, and scheduled publication date.

Thank you for your contribution. We hope that you will consider the **Journal** for publication of future research articles from your laboratory.

With my very warmest regards.

Sincerely yours,

Gary S. Stein
For the Editorial Board

GSS:hk
Enclosures

Published by Wiley-Liss, a Division of John Wiley & Sons, Inc., 605 Third Ave., New York, NY 10158-0012

Green Tea Extracts Decrease Carcinogen-Induced Mammary Tumor Burden In Rats and Rate of Breast Cancer Cell Proliferation in Culture

Kathryn T. Kavanagh[1,4], Laurie J. Hafer[1,4], Dong W. Kim[2,4], Koren K. Mann[3,4], David H. Sherr[3,4], Adrianne E. Rogers[1,4], and Gail E. Sonenshein[2,4,*]

Departments of [1]Pathology and Laboratory Medicine, [2]Biochemistry and [3]Environmental Health, and [4]Program in Research on Women's Health. Boston University Schools of Medicine and Public Health

Running Title: Inhibitory Effects of Green Tea Extracts on Breast Cancer

*Correspondence to: Gail E. Sonenshein, Department of Biochemistry, Boston University School of Medicine, 715 Albany Street, Boston MA 02118. E-mail: gsonensh@bu.edu.

[5]Abbreviations: GTP, green tea polyphenol; EGCG, epigallocatechin-3 gallate; DMBA, 7,12-dimethylbenz(*a*)anthracene; S-D, Sprague-Dawley; FBS, fetal bovine serum; MTS, (3-(4,5-dimethylthiazol-2-yl)-5-(3-carboxymethoxyphenyl)-2-(4-sulphophenyl)-2H-tetrazolium inner salt; ER, estrogen receptor; CDK, cyclin-dependent kinase; CKI, cyclin-dependent kinase inhibitor; IPTG, isopropyl-beta-D- thiogalactopyranoside.

Epidemiological evidence suggests tea (*Camellia sinesis L.*) has chemopreventive effects against various tumors. Green tea contains many polyphenols, including epigallocatechin-3 gallate (EGCG), which possess anti-oxidant qualities. Reduction of chemically induced mammary gland carcinogenesis by green tea in a carcinogen-induced rat model has been suggested previously, but the results reported were not statistically significant. Here we have tested the effects of green tea on mammary tumorigenesis using the 7,12-dimethylbenz(*a*)anthracene (DMBA) Sprague-Dawley (S-D) rat model. We report that green tea significantly increased mean latency to first tumor and reduced tumor burden and number of invasive tumors per tumor bearing animal; although, it did not affect tumor number in the female rats. Furthermore, we show that proliferation and/or viability of cultured Hs578T and MDA-MB-231 estrogen receptor negative breast cancer cell lines was reduced by EGCG treatment. Similar negative effects on proliferation were observed with the DMBA-transformed D3-1 cell line. Growth inhibition of Hs578T cells correlated with induction of $p27^{Kip1}$ cyclin-dependent kinase inhibitor expression. Hs578T cells expressing elevated levels of $p27^{Kip1}$ protein due to stable ectopic expression displayed increased G1 arrest. Thus, green tea had significant chemopreventive effects on carcinogen-induced mammary tumorigenesis in female S-D rats. In culture, inhibition of human breast cancer cell proliferation by EGCG was mediated in part via induction of the $p27^{Kip1}$ cyclin-dependent kinase inhibitor.

Keywords: Green tea, breast cancer, EGCG, DMBA, $p27^{Kip1}$

The incidence of breast cancer, the second leading cause of death from cancer among women in the United States, has been increasing since the 1980's. Interestingly, breast cancer mortality rates are race-dependent. In 1999, the mortality rate of breast cancer per 100,000 Caucasians was 26.0, of African-Americans 31.5 and of Asian-Americans 11.6. Studies show that migration of young Asian women to the United States dramatically increases their risk of breast cancer and mortality from breast cancer [Haenszel, et al. 1968; Kelsey and Gannon, 1990; Ziegler, et al. 1993]. In an effort to explain this phenomenon, epidemiologists have put forth various hypotheses, including differences in diet and environmental exposure to carcinogens [Haenszel, et al. 1968; Kelsey and Gannon, 1990; Ziegler, et al. 1993]. Dietary comparisons of the Asian diet and the typical Western diet show, among many differences, that the Asian population consume more green tea.

Tea (*Camellia sinesis L.)* is prepared as green, black or oolong tea. Green tea, which is made by steaming or drying fresh tea leaves at elevated temperatures, retains its chemical composition of polyphenols, which include flavanols, flavandiols, flavonoids and phenolic acids. Polyphenols make up approximately 40% of the dry weight of green tea leaves. The green tea polyphenols (GTP)[5], which include epicatechin, epicatechingallate, epigallocatechin and epigallocatechin-3 gallate (EGCG), possess anti-oxidant qualities. Statistics indicate that the incidence of breast cancer in regions where green tea is consumed in large quantities, including China and Japan, is much lower than in western societies. Epidemiologic studies have indicated that green tea reduces the risk of many other cancers, including stomach, lung, colon, rectum, liver, and pancreas [Mukhtar et al. 1994a; Goldbohm et al. 1996; National Cancer Institute 1996; Yang et al. 1996; Zheng et al. 1996; Ji et al. 1997]. Concentrated, purified polyphenol extracts of green tea have been shown in laboratory animals to have anticarcinogenic activity against a tumors of the duodenum [Fujita et al., 1989], esophagus [Wang et al., 1994; Stoner and Mukhtar, 1995], lung [Taniguchi et al., 1992; Wang et al., 1992a] and skin [Wang et al., 1992b; Katiyar et al., 2000;

Wang et al., 1989]. Reduction of chemically induced mammary gland carcinogenesis by green tea has been suggested by Hirose et al. [1997] and Tanaka et al. [1997], but the results reported were not statistically significant. In those studies, green tea was administered in the feed rather than the drinking fluid. In a series of three bioassays, a significant inhibitory effect of black tea on mammary tumorigenesis was found in rats fed a high fat diet [Rogers et al., 1998]. The toxicity of tea extracts is low, and they are potentially important cancer chemopreventive agents. Several possible mechanisms for the protective effect of green tea on carcinogenesis have been proposed: (1) modulation of carcinogen-metabolizing enzymes, (2) trapping of ultimate carcinogens, (3) inhibitory action against nitrosation reactions, (4) inhibition of cell proliferation-related activities [rev. in Stoner and Mukhtar, 1995]. Here we have examined the effects of green tea extracts on breast cancer using the Sprague-Dawley (S-D) rat carcinogen model and breast cancer cells in culture. In the rat model, approximately 90% of female S-D rats given a single intragastric 15-25 mg/kg dose of 7,12-dimethylbenz(*a*)anthracene (DMBA) develop mammary tumors within 7-20 weeks [Rogers and Conner, 1990]. We find that green tea extracts given in drinking water reduce the mammary tumor burden. Second, treatment of cultured human breast cancer cells with GTPs or EGCG inhibits their growth, correlating with increased expression of the cyclin-dependent kinase inhibitor $p27^{Kip1}$. At higher doses, cell death was observed.

MATERIALS AND METHODS

Rat Studies

Virgin female S-D rats were treated according to a protocol approved by the Boston University Institutional Animal Care and Use Committee. Forty S-D, 4-week-old female weanling rats (weighing approximately 40-50g), were purchased from Charles River Laboratories (Wilmington, MA). They were immediately weighed and housed individually in an

environmentally controlled animal facility at the Boston University Laboratory Animal Science Center. Rats were randomized into four groups of approximately equal average body weight, and fed the AIN-76A purified diet. Body weights were recorded weekly. The composition of the treatment groups was as follows:

		Fluid Source		
Group	**No. of Rats**	**DMBA**	**Water**	**Green Tea**
CG1	5	0	+	0
TG1	5	0	0	+
CG2	15	+	+	0
TG2	15	+	0	+

Green tea powder (kindly supplied by Lipton Tea Co., Inc., Englewood Cliffs, NJ) was reconstituted in deionized water to a concentration of 0.3%. (The certificate of analysis of the green tea powder indicated that the catechin composition, which had been assessed by HPLC, was as follows: 11.79% EGCG, 7.87% (-)-epigallocatechin, 5.76% (-)-epicatechin gallate, 4.21% (-)-epicatechin, 1.39% (+)-gallocatechin, 1.33% (+)-catechin, 0.39% (+)-gallocatechin gallate.) Rats in the control groups (CG1 and CG2) were given deionized water to drink, and rats in the TG1 and TG2 groups were given 0.3% green tea as their sole fluid source beginning two days after entry into the facility. Rats were given 15mg/kg DMBA in 0.2mL sesame oil or 0.2mL sesame oil alone by gastric gavage at 8 weeks of age and palpated for tumors weekly starting 4 weeks later. Rats were euthanized by CO_2 inhalation and necropsied when they bore a tumor that was $\geq$3cm or ulcerated or at termination of the experiment at 17 weeks post-DMBA administration. All tumors, grossly normal mammary glands and uteri were excised. Sections of tumors and grossly normal glands were fixed in ice-cold 4% paraformaldehyde (4°C) for histology and immunohistochemistry. The

remaining tissue was frozen on dry ice for molecular/biochemical studies. Frozen tissues were stored at –80°C.

Analysis of Tumor Endpoints

Chi-square analysis was used to compare the tumor incidences between treatment groups. One-way analysis of variance was used to compare the tumorigenesis endpoints (tumor number, tumor weight, tumor burden, tumor latency) between treatment groups. The post hoc tests used were Scheffe's and Tukey's; these were performed using SAS 6.12 and SPSS 7.0. A p-value ≤ 0.05 was considered statistically significant.

Cell Growth and Treatment Conditions

The estrogen receptor (ER) negative Hs578T human breast cancer cell line was derived from a mammary carcinosarcoma and is epithelial in origin [Hackett et al., 1997]. Hs578T cells were propagated in DMEM with 10% heat-inactivated fetal bovine serum (FBS) (Gibco), 4.5 g/L glucose, 10 ug/ml of insulin (Sigma), and 100 ug/ml streptomycin (Gibco), and 100 U/ml penicillin (Gibco). The ER negative MDA-MB-231 human cancer cell line was derived from a patient with poorly differentiated adenocarcinoma of the breast. The cells were grown in DMEM essentially as above except with addition of 0.29 mg/L L-glutamine. The D3-1 line was derived by DMBA-mediated transformation of ER negative MCF-10F human mammary epithelial cells, which were established from a patient with fibrocystic disease and do not display characteristics of a malignant phenotype [Soule et al., 1993]. D3-1 cells were cultured as published previously [Calaf and Russo, 1993]. GTPs and EGCG were purchased from LKT Laboratories Inc., St Paul, Minnesota. GTP was dissolved in ddH_2O. EGCG was dissolved in sterile 50% DMSO at a concentration of 100 mg/ml, and diluted with ddH_2O to a 1 mg/ml working strength solution. Cells were incubated with EGCG for 24, 48 or 72 h as indicated or the volume of diluted DMSO equivalent to the highest dose employed.

For the non-radioactive cell proliferation assay (Promega), cells were seeded at the indicated confluence in 96 well tissue culture dishes. Green tea polyphenols or EGCG was added at the indicated concentration and cultures incubated, in triplicate, for 4-6 h in the presence of (3-(4,5-dimethylthiazol-2-yl)-5-(3-carboxymethoxyphenyl)-2-(4-sulphophenyl)-2H-tetrazolium inner salt (MTS) solution (333 ug/ml) and 25 uM phenazine methosulfate according to the manufacturer's directions (Promega, Madison, WI). The A490 was measured using an ELISA plate reader. For assessment of apoptosis, the TUNEL assay was performed using the ApopTag peroxidase kit from Intergen Company according to the manufacturer's directions. Statistical analysis was performed between the control and treated cultures at the latest time points analyzed in each experiment using the Student's t test. A p-value ≤ 0.05 was considered statistically significant.

Immunoblot analysis

Cells were scraped in PBS and lysed in RIPA buffer (10 mM Tris HCl pH 7.5, 150 mM NaCl, 1% NP40, 0.1% SDS and 1% sodium sarcosyl, 0.2 mM PMSF, 10 μg/ml leupeptin, 1mM dithiothreitol). Following incubation on ice for 5 minutes, the DNA was sheared either by sonication for 5-10 seconds or by passing the lysate 20 times through a 23g and then a 25g needle. The debris was removed by centrifugation at 13,000 rpm for 30 minutes at 4^0C and the total cellular proteins, contained in the supernatant, collected. Protein concentrations were determined using the Bio-Rad *Dc* protein assay. For immunoblot analysis, proteins were resolved on a 10% polyacrylamide-SDS gel and subjected to immunoblotting as we have described previously [Sovak et al., 1997]. The antibody against the cyclin-dependent kinase (CDK) inhibitor (CKI) $p27^{Kip1}$ (13231A) was purchased from Pharmingen (San Diego CA). Densitometry was performed and values presented normalized to the β-actin loading control.

Isolation of Hs578T Stable Transfectants

The LacSwitch inducible system consists of a p3'SS eukaryotic Lac-repressor-expressing vector carrying the *lac I* gene, and a eukaryotic lac-operator-containing $p27^{Kip1}$ vector driven by the RSV-LTR promoter, termed pOPRSVI-*p27*, prepared as described previously [Wu et al., 1999]. Hs578T cells were transfected sequentially, essentially as described previously [Sovak et al., 1997]. Briefly, the p3'SS vector was introduced by the calcium phosphate, and transfectants selected with 50 μg/ml of Hygromycin B. A mixed population of these cells (Hs578T-lacR) was obtained and expression of the Lac I repressor protein confirmed (data not shown). These cells were subjected to a second round of transfection with either 20 μg of pOPRSVI-*sense-p27* vector (carrying the *neo* resistance gene), or 2.5 ug of pSV2*neo* vector DNA. Double transfected cells were selected with both hygromycin and 1200 μg/ml G418. Mixed population of cells (Hs578T-*p27S* and Hs578T-*neo*) were isolated initially. Three single cell clones were isolated by the method of limiting dilution. For induction, cells were treated with the indicated dose of isopropyl-beta-D-thiogalactopyranoside (IPTG). The Lac I repressor protein antibody was obtained from Stratagene (#217449).

FACS analysis

Cells were washed in cold PBS, trypsinized and collected by centrifugation. Cells were resuspended in 0.5 ml hypotonic fluorochrome solution containing 5.0 ug/ml propidium iodide (P.I., Sigma), 1% sodium citrate, and 0.1 % Triton X-100 (Sigma), and analyzed in a Becton-Dickson FACScan flow cytometer, as we have described previously [Wu et al., 1997].

RESULTS

Effect of Green Tea on Mammary Tumorigenesis

In S-D rats, a single intragastric dose of DMBA induces mammary tumors in approximately 90% of animals within 7-20 weeks [Rogers and Conner, 1990]. To test the ability of green tea to reduce or ablate mammary tumor formation, animals were treated with 15mg/kg DMBA, and given 0.3% green tea or water as their sole fluid source. The effects of green tea on cumulative probability of bearing a palpable mammary tumor, tumor number, burden, and latency were all assessed. No effect of tea on body weight gain was observed (data not shown). What appeared to be a slight initial reduction in probability of palpable tumors in the green tea-fed rats compared to the water-fed rats failed to reach statistical significance (Fig. 1). In tumor-bearing rats, the mean latency to first tumor was significantly longer in the green tea-fed group (84 days) than in the water-fed group (66 days) ($p=0.001$) (Table 1). Importantly, there was a statistically significant decrease in mean tumor burden per tumor bearing animal (TBA) in the green tea-fed rats (2.5 +/-4.5 gm) compared to the water-fed rats (8.3 +/-6.9 gm) ($p=0.03$) (Table 1). The water-fed rats had 3.0 tumors per TBA, and the green tea-fed rats had 1.9; this apparent decrease was not significant (Table 1). Of all tumors detected, 89% (42/47) were malignant. They were generally well-differentiated papillary adenocarcinomas; no association of histopathologic subtypes, such as comedo carcinoma, with treatment was discerned. There was no significant difference in malignant tumors per TBA with green tea consumption (1.7 +/- 1.5) compared to water-fed controls (2.8 +/- 1.7). A significant reduction was observed in the mean number of invasive malignant tumors per TBA with green tea consumption (0.2 +/- 0.4) compared to water-fed rats (1.5 +/- 1.8) ($p=0.02$) (Table 2). Green tea had no significant effect on the number of noninvasive tumors per TBA (Table 2). In summary, green tea significantly increased mean latency to first tumor and reduced tumor burden and number of invasive tumors per tumor bearing animal.

Green Tea Polyphenols Decrease Growth of Hs578T Breast Cancer Cells

In the clinic, ER negative tumors are not responsive to anti-estrogenic treatments such as tamoxifen, and generally indicate a poorer prognosis. Therefore we sought to determine whether treatment with green tea extracts decreases the growth of ER negative breast cancer cells, and first selected the Hs578T cell line. Hs578T cells were treated with concentrations of GTPs ranging from 0-160 μg/ml. Cell growth was assessed every 24 h for a 72 h period by cell numbers using an MTS assay (Fig 2A). Incubation in the presence of 40 μg/ml GTPs had no detectable effect on Hs578T cell growth ($p=0.95$), whereas, 80 μg/ml GTP slowed the growth of these breast cancer cells ($p<0.05$). No growth, i.e., no increase in cell numbers, was seen with a higher dose of 160 μg/ml GTP ($p<0.01$). Similar effects of GTPs were obtained by cell counting using a hemocytometer (data not shown). Thus, treatment with GTPs inhibits growth of Hs578T cells in a dose-dependent fashion.

We next assessed the effects of EGCG, one of the more potent anti-carcinogenic components of GTPs, on growth of Hs578T cells (Fig. 2B). EGCG slowed the growth of the Hs578T cells in a dose-dependent fashion ($p<0.01$ at all doses tested). A slower growth was seen at a EGCG concentration of 40 μg/ml, while no increase in cell numbers was seen at 80 μg/ml EGCG. At 160 μg/ml EGCG, a decline in cell numbers was observed (Fig. 2B). Thus, both GTP and EGCG slow proliferation of Hs578T breast cancer cells. A lower concentration of EGCG (80 μg/ml) than GTP mixture (160 μg/ml) was effective in preventing an increase in cell numbers over time.

The drop in Hs578T cell numbers with the highest dose of EGCG suggested cell death was occurring. To monitor for cell death, trypan blue exclusion analysis was performed (Fig. 3). To ensure that floating, dead cells were not lost during the preparation, cells on the dish and in the media were combined and trypan blue positive and negative cells counted. At 80 μg/ml EGCG, a

low percentage of the Hs578T cells stained trypan blue positive at 24 and 48 h (between 7-8%), indicating that the cells were largely viable. A substantial increase in the number of dead cells was seen with 160 μg/ml EGCG (~45% trypan blue positive cells) (Fig. 3). A TUNEL assay indicated apoptosis was occurring at doses of 80 and 160 μg/ml EGCG (data not shown). Taken together, these findings indicate that growth of Hs578T cells begins to slow at 40 μg/ml EGCG, while higher doses of 80-160 μg/ml EGCG inhibit growth and/or cause apoptosis of Hs578T breast cancer cells.

EGCG Slows Growth of Multiple ER Negative Breast Cancer Cell Lines

To determine whether the growth inhibitory effects of EGCG could be extended to other ER negative cells, the MDA-MB-231 and D3-1 breast cancer cell lines were selected. The D3-1 line was derived by DMBA-mediated transformation of non-malignant MCF-10F human mammary epithelial cells [Calaf and Russo, 1993]. MDA-MB-231 cells displayed an EGCG dose-response curve similar to that of Hs578T cells (Fig. 2C), while the D3-1 cells were somewhat more sensitive (Fig. 2D). The apparent higher sensitivity of the D3-1 line was extended to trypan blue analysis in order to assess EGCG-mediated death of D3-1 cells. A significant level of cell death was detected even at 80 μg/ml, and 90-100% of the cultured cells had died within 48-72 h of incubation in the presence of 160 μg/ml EGCG (Fig. 4). Thus, EGCG slows growth and induces death of ER- breast cancer cell lines in a dose-dependent fashion.

$p27^{Kip1}$ Cyclin-Dependent Kinase Inhibitor Expression is Induced by EGCG Treatment

Since the $p27^{Kip1}$ CKI has been implicated in control of cell cycle progression, we measured the effects of EGCG treatment on the levels of $p27^{Kip1}$ CKI protein in Hs578T cells. Cultures of exponentially growing cells were treated for 24 h with 40 or 80 μg/ml EGCG, as appropriate to inhibit cell proliferation. Whole cell extracts were prepared and subjected to immunoblot analysis for $p27^{Kip1}$ protein expression (Fig. 5A). A small increase in the $p27^{Kip1}$ levels was observed in response to treatment with 40 μg/ml EGCG (1.5-fold relative to untreated control cells), which causes a slight

decrease in growth. A larger increase in $p27^{Kip1}$ level was noted with 80 μg/ml EGCG (2.8-fold relative to untreated cells). We then assessed the effects of a longer (48 h) period of EGCG treatment (Fig. 5B). Growth for 48 hours alone resulted in an increase in $p27^{Kip1}$ levels, likely due to the increase in cell density (2.8-fold). EGCG treatment clearly elevated the $p27^{Kip1}$ levels even further (5.5-fold). Thus, growth arrest of HS578T cells in response to EGCG treatment is accompanied by an increase in the level of expression of the CKI $p27^{Kip1}$.

Ectopic Expression of $p27^{Kip1}$ Arrests Growth of Hs578T Cells

To determine the role of induction of $p27^{Kip1}$ protein in Hs578T breast cancer cell, the LacSwitch inducible expression system was used. Mixed populations of stable Hs578T-*p27S* and Hs578T-*neo* population of cells were isolated. Since we have found that the response of the mixed populations is relatively minimal due to the presence of cells expressing only low levels, three single cell clones of Hs578T- *p27S* cells were isolated by limiting dilution (Hs578T-*p27S* #2, #3, #4). To test for induction of $p27^{Kip1}$ expression, the mixed populations of Hs578T-*p27S* and Hs578T-*neo* cells, and the three Hs578T- *p27S* clones were treated with 0, 10 or 20 mM ITPG, as indicated (Fig. 6A). Total cellular proteins were extracted and samples (50 ug) subjected to immunoblot analysis for $p27^{Kip1}$ expression. A very high level of induction of the $p27^{Kip1}$ protein was detected in the Hs578T-*p27S* cells at both concentrations of IPTG (Fig. 6A, upper panel). In contrast, control Hs578T-*neo* cells showed essentially no induction of the $p27^{Kip1}$ protein. As expected, the Lac I repressor protein was detected at high levels in extracts from both cell populations, confirming equal loading (Fig. 6A, lower panel). One of these clones (Hs578T-*p27S* #3) showed a very high level of $p27^{Kip1}$ induction upon 10 mM IPTG treatment (Fig. 6B, upper panel); whereas, the two other clonal isolates (Hs578T-*p27S* #4, and Hs578T-*p27S*#2) displayed no significant increase in $p27^{Kip1}$ levels (Fig. 6B, lower panel and data not shown). Thus, we selected the Hs578T-*p27S* mixed population and Hs578T-*p27S* #3 for study of the effects of $p27^{Kip1}$

induction on cell cycle, while the Hs578T-*neo* mixed population and Hs578T-*p27S* #4 cells served as negative controls.

The Hs578T-*p27S*, Hs578T-*neo*, Hs578T-*p27S* #3 or Hs578T-*p27S* #4 cells were treated, in triplicate, with IPTG for 24 h and analyzed on a Becton-Dickson FACScan flow cytometer (Fig. 7 and Table 3). Approximately, 64.4 +/- 0.4 % of the Hs578T-*p27S* cells treated with IPTG were in the G0/G1 state, compared to 57.2 +/- 1.9 % when untreated. As expected, the Hs578T-*neo* cells had essentially equivalent cell cycle distribution in the presence or absence of IPTG. IPTG treatment of Hs578T-*p27S* #3 cells resulted in G0/G1 arrest of 82 +/- 0.5 %, compared to 62.5 +/- 1.9 % in untreated cells (Fig. 7). Clone Hs578T-*p27S* #4 cells, which showed no induction of $p27^{Kip1}$ levels, displayed no significant difference in the cell cycle distribution with respect to IPTG treatment (Fig. 7). Taken together these results indicate the induction of the $p27^{Kip1}$ protein participate in the G0/G1 arrest of Hs578T breast cancer cells.

DISCUSSION

Here we show that green tea extracts given to S-D rats in their drinking fluid significantly decrease carcinogen-induced tumor burden and invasiveness and significantly increase latency to first tumor. The cumulative probability of bearing a palpable tumor also was numerically decreased, although this was not statistically significant. Similarly, doses of GTP and EGCG between ~40 to 80 μg/ml slowed growth of various ER negative breast cancer cell lines in culture, including Hs578T, MDA-MB-231 and D3-1. Slower growth could be related in part to induction of $p27^{Kip}$ protein, which causes an arrest of cells at the G1/S phase transition. Higher doses of EGCG (~80 to 160 μg/ml) were shown to cause death of breast cancer cells, at least in part due to apoptosis as judged by TUNEL assay (data not shown). Thus, these data extend the findings of other groups on the anti-carcinogenic properties of green tea [rev. in Yang et al., 1997]. Overall, these results

confirm the anti-carcinogenic properties of green tea polyphenols on mammary tumor formation *in vivo*. Importantly, the data presented here were obtained, for the first time, using drinking fluid as the route of administration of the green tea, rather than feed, thus modeling human exposure to green tea polyphenols. We demonstrate also the ability of GTPs to slow growth of breast cancer cells in culture. These observations provide both *in vivo* and cell culture evidence in support of a role for green tea components in chemoprevention and, possibly, chemotherapy of breast cancer.

The $p27^{Kip1}$ CKI was originally characterized as a protein able to interrupt CDK2 kinase activity in TGF-β1-treated cells, and in a yeast two hybrid system as being able to interact with cyclin D and CDK4 [Polyak et al., 1994; Toyoshima and Hunter, 1994]. The CKI $p27^{Kip1}$ is now known to bind to and inhibit complexes formed by cyclin E-CDK2, cyclin A-CDK2, and cyclin D-CDK4, playing essential roles in transition through the G1 phase, in particular the restriction point [Sherr and Roberts, 1999]. Here we demonstrate that increased levels of $p27^{Kip1}$ can prevent cell cycle progression of Hs578T breast cancer cells, with arrest occurring prior to entry into S phase. The ability of EGCG to induce $p27^{Kip1}$ expression in breast cancer cells provides a mechanism for the observed reduction in growth rate. Similar effects on $p27^{Kip1}$ were reported recently by Liang et al. [1999]. Interestingly, a high level of ectopic expression of $p27^{Kip1}$ failed to result in apoptosis or cell death of Hs578T cells, indicating that other molecular events are induced by EGCG treatment.

Interestingly, many human malignancies, including cancers of the breast, stomach, colon, lung, esophagus, prostate and pituitary [reviewed in Cariou et al., 1998; Lloyd et al., 1999], are typified by very low basal levels of $p27^{Kip1}$ protein. Reduced $p27^{Kip1}$ protein levels has been correlated with more aggressive, poorly differentiated cancers [Cariou et al., 1998, Han et al., 1999] and indicate a poorer prognosis [Catzavelos et al., 1997; Gillett et al., 1999; Han et al., 1999]. In breast cancer, several studies have correlated decreased $p27^{Kip1}$ levels with increased malignant behavior. Catzavelos et al. [1997] completed an informative study of 168 breast cancer patients who

had undergone primary surgery between 1986 and 1992. Patients were divided into two categories based on their degree of elevation of $p27^{Kip1}$ protein levels. High $p27^{Kip1}$ protein levels were found in patients with less aggressive types of tumor, while lower levels were detected in those with a high grade of malignant tumor. Furthermore, those patients displaying axillary lymph node involvement displayed similar or even lower $p27^{Kip1}$ protein levels in the nodes in question. Moreover, Kaplan-Meier curves of disease-free survival were constructed and indicated a significantly shorter disease-free survival with decreased $p27^{Kip1}$ protein levels. These findings led the investigators to conclude that a decrease in $p27^{Kip1}$ level facilitates breast cancer progression. Similar results were obtained from a study of 102 female breast cancer patients with lymph node metastasis conducted by Tsuchiya et al. [1999]. In this study, a significant positive correlation was also found between $p27^{Kip1}$ levels and estrogen receptor (ER) status. Similarly, Gillett et al. [1999] observed that high $p27^{Kip1}$ protein levels were associated with smaller, well-differentiated, more slowly proliferating tumors with ER positive status. In addition, these patients were also shown to have a significantly longer survival than those with low $p27^{Kip1}$ levels, unless they also had high levels of cyclin D1. In effect, overexpression of cyclin D1 appeared to overcome the detrimental effect of low $p27^{Kip1}$ levels. Similar results have been shown by other groups [Fredersdorf et al., 1997; Porter et al., 1997; Tan et al., 1997].

In animal models, green tea extracts inhibit chemical carcinogenesis, including cancers of the gastrointestinal tract, lung and skin in mice [Fujita et a., 1989; Wang et al. 1989; Wang et al., 1991; Conney et al. 1992; Huang et al., 1992; Katiyar et al. 1992; Taniguchi et al., 1992; Wang et al., 1992a; Wang et al., 1992b; Pingzhang et al. 1994; Wang et al. 1994; Wang et al. 1995]. It has been reported also that EGCG inhibits the growth of human breast and prostate tumors transplanted into athymic mice [Liao et al. 1995]. Two studies of mammary gland carcinogenesis in rats provided suggestive evidence of a chemopreventive effect of green tea [Hirose et al. 1994; Hirose et

al. 1995]. One study of rats fed a high fat diet and given black tea to drink showed a reduction in tumor multiplicity compared to rats given water [Weisburger et al. 1997]; results in rats fed control diet were not reported. One study using a diet containing 1% green tea catechins fed to female Sprague-Dawley rats showed that tea was effective in reducing mammary gland tumorigenesis in the promotion, but not the progression, stages of carcinogenesis [Hirose et al. 1997]. Consistent with these findings, several studies have also found that green tea treatment of breast cancer cells *in vitro* reduces their rate of proliferation [Araki et al., 1995; Chen et al., 1998; Liang et al., 1999]. In these studies, we have shown the effects of green tea on carcinogen-induced tumor burden in rats and extended the *in vitro* findings to additional cell lines.

ACKNOWLEDGMENTS

We thank J. Russo for generously providing cell lines, and Lipton Tea company for providing green tea. We thank G. Zanieski for assistance in preparation of the Hs578T transfectants, J. Foster for the use of the scanning densitometer, and D. Sloneker for assistance in preparation this manuscript. This work was supported by Department of Army research grants DAMD17-94-J-4468 (G.E.S.), DAMD17-98-1 (G.E.S.), DAMD 17-98-1-8034 (DWK), DAMD17-99-1-9083 (K.T.K.), and Training Grant DAMD 17-94-J-442194 (K.T.K., L.H.), and Karin Grunebaum Cancer Research Fellowships (K.T.K., DWK).

REFERENCES

Araki R, Inoue S, Osborne MP, Telang NT. 1995. Chemoprevention of mammary preneoplasia. In vitro effects of a green tea polyphenol. Ann NY Acad Sci 768:215-222.

American Cancer Society, CA. 1999. A Cancer Journal for Clinicians, 49: 1-64

Calaf G, Russo J. 1993. Transformation of human breast epithelial cells by chemical carcinogens. Carcinogenesis 14:483-492.

Cariou S, Catzavelos C, Slingerland JM. 1998. Prognostic implicatins of expression of the cell cycle inhibitor protein p27Kip1. Breast Cancer Res Treatment 52:29-41.

Catzavelos C, Bhattacharya N, Ung YC, Wilson JA, Roncari L, Sandhu C, Shaw P, Yeger H, Morava-Protzner I, Kapusta L, Franssen E, Pritchard KI, Slingerland JM. 1997. Decreased levels of the cell-cycle inhibitor p27Kip1 protein: prognostic implications in primary breast cancer. Nat Med 3:227-230.

Chen ZP, Schell JB, Ho CT, Chen KY. 1998. Green tea epigallocatechin gallate shows a pronounced growth inhibitory effect on cancerous cells but not on their normal counterparts. Cancer Lett 129:173-179.

Conney AH, Wang Z-Y, Huang M-T, Ho C-T, Yang CS. 1992. Inhibitory effect of green tea on tumorigenesis by chemicals and ultraviolet light. Preventative Medicine 21:362-369.

Fredersdorf S, Burns J, Milne AM, Packham G, Fallis L, Gillett CE, Royds JA, Peston D, Hall PA, Hanby AM, Barnes DM, Shousha S, O'Hare MJ, Lu X. 1997. High level expression of p27(kip 1) and cyclin D1 in some numan breast cancer cells: inverse correlation between the expression of p27(kip 1) and degree of malignancey in human breast and colorectal cancers. Proc Natl Acad Sci USA 94:6380-6385.

Fujita Y, Yamane T, Tanaka M, Kuwata K, Okuzumi J, Takahashi T, Fujiki H. 1989. Inhibitory effect of (-)-epigallocatechin gallate on carcinogenesis with N-ethyl-N-nitro-Nnitrosoguanidine in mouse duodenum. Jpn J Cancer Res 80:503-505.

Gillet CE, Smith P, Peters G, Lu X, Barnes DM. 1999. Cyclin-dependent kinase inhibitor p27Kip1 expression and interaction with other cell cycle-associated proteins in mammary carcinoma. J Pathol 187:200-206.

Goldbohm RA, Hertog MG, Brants HAM, van Poppel G, van den Brandt PA. 1996. Consumption of black tea and cancer risk: A prospective cohort study. J Natl Cancer Institute 88:93-100.

Hackett AJ, Smith HS, Springer EL, Owens RB, Nelson-Rees WA, Riggs JL, Gardner MB. 1997. Two syngeneic cell lines from human breast tissue: the aneuploid mammary epithelial (Hs578T) and the diploid myoepithelial (Hs578Bst) cell lines. J Nat Cancer Inst 58:1795-1806.

Haenszel W, Kurihara M. 1968. Studies of Japanes migrants. I. Mortality from cancer and other disease among Japanese in the United States. J Natl Cancer Institute 40:43-68.

Han S, Park K, Kim HY, Lee MS, Kim HJ, Kim YD. 1999. Reduced expression of p27Kip1 protein is associated with poor clinical outcome of breast cancer patients treated with systemic chemotherapy and is linked to cell proliferation and differentiation. Breast Cancer Res Treat 55:161-167.

Hirose M, Akagi K, Hasegawa R, Yaono M, Satoh T, Hara Y, Wakabayashi K, Ito N. 1995. Chemoprevention of 2-amino-1-methyl-6-phenylimidazo[4,5-b]-pyridine (PhIP)-induced mammary gland carcinogenesis by antioxidants in F344 female rats. Carcinogenesis 16:217-221.

Hirose M, Hoshiya T, Akegi K, Futakuchi M, Ito N. 1994. Inhibition of mammary gland carcinogenesis by green tea catechins and other naturally occurring antioxidants in female Sprague-Dawley rats pretreated with 7, 12-dimethylbenz(*a*)anthracene. Cancer Lett 83:149-156.

Hirose M, Mizoguchi Y, Yaono M, Tanaka H, Yamaguchi T, Shirai T. 1997. Effects of green tea catechins on the progression or late promotion stage of mammary gland carcinogenesis in female Sprague-Dawley rats pretreated with 7,12-dimethylbenz(*a*)anthracene. Cancer Lett 112:141-147.

Ji B-T, Chow W-H, Hsing AW, McLaughlin JK, Dai Q, Gao Y-T, Blot WJ, Fraumeni JF, Jr.

1997. Green tea consumption and the risk of pancreatic and colorectal cancers. Intl J Cancer 70:255-258.

Katiyar S, Agarwal R, Wood GS. 1992. Inhibition of 12-O-tetradecanoylphorphol-13-acetate-caused tumor promotion in 7,12-dimethylbenz(a)anthracene-initiated SENCAR mouse skin by a polyphenolic fraction isolated from green tea. Canc Res 52:6890-6897.

Katiyar SK, Ahmad N, Mukhtar H. 2000. Green tea and skin. Arch Dematol 136:989-994.

Kelsey JL, Gannon MD. 1990. Epidemiology of breast cancer. Epidemiological Rev 12:228-240.

Liang YC, Huang YT, Tsai SH, Lin-Shiau SY, Chen CF, Lin JK. 1999. Suppression of inducible cyclooxygenase and inducible nitric oxide synthase by apigenin and related flavonoids in mouse macrophages. Carcinogenesis 20:1945-1952.

Liao S, Umekita Y, Guo J, Kokontis JM, Hiipakka RA. 1995. Growth inhibition and regression of human prostate and breast tumors in athymic mice by tea epigallocatechin gallate. Cancer Lett 96:239-245.

Lloyd RV, Erickson LA, Jin L, Kulig E, Qian X, Cheville JC, Scheithauer BW. 1999. p27Kip1: a multifunctional cyclin-dependent kinase inhibitor with prognostic significance in human cancers. Am J Pathol 154:313-323.

Mukhtar H, Katiyar S, Agarwal R. 1994. Cancer chemoprevention by green tea components. In Jacobs MM (ed): "Diet and Cancer: Markers, Prevention and Treatment." New York: Plenum Press, pp 113-122.

National Cancer Institute, DCPC Chemoprevention Branch and Agent Development Committee. 1996. Clinical development plan: Tea extracts, green tea polyphenols, epigallocatechin gallate. J. Cell Biochem 265:236-257

Pingzhang Y, Jinying Z, Shujun C, Hara Y, Qingfan Z, Zhengguo L. 1994. Experimental studies of

the inhibitory effects of green tea catechin on mice large intestianl cancers induced by 1,2-dimethylhydrazine. Canc Lett 79:33-38.

Polyak K, Kato, JY, Solomon, MJ, Sherr, CJ, Massague, J, Roberts, JM, Koff, A. 1994. p27Kip1, a cyclin-Cdk inhibitor, links transforming growth factor-beta and contact inhibition to cell cycle arrest. Genes Dev 8: 9-22.

Porter PL, Malone KE, Heagerty PJ, Alexander GM, Gatti LA, Firpo EJ, Daling JR, Roberts JM 1997. Expression of cell-cycle regulators p27Kip1 and cyclin E, alone and in combination, correlate with survival in young breast cancer patients. Nat Med 3:222-225.

Rogers AE, Conner BH. 1990. Dimethylbenzanthracene-induced mammary tumorigenesis in ethanol-fed rats. Nutr Res 10:915-928.

Rogers AE, Hafer LJ, Iskander YS, Yang S. 1998. Black tea and mammary gland carcinogenesis by 7,12-dimethylbenz[a]anthracene in rats fed control or high fat diets. Carcinogenesis 19:1269-1273.

Sherr C, Roberts, JM. 1999. CDK inhibitors: positive and negative regulators of G1-phase progression. Genes Dev 13:1501-1512.

Soule HD, Vazguez J, Long A, Albert S, Brennan M. 1973. A human cell line from a pleural effusion derived from a breast carcinoma. J Nat Cancer Inst 51:1409-1416.

Sovak MA, Bellas RE, Kim DW, Zanieski GJ, Rogers AE, Traish AM, Sonenshein GE. 1997. Aberrant Nuclear Factor-kB/Rel expression and the pathogenesis of breast cancer. J Clin Invest 100:2952-2960.

Stoner GD, Mukhtar H. 1995. Polyphenols as cancer chemotherapeutic agents. J Cell Biochem 22:169-180.

Tan P, Cady B, Wanner M, Worland P, Cukor B, Magi-Galluzzi C, Lavin P, Draetta G, Pagano M,

Loda M. 1997. The cell cycle inhibitor p27 is an independent prognostic marker in small (T1a,b) invasive breast carcinomas. Canc Res 57:1259-1263.

Tanaka H, Hirose M, Kawabe M, Sano M, Takesada Y, Hagiwara A, Shirai T. 1997. Post-initiation inhibitory effects of green tea catechins on 7,12-dimethylbenz[*a*]anthracene-induced mammary gland carcinogenesis in female Sprague-Dawley rats. Cancer Lett 116:47-52.

Taniguchi S, Fujiki H, Kobayashi H, Go H, Miyado K, Sadano H, Shimokawa R. 1992. Effect of (-)-epigallocatechin gallate, the main constituent of green tea, on lung metastasis with mouse B16 melanoma cell lines. Cancer Lett 65:51-54.

Toyoshima H, Hunter T. 1994. p27, a novel inhibitor of G1 cyclin-Cdk protein kinase activity, is related to p21. Cell 78:67-74.

Tsuchiya A, Zhang GJ, Kanno M. 1999. Prognostic impact of cyclin-dependent kinase inhibitor p27Kip1 in node-positive breast cancer. J Surg Oncol 70:230-234.

Wang ZY, Hong JY, Huang MT, Reuhl KR, Conney AH, Yang CS. 1992a. Inhibition of N-nitroso-diethylamine and 4-(methylnitrosamino)-1-(3-pyridyl)-1-butanone-induced tumorigenesis in A/J mice by green tea and black tea. Canc Res 52:1943-1947.

Wang ZY, Huang MT, Ho CT, Chang R, Ma W, Ferraro T, Reuhl KR, Yang CS, Conney AH. 1992b. Inhibitory effect of green tea on the growth of established skin papillomas in mice. Cancer Res 52:6657-6665

Wang Z-H, Hong J-Y, Huang M-T, Reuhl K, Conney AH, Yang CS. 1994. Inhibition of N-nitroso-diethylamine and 4-(methylnitrosamino)-1-(3-pyridyl)-1-butanone bioactivation, DNA methylation, and lung tumorigenesis by green tea and black tea in A/J mice. Canc Res 54:4641-4647.

Wang Z-R, Agarwal R, Bickers DR, Mukhtar H. 1991. Protection against ultraviolet B radiation-

induced photocarcinogenesis in hairless mice by green tea polyphenols. Carcinogenesis 12:1527-1530.

Wang ZY, Khan WA, Bickers DR, Mukhtar H. 1989. Protection against polycyclic aromatic hydrocarbon-induced skin tumor initiation in mice by green tea polyphenols. Carcinogenesis 10:411-415.

Wang ZY, Wang L-D, Lee M-J, Ho C-T, Huang M-T, Conney AH, Yang CS. 1995. Inhibition of N-nitrosomethylbenzylamine-induced esophageal tumorigenesis in rats by green and black tea. Carcinogenesis 16:2143-2148.

Weisburger JH, Rivenson A, Garr K, Aliaga C. 1997. Tea, or tea or milk, inhibit mammary gland and colon carcinogenesis in rats. Canc Lett 114:323-327.

Wu M, Lee H, Bellas RE, Schauer SL, Arsura M, Katz D, FitzGerald MJ, Rothstein TL, Sherr DH, Sonenshein GE. 1996. Inhibition of NF-κB/Rel induces apoptosis of murine B cells. EMBO J 15:4682-4690.

Wu M, Bellas RE, Shen J, Yang W, Sonenshein GE. 1999. Increased p27Kip1 cyclin-dependent kinase inhibitor gene expression following anti-IgM treatment promotes apoptosis of WEHI 231 B cells. J Immunol 163:6530-6535.

Yang CS, Chen L, Lee M-J, Landau JM. 1996. Effects of tea on carcinogenesis in animal models and humans. Dietary phytochemicals in cancer prevention and treatment. New York: Plenum Press.

Yang CS, Lee MJ, Chen L, Yang GY. 1997. Polyphenols as inhibitors of carcinogenesis. Environ Health Perspect 105 Suppl 4:971-976.

Zheng W, Doyle TJ, Kushi LH, Seilers TA, Hong C-P, Folsom AR. 1996. Tea consumption and cancer incidence in a prospective cohort study of postmeopausal women. Amer J Epidemiology 144:175-182.

Ziegler RG, Hoover RN, Pike MC, Hildesheim A, Nomura AM, West AM, Wu-Williams AH, Kolonel LN, Horn-Ross PL, Rosenthal JF. 1993. Migration patterns and breast cancer risk in Asian-American women. J Nat Cancer Institute 85:1819-1827.

Figure Legends

Fig. 1. Cumulative probability of bearing a palpable tumor in DMBA-treated female Sprague-Dawley rats as a function of green tea. Rats were given 15 mg/kg body weight DMBA at eight weeks of age.

Fig. 2. GTPs and EGCG slow growth estrogen receptor negative breast cancer cells in a dose-dependent fashion.

A) Effects of GTPs on Hs578T cells. Hs578T cells were plated, in triplicate, at a density of 3.9 x 10^3 cells/cm^2 in 96 well plates. After overnight incubation, GTP was added at a concentration of 0, 40, 80 or 160 μg/ml, as indicated. Cultures incubated for an additional 24, 48 or 72 h. Cell proliferation was quantified by conversion of MTS dye to its formazan product read at OD490nm. The data are presented as the mean +/- SD.

B) Effects of EGCG on Hs578T cells. Hs578T cells were plated, in triplicate, at a density of 3.9 x 10^3 cells/cm^2. After overnight incubation, EGCG was added at the indicated concentration dissolved in DMSO or the DMSO vehicle alone was added as control (0 μg/ml). Cultures were then incubated and processed as above in Part A.

C) Effects of EGCG on MDA-MB-231 cells. MDA-MB-231 cells were plated, in triplicate, at a density of 6 x 10^3 cells/cm^2. After overnight incubation, EGCG was added and cultures processed as above. A significant decrease in cell numbers was seen at all doses ($p<0.05$).

D) Effects of EGCG on D3-1 cells. D3-1 cells were plated, in triplicate, at a density of 7 x 10^3 cells/cm^2, and treated with EGCG and processed as above. A statistically significant decrease was achieved at 80 and 160 μg/ml EGCG ($p<0.05$).

Fig. 3. Higher doses of EGCG kills Hs578T cells as measured by trypan blue staining. Hs578T cells were plated, in triplicate, at 2.6 x 10^3 cells/cm^2 in 6 well plates. After overnight incubation, EGCG was added at 80 or 160 μg/ml in DMSO or the DMSO vehicle alone was added as control (0 μg/ml). After an additional 24- or 48-h period, both adherent and floating cells were harvested and subjected to trypan blue analysis for dead cells. Values of the percentage of trypan blue positive cells are given as the mean +/- SD.

Fig. 4. EGCG reduces viability of D3-1 cells. D3-1 cells were plated, in triplicate, at a 7 x 10^3 cells/cm^2. After overnight incubation, EGCG was added at 40, 80 or 160 μg/ml in DMSO or the DMSO vehicle alone was added as control (0 μg/ml). After an additional 24, 48 or 72 h period, both adherent and floating cells were harvested and subjected to trypan blue analysis for dead cells. Values of the percentage of trypan blue positive cells are given as the mean +/- SD.

Fig. 5. EGCG induces $p27^{Kip1}$ expression. A) Hs578T cells were incubated in the presence of 0, 40, or 80 μg/ml in DMSO for a 24-h period and total protein extracts prepared and subjected to immunoblotting for expression of $p27^{Kip1}$ and β-actin protein. B) Twenty-four hours after plating, Hs578T cultures were either harvested directly (0 h) or incubated for 48 h in the presence of 80 μg/ml EGCG or the equivalent volume of DMSO. Total protein extracts were prepared, and analyzed as in Part A.

Fig. 6. Ectopic expression of $p27^{Kip1}$ protein is induced by IPTG treatment in Hs578T-*p27S* cells. A) Cultures of mixed populations of Hs578T-*p27* and -*neo* cells were treated with 0, 10, or 20 mM IPTG for 28 h and total cellular proteins were extracted. Samples (50 ug) were subjected to

immunoblot analysis using antibodies to the $p27^{Kip1}$ (Pharmingen 13231A) (upper panel) and the Lac I repressor protein (Stratagene #217449) (lower panel).

B) Three clonal isolates were derived from the Hs578T-*p27S* cells by limiting dilution, tested for induction of $p27^{Kip1}$ protein upon treatment in the absence or presence of 10 mM IPTG, as above in part A. Hs578T-*neo* cells were tested similarly, as negative control.

Fig. 7. FACS analysis of individual Hs578T-*p27S* clones.

Hs578T-*p27S* #3 clonal populations, and Hs578T-*neo* cells were treated in triplicate with 10 mM IPTG for 24 h, and analyzed on a Becton-Dickson FACScan flow cytometer for cell cycle distribution. The upper panel shows a representative flow cytometry results for Hs578T-*p27S* #3 and the Hs578T-*neo* cells in the absence or presence of IPTG.

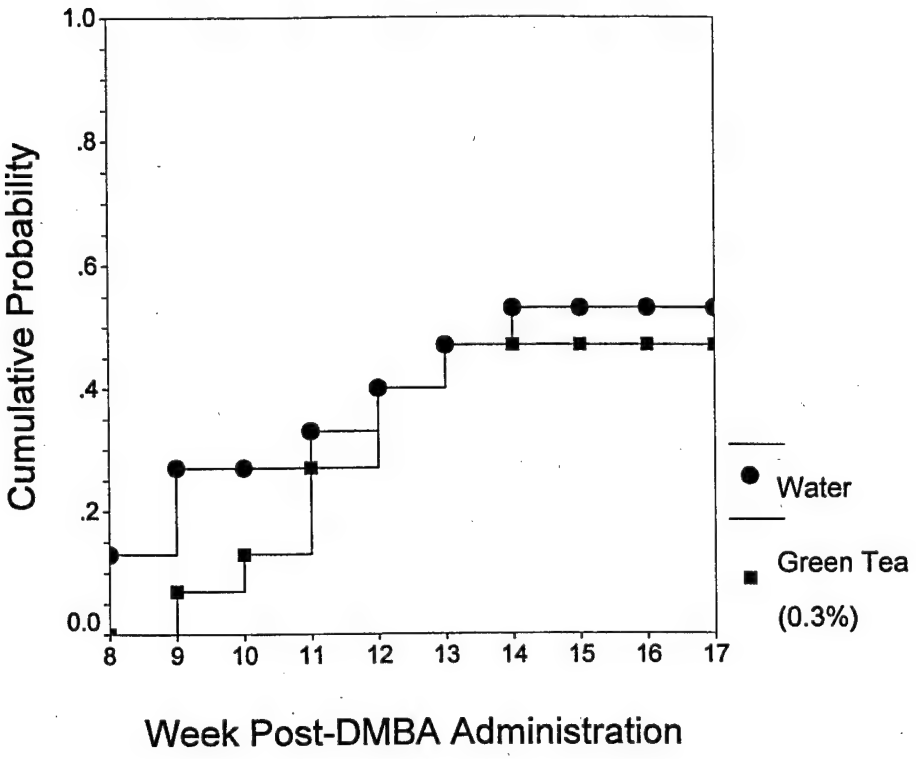

Fig.1, Kavanagh et al

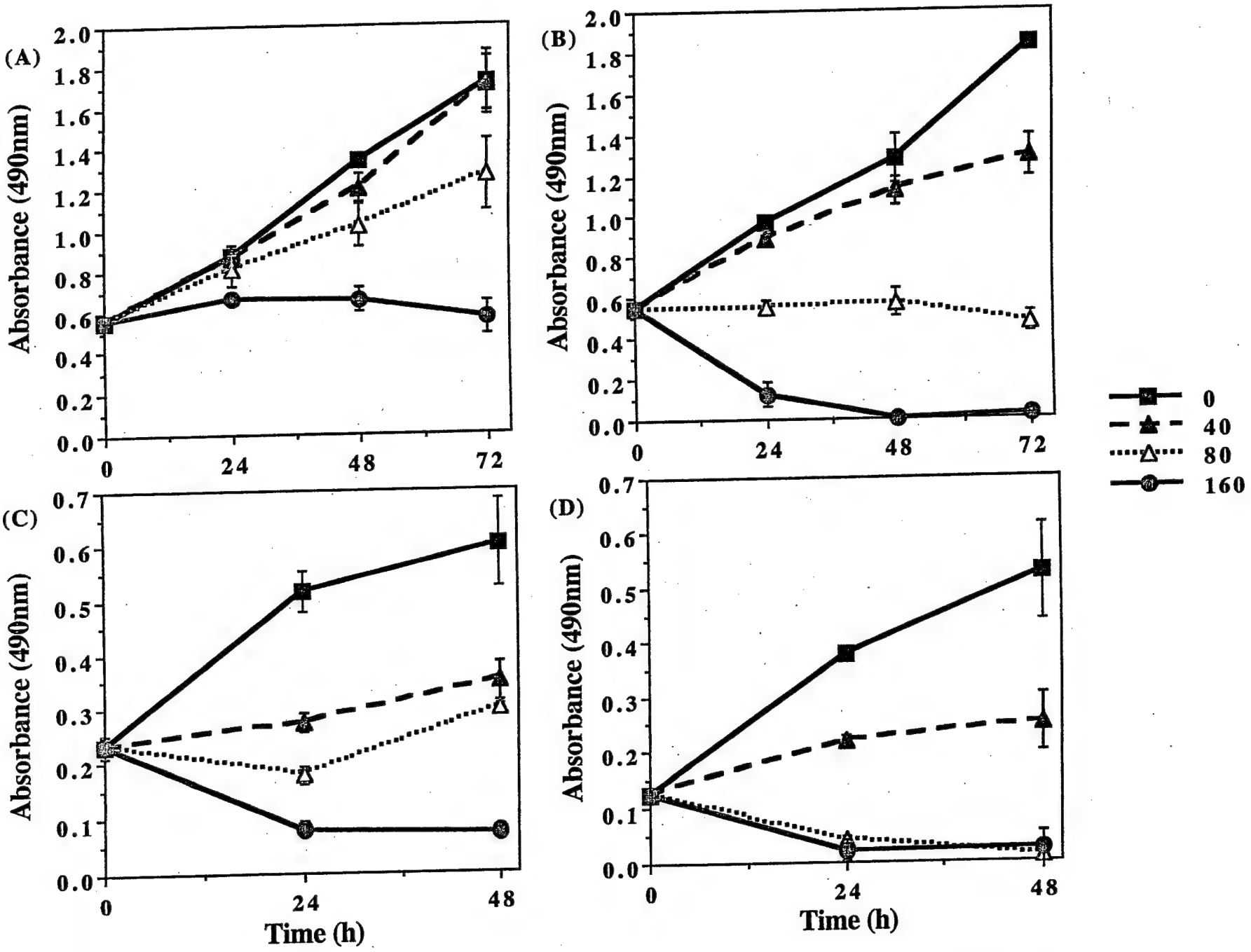

Fig.2, Kavanagh et al

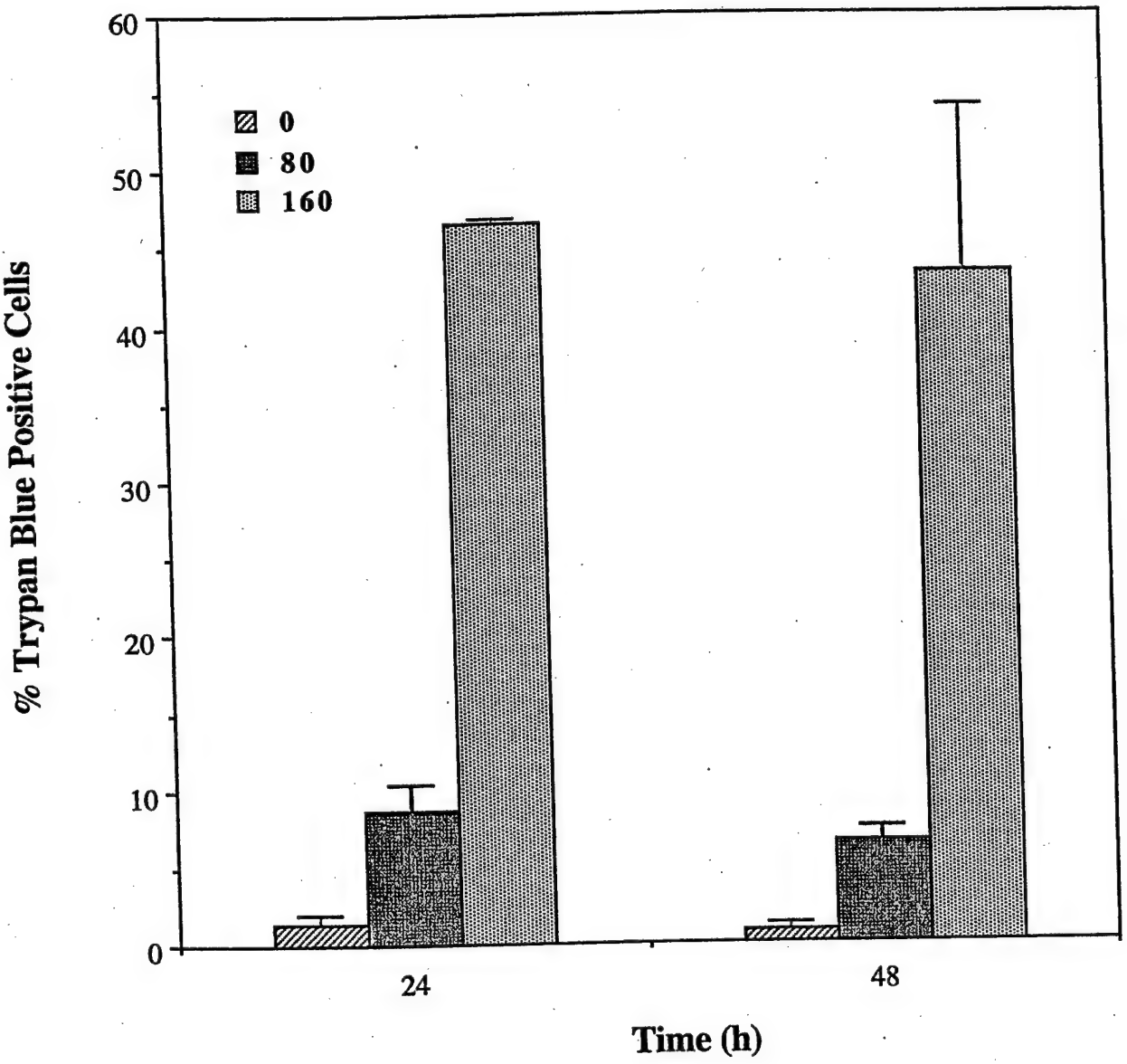

Fig.3, Kavanagh et al

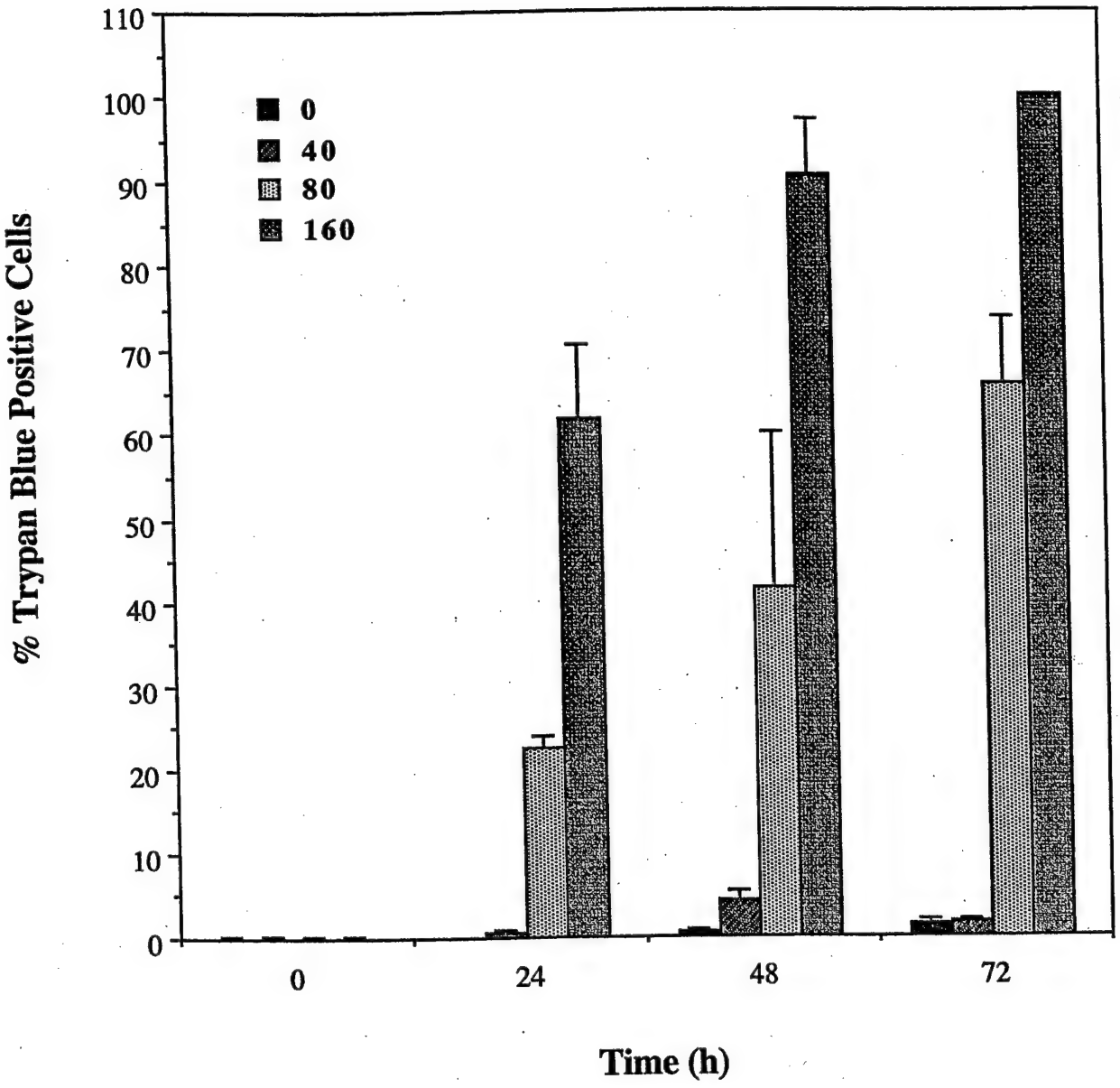

Fig.4, Kavanagh et al

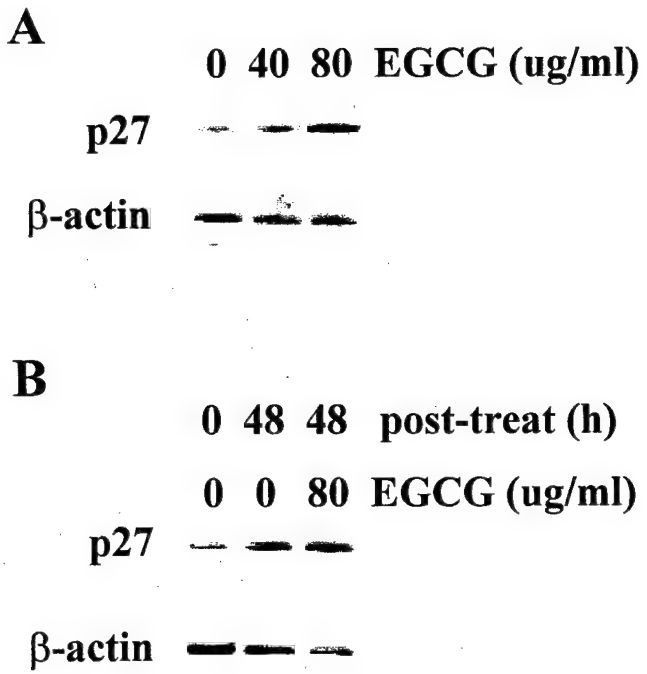

Fig. 5, Kavanagh et al.

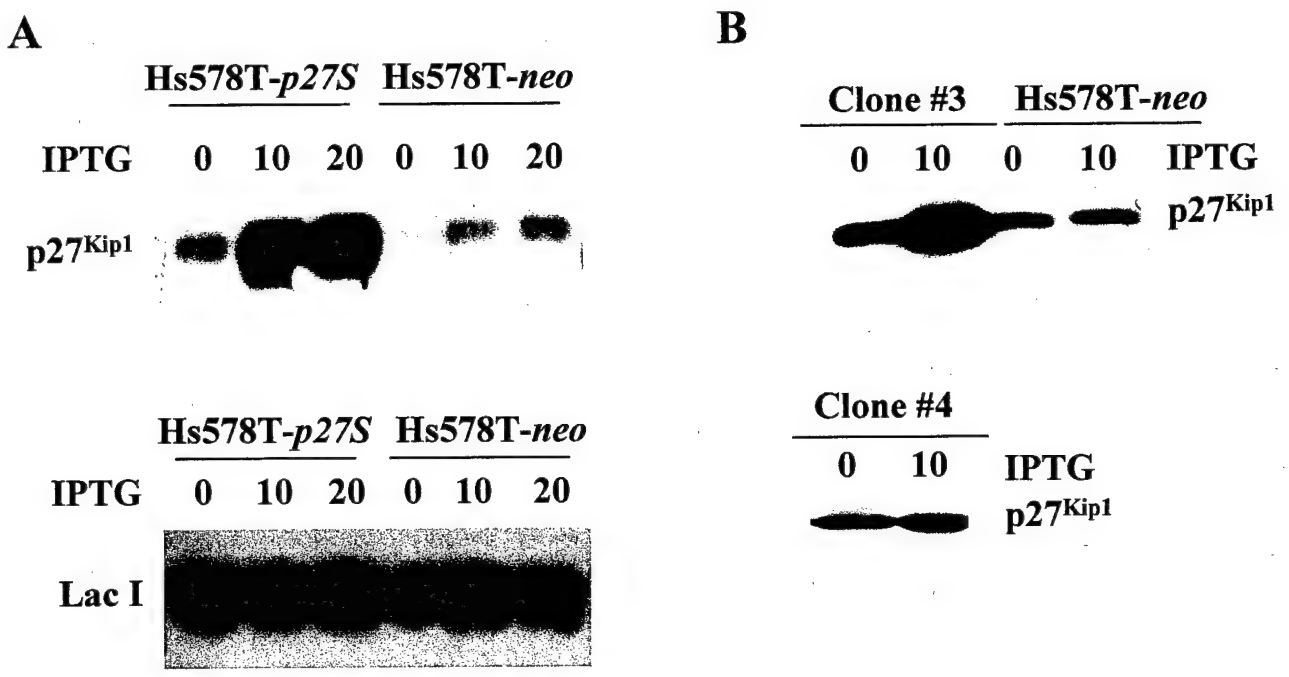

Fig. 6, Kavanagh et al

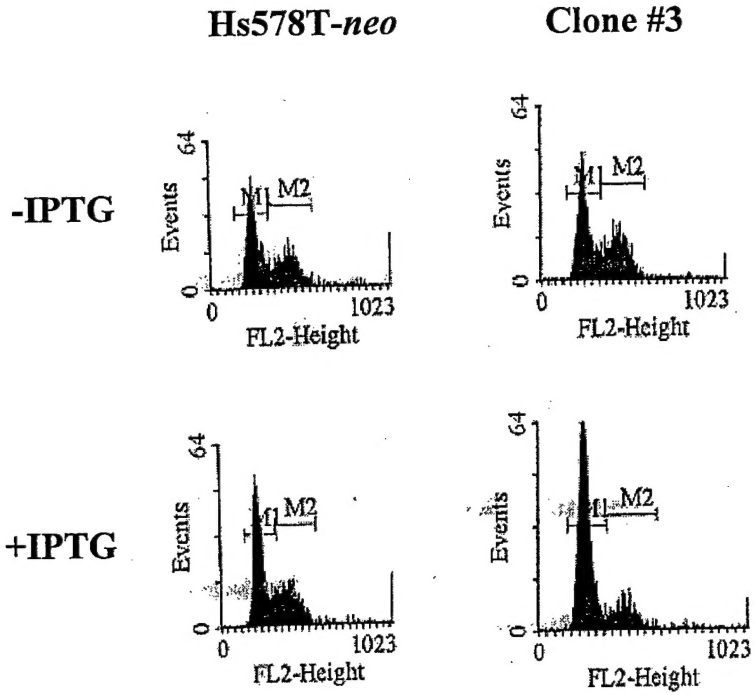

Fig. 7, Kavanagh et al

Table 1

DMBA-induced Mammary Tumor Incidence, Number and Weight in Female Sprague-Dawley Rats Drinking Tea or Water

Group	Tumor Incidence (%)[a]	Tumor No. per TBA[b]	Tumor Wt. (g) per TBA	Latency (days) to 1st Tumor
Water (CG2)	53	3.0±1.6	8.3±6.9	66±14[d]
Green tea (TG2)	80	1.9±1.6	2.5+4.5 [c]	84±21

[a]15 rats per group

[b]TBA = tumor bearing animal; values given are mean + S.D.

[c]significantly less than water-fed (CG2) control animals (p=0.03)

[d]significantly shorter than green tea-fed (TG2) animals (p=0.001)

Table 2

Number of Noninvasive and Invasive Tumors per Tumor Bearing Animal (TBA)

Histology	Group	Number/TBA*
Noninvasive	Water (CG2)	1.2±1.0
	Green tea (TG2)	1.5±1.4
Invasive	Water (CG2)	1.5±1.8
	Green tea (TG2)	0.2±0.4[a]

* mean + S.D.

[a] significantly less than water-fed (CG2) control animals (p=0.025)

Table 3. Summary of FACS Analysis of Hs578T-*p27S* and Hs589T-*neo* Cells

Cell Types		Average G_0/G_1 +/-Standard Deviation
Hs578T-*p27S*	MP Untreated	57.2 +/- 1.9
	MP + IPTG	64.4 +/- 0.4
	Clone#3 Untreated	62.5 +/- 1.9
	Clone#3 + IPTG	82.1 +/- 0.5
	Clone#4 Untreated	60.6 +/- 1.0
	Clone#4 + IPTG	60.6 +/- 1.6
Hs578T-*neo*	MP Untreated	56.0 +/- 1.1
	MP + IPTG	58.4 +/- 1.1

FACS analysis was performed to determine the cell cycle distribution of the cells upon induction of the p27kip1 proteins in the mixed population (MP) of Hs578T-*p27S* cells, and the clonal populations (Clone #3 and Clone #4). The MP Hs578T-*p27S*, Clone #3, Clone #4, and MP Hs578T-*neo* control cells were treated in triplicate with 20 mM IPTG. After 24 hours, the cells were washed in cold PBS, trypsinized and pelleted, and resuspended in 0.5 ml hypotonic fluorochrome solution containing 5.0 ug/ml PI, 1% sodium citrate, and 0.1% Triton X-100. Cells were then analyzed in Becton-Dickson FACScan flow cytometer for cell cycle distribution. The results of the average cell cycle distribution of the cells are summarized above.